Physics – Uspekhi **47** (7) 643 – 670 (2004)

REVIEWS OF TOPICAL PROBLEMS PACS numbers: **12.10.–g**, **12.60.–i**, 14.80.Bn

The search for new physics at the Large Hadron Collider

N V Krasnikov, V A Matveev

DOI: 10.1070/PU2004v047n07ABEH001767

Contents

Abstract. **This is a review of various aspects of the Large Hadron Collider project for the search for new physics (namely, the Higgs boson, supersymmetry, and exotics). The basic parameters of the CMS and ATLAS detectors are also discussed.**

1. Introduction

The Standard Model (SM) [1], which describes strong and electroweak interactions of elementary particles, is based on several main principles: renormalizability, gauge invariance, and spontaneous gauge-symmetry breaking. The renormalizability principle [2], often considered as something beyond experimental verification, is one of the most important (if not the most important) principles of local quantum field theory. The gauge group of the SM, $SU_c(3) \otimes SU_L(2) \otimes U(1)$, is spontaneously broken to the gauge group $SU_c(3) \otimes U_{em}(1)$ via a finite vacuum expectation value of the scalar field, which leads to the vector bosons $W^{\pm}$ and Z acquiring mass (these vector bosons are the carriers of the weak interaction), while the photon remains massless. After the spontaneous symmetry breaking, one physical degree of freedom remains in the scalar sector, and this is a scalar boson (the Higgs boson), the last undiscovered particle of the SM. We note that the existence of the Higgs boson is a direct consequence of the renormalizability of the SM. The gauge group $SU_c(3)$ describes strong interactions (quantum chromodynamics, or QCD). Eight vector gluons carry the color charges. In view of the asymptotic freedom, the effective QCD coupling constant α_s is small for large transferred momenta, which makes it possible to reliably calculate the cross sections of deep inelastic processes. Quarks and leptons are the fundamental fermions of the SM; left-handed states are doublets with respect to the gauge group $SU_L(2)$, while right-handed states transform as singlets. The SM has three generations of fermions, which differ only in fermion mass.

Despite the amazing achievements of the SM in describing the experimental data, there are many reasons why it cannot be considered the final theory. In this model, the neutrinos are massless particles, with the result that there are no neutrino oscillations. But there presently exist clear indications that neutrino oscillations indeed occur [3]; this follows from the detection of neutrinos born in the atmosphere and from the deficit of solar electron-neutrino flux. The SM can easily be extended by incorporating massive neutrinos into it. But a plausible explanation for the smallness of the neutrino mass is highly nontrivial and, apparently, requires qualitatively new physics beyond the SM. In the SM, the finite vacuum expectation value of the Higgs field generates the masses of the W and Z bosons and the fermions. For the self-consistency of the SM, the Higgs boson mass must be small: $M_H \leqslant 1$ TeV. The radiative corrections to the tree-level mass of the Higgs boson diverge quadratically, namely, $\delta M_H^2 \sim \Lambda^2$, where Λ is a certain ultraviolet cutoff parameter. In

N V Krasnikov, V A Matveev Institute for Nuclear Research, Russian Academy of Sciences,
prosp. 60-letiya Oktyabrya 7a, 117132 Moscow, Russian Federation
Tel. (7-095) 135 21 71, 135 77 60
E-mail: krasniko@ms2.inr.ac.ru

Received 29 October 2003
Uspekhi Fizicheskikh Nauk **174** (7) 697 – 725 (2004)
Translated by E Yankovsky; edited by A M Semikhatov

elementary particle physics, the natural value of the ultraviolet cutoff is usually assumed to be equal to the Planck scale $M_{\rm Pl} \sim 10^{19}$ GeV or the scale of the Grand Unification Theory (GUT), $M_{\rm GUT} \sim 10^{16}$ GeV. Hence, the natural value of the Higgs boson mass must be $O(\Lambda)$. To explain why the Higgs boson mass is so small compared to the Planck scale or the GUT scale, one needs to heavily reduce the radiative corrections to the Higgs boson mass, which is highly nontrivial (the problem of fine-tuning the parameters, or the problem of gauge hierarchies). At present, the supersymmetric solution [4, 5] to the problem of gauge hierarchies is commonly accepted. The supersymmetric explanation predicts that there are particles with masses smaller than or equal to $O(1)$ TeV.

Another possible explanation is based on models involving technicolor [6]. We cannot exclude the possibility that the natural scale of ultraviolet cutoff is $\Lambda \sim O(1)$ TeV. In any case, all proposed solutions to the gauge hierarchy problem predict the existence of new physics on the scale $O(1)$ TeV.[1] Another nontrivial problem is that the SM is unable to predict fermion masses that differ in value by five orders of magnitude (the fermion mass problem).

The research program at the Large Hadron Collider (LHC) [7], which will be the biggest particle accelerator complex ever built, consists of many goals. Among these, the most important are

(1) the discovery of the Higgs boson; and

(2) the discovery of supersymmetry.

The LHC [7] will mainly accelerate two proton beams with the total energy $\sqrt{s} = 14$ TeV. In the low-luminosity stage (the first two to three years of operation), the luminosity is planned to be $L_{\rm low} = 10^{33}$ cm^{-2} s^{-1} with the integrated luminosity $L_{\rm t} = 10$ fb^{-1} per annum. In the high-luminosity stage, the luminosity is planned to be $L_{\rm high} = 10^{34}$ cm^{-2} s^{-1} with the integrated luminosity $L_{\rm t} = 100$ fb^{-1} per annum. The LHC will also accelerate heavy ions, e.g., Pb – Pb ions, with the center-of-mass energy 1150 TeV and luminosities up to 10^{27} cm^{-2} s^{-1}. Proton bunches will smash into each other at four points, where detectors will be located. Two multipurpose detectors are planned to be built, the Compact Muon Solenoid (CMS) [8] and A Toroidal LHC Apparatus (ATLAS) [9], as well as the ALICE detector for studying the physics of heavy ions [10] and the LHC-B detector for studying B-physics [11].

The LHC is set to become operational in 2007. There are many areas of research that will be carried out at the LHC [12], such as

(a) the search for the Higgs boson;

(b) the search for supersymmetry;

(c) the search for new physics outside the scope of the SM and MSSM (Minimal Supersymmetric Standard Model);

(d) B-physics;

(e) heavy-ion physics;

(f) top-quark physics; and

(g) standard physics (QCD and electroweak interactions).

[1] There is an important difference between the prediction that there is a Higgs boson and the prediction that there is new physics in the teraelectronvolt region. Indeed, electroweak models without a Higgs boson are unrenormalizable, with the result that we simply cannot do quantitative calculations with these models at the quantum level. The Standard Model with a small Higgs boson mass is a self-consistent renormalizable local quantum field theory. But staying within it, we cannot explain the fact that the Higgs boson mass is so small (the smallness of the electroweak scale) compared to the Planck scale.

In this article, we review the work done in the search for new physics at the Large Hadron Collider. We describe the progress in the search for the Higgs boson, supersymmetry, and exotics (the new physics beyond the Standard and Minimal Supersymmetric Models) that will be carried out at the LHC. We also describe the main parameters of the CMS [8] and ATLAS [9] detectors (see Section 2). In Section 3, we review the work done in the search for the Higgs boson. In Sections 4 and 5, we review the work done in the search for supersymmetry and exotics. Finally, Section 6 is devoted to concluding remarks.

2. The CMS and ATLAS detectors

One of the most important problems the LHC can help to solve is the study of spontaneous symmetry breaking in the electroweak sector of the Standard Model. Here, the search for the Higgs boson [13] is used as a typical problem for optimization of both the CMS detector and the ATLAS detector. For this search, the detector must be sensitive to the following processes in order to ensure the discovery of the Higgs boson, beginning with the LEP restriction $M_{\rm H} \geqslant 114.4$ GeV [14] up to $m_{\rm H} = 1$ TeV:

(1) $\rm H \to \gamma\gamma$ at $114 \leqslant m_{\rm H} \leqslant 150$ GeV;

(2) $\rm H \to b\bar{b}$ from WH, ZH, and $\rm t\bar{t}H$ by tagging $\rm l^{\pm}$ ($\rm l^{\pm} = e^{\pm}$ or $\mu^{\pm}$) and b-quarks;

(3) $\rm H \to ZZ^* \to 4l^{\pm}$ for 130 GeV $\leqslant m_{\rm H} \leqslant 2m_{\rm Z}$; and

(4) $\rm H \to ZZ \to 4l^{\pm}, 2l^{\pm}2\nu$ for $m_{\rm H} \geqslant 2m_{\rm Z}$.

The second most important task of the LHC project is to discover supersymmetry, i.e., to detect superparticles. Here, the main signature in the search for supersymmetry is left by events with 'lost' transverse energy, which is a consequence of the undetectability of the lightest supersymmetric particle. Hence, there should be rigorous restrictions on the leak-proofness of the detector. Moreover, the search for a new physics different from supersymmetry (new gauge bosons $\rm W'$ and $\rm Z'$, extra dimensions, etc.) requires very precise measurements of lepton momenta and charge identification for transverse momenta up to several teraelectronvolts. Another possible signature of the new physics (composite quarks) requires measuring hadronic jets with transverse momenta up to several teraelectronvolts. An important problem that the LHC project will investigate is the physics of b- and t-quarks.

Hence, the main requirements imposed on the design of the CMS and ATLAS detectors are

(1) good electromagnetic calorimetry used in identifying electrons and photons and in measuring their momenta;

(2) good leak-proof hadronic calorimetry;

(3) an effective high-luminosity tracker for measuring the lepton momenta and tagging b-quarks;

(4) exact measurement of muon momenta for p_T ranging from several gigaelectronvolts to several teraelectronvolts; and

(5) large coverage in the pseudorapidity η $[\eta \equiv -\ln\tan(\theta/2)]$ (with a geometry close to 4π).

2.1 The CMS detector

The CMS detector [8] consists of an inner detector (tracker), electromagnetic calorimeter, hadron calorimeter, and muon spectrometer. A schematic view of the CSM detector is given in Fig. 1.

In the CMS detector, the tracker is placed in a magnetic field of 4 T, which ensures the necessary magnetic field

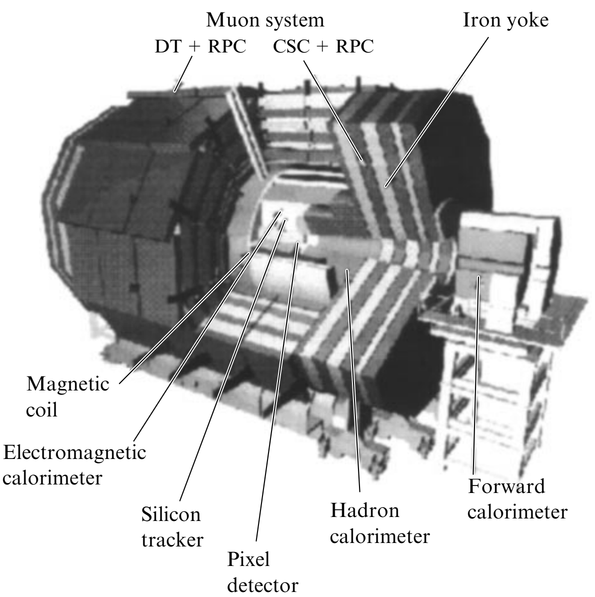

Figure 1. Schematic of the CMS detector.

strength to make exact measurements of the charged particles. The tracker system consists of silicon pixels and silicon stripped detectors. The expected accuracy of measurement in the barrel rapidity region is $\delta p_T/p_T = 0.01$ at $p_T = 100$ GeV. The accuracy of determining the momentum decreases by a factor of approximately five at $p_T = 1$ TeV.

The operation of the electromagnetic calorimeter of the CMS detector is based on the properties of lead tungstate $PbWO_4$, with a pseudorapidity coverage as high as $|\eta| < 3$. The low-luminosity energy resolution is given by the formula

$$\frac{\Delta E}{E} = \frac{0.03}{\sqrt{E}} \oplus 0.005\,. \tag{1}$$

The calculations (see Ref. [8]) lead to the following accuracy in determining the invariant mass of the diphoton pair in the reaction $\mathrm{H} \to \gamma\gamma$ ($m_{\mathrm{H}} = 100$ GeV):

• $\delta m_{\gamma\gamma} = 475$ MeV (low luminosity, $L_{\mathrm{low}} = 10^{33}\ \mathrm{cm}^{-2}\,\mathrm{s}^{-1}$); and

• $\delta m_{\gamma\gamma} = 775$ MeV (high luminosity, $L_{\mathrm{high}} = 10^{34}\ \mathrm{cm}^{-2}\,\mathrm{s}^{-1}$).

The hadron calorimeter encompasses the electromagnetic calorimeter and operates in conjunction with it in measuring the energies and direction of the hadronic jets and in providing the air-tight operation of the detector in order to exactly measure transverse momentum. The pseudorapidity region $|\eta| \leqslant 3$ is covered by the barrel and endcap parts of the hadron calorimeter, which are in the CMS magnetic field. The expected energy resolution for hadronic jets in this region is $\Delta E/E = 1.1/\sqrt{E} \oplus 0.05$. The pseudorapidity region $3.0 \leqslant |\eta| \leqslant 5.0$ is covered by a separate forward calorimeter. The expected energy resolution for hadronic jets in this pseudorapidity region is

$$\frac{\Delta E}{E} = \frac{1.8}{\sqrt{E}} \oplus 0.1\,. \tag{2}$$

At the LHC, the effective detection of muons from the decays of the Higgs boson and the decays of W, Z, and $\mathrm{t\bar{t}}$ requires a larger pseudorapidity coverage. It is expected that muons from pp collisions will provide a pure and clear signature for a broad class of processes involving new physics. Many of these processes are rare, and hence high luminosity is needed to detect them. The muon spectrometer identifies the muons and their exact momenta, which range from several gigaelectronvolts to several teraelectronvolts. The detector barrel covers the pseudorapidity region $|\eta| \leqslant 1.3$. The endcap part covers the pseudorapidity region $1.3 \leqslant |\eta| \leqslant 2.4$. For $0 \leqslant |\eta| \leqslant 2$, the accuracy in determining the muon momenta in the CMS is expected to be 0.015–0.05 at $p_T = 100$ GeV and 0.05–0.2 at $p_T = 1$ TeV.

2.2 The ATLAS detector

The design of the ATLAS detector [9] is similar to that of the CMS detector. It also consists of an inner detector (tracker), an electromagnetic calorimeter, a hadron calorimeter, and a muon spectrometer (Fig. 2).

The inner detector consists of silicon pixels, a silicon stripped detector, and a transitional radiation detector. The accuracy of measuring the momenta of the charged particles is expected to be $\Delta p_T/p_T = 0.2$ at $p_T = 500$ GeV. A liquid-argon electromagnetic calorimeter covers the pseudorapidity region $|\eta| < 3$. The expected energy resolution is

$$\frac{\Delta E}{E} = \frac{0.1}{\sqrt{E}} \oplus 0.007 \quad \text{at} \quad |\eta| \leqslant 2.5\,.$$

The accuracy of determining the diphoton invariant mass is expected to be 1.4 GeV for the Higgs boson mass $m_{\mathrm{H}} = 100$ GeV at $L_{\mathrm{high}} = 10^{34}\ \mathrm{cm}^{-2}\,\mathrm{s}^{-1}$.

The accuracy of measuring the hadronic jets by the hadron calorimeter is expected to be

$$\frac{\Delta E}{E} = \frac{0.5}{\sqrt{E}} \oplus 0.03\,.$$

The forward calorimeter covers the pseudorapidity region $3 \leqslant |\eta| \leqslant 5$ with an energy resolution better than $\Delta E/E = 1/\sqrt{E} \oplus 0.1$. The muon system measures the muon paths,

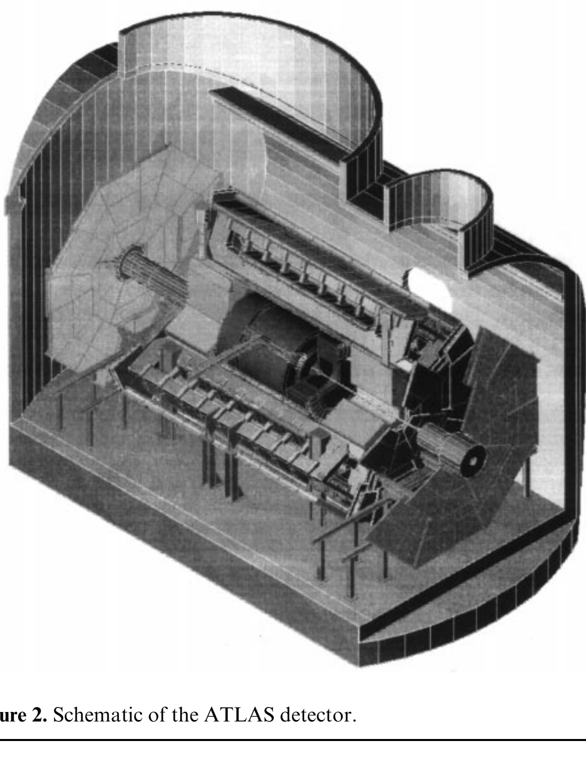

Figure 2. Schematic of the ATLAS detector.

with the muon momenta estimated as $\Delta p_T/p_T = 0.02$ ($p_T = 100$ GeV) and $\Delta p_T/p_T = 0.08$ ($p_T = 1$ TeV) for $|\eta| \leqslant 2.2$.

3. The search for the standard Higgs boson

3.1 Lagrangian of the Standard Model

The SM is a renormalizable model of local quantum field theory describing strong and electroweak interactions. It has the gauge group $\mathrm{SU_c}(3) \otimes \mathrm{SU_L}(2) \otimes \mathrm{U}(1)$ and the minimal Higgs structure consisting of one complex isodoublet of Higgs fields. The spontaneous gauge-group breaking,

$$\mathrm{SU_c}(3) \otimes \mathrm{SU_L}(2) \otimes \mathrm{U}(1) \to \mathrm{SU_c}(3) \otimes \mathrm{U}(1)\,,$$

which occurs because of a finite vacuum expectation value of the Higgs isodoublet, provides the simplest implementation of the Higgs mechanism [13], which generates the masses of the gauge $\mathrm{W}^{\pm}$ and Z bosons, quarks, and leptons. In the SM, as a result of spontaneous electroweak gauge symmetry breaking, only one scalar particle, the Higgs boson, is left in the physical (gauge-invariant) sector. The Lagrangian of the SM consists of several parts [15]:

$$L_{\mathrm{WS}} = L_{\mathrm{YM}} + L_{\mathrm{HYM}} + L_{\mathrm{SH}} + L_{\mathrm{f}} + L_{\mathrm{Yuk}}\,. \tag{3}$$

Here, L_{YM} is the Lagrangian of the gauge fields,

$$L_{\mathrm{YM}} = -\frac{1}{4} F^i_{\mu\nu}(W) F^{\mu\nu}_i(W) - \frac{1}{4} F^{\mu\nu}(W^0) F_{\mu\nu}(W^0) - \frac{1}{4} F^a_{\mu\nu}(G) F^{\mu\nu}_a(G)\,, \tag{4}$$

where $F^i_{\mu\nu}(W)$, $F^a_{\mu\nu}(G)$, and $F_{\mu\nu}(W^0)$ are given by

$$F^i_{\mu\nu}(W) = \partial_\mu W^i_\nu - \partial_\nu W^i_\mu + g_2 \epsilon^{ijk} W^j_\mu W^k_\nu\,, \tag{5}$$

$$F_{\mu\nu}(W^0) = \partial_\mu W^0_\nu - \partial_\nu W^0_\mu\,, \tag{6}$$

$$F^a_{\mu\nu}(G) = \partial_\mu G^a_\nu - \partial_\nu G^a_\mu + g_s f^{abc} G^b_\mu G^c_\nu\,, \tag{7}$$

with W^i_μ and W^0_μ being the $\mathrm{SU_L}(2) \otimes \mathrm{U}(1)$ gauge fields, G^a_μ the gluon fields, and ϵ^{ijk} and f^{abc} the structure constants of the SU(2) and SU(3) gauge groups. The Lagrangian L_{HYM} describes the coupling of the Higgs doublet to the $\mathrm{SU_L}(2) \otimes \mathrm{U}(1)$ gauge fields,

$$L_{\mathrm{HYM}} = (\mathrm{D}_{\mathrm{L}\mu} H)^+ (\mathrm{D}^\mu_{\mathrm{L}} H)\,, \tag{8}$$

where the covariant derivatives are defined as follows:

$$\mathrm{D}_{\mathrm{L}\mu} = \partial_\mu - \mathrm{i} g_1 \frac{Y}{2} W^0_\mu - \mathrm{i} g_2 \frac{\sigma^i}{2} W^i_\mu\,, \tag{9}$$

$$\mathrm{D}_{\mathrm{R}\mu} = \partial_\mu - \mathrm{i} g_1 \frac{Y}{2} W^0_\mu\,, \tag{10}$$

$$\mathrm{D}^q_{\mathrm{L}\mu} = \partial_\mu - \mathrm{i} g_1 \frac{Y}{2} W^0_\mu - \mathrm{i} g_2 \frac{\sigma^i}{2} W^i_\mu - \mathrm{i} g_s t^a G^a_\mu\,, \tag{11}$$

$$\mathrm{D}^q_{\mathrm{R}\mu} = \partial_\mu - \mathrm{i} g_1 \frac{Y}{2} W^0_\mu - \mathrm{i} g_s t^a G^a_\mu\,. \tag{12}$$

Here, g_1 is the U(1) gauge coupling constant, Y is the hypercharge defined by the relation

$$Q = \frac{\sigma_3}{2} + \frac{Y}{2}\,,$$

σ^i are the Pauli matrices, t^a are SU(3) matrices in the fundamental representation, and

$$H = \begin{pmatrix} H_1 \\ H_2 \end{pmatrix}$$

is the Higgs SU(2) isodoublet with $Y = 1$. The Lagrangian L_{SH} describing the self-interaction of the Higgs field isodoublet is

$$L_{\mathrm{SH}} = -V_0(H) = M^2 H^+ H - \frac{\lambda}{2} (H^+ H)^2\,, \tag{13}$$

where $H^+ H = \sum_i H^*_i H_i$ and λ is the Higgs self-coupling constant. The Lagrangian L_{f} describes the interaction of fermions with gauge fields. Fermions transform as doublets or singlets under the gauge group $\mathrm{SU_L}(2) \otimes \mathrm{U}(1)$,

$$R_1 = e_{\mathrm{R}}\,, \quad R_2 = \mu_{\mathrm{R}}\,, \quad R_3 = \tau_{\mathrm{R}}\,, \tag{14}$$

$$L_1 = \begin{pmatrix} \nu \\ e \end{pmatrix}_{\mathrm{L}}, \quad L_2 = \begin{pmatrix} \nu' \\ \mu \end{pmatrix}_{\mathrm{L}}, \quad L_3 = \begin{pmatrix} \nu'' \\ \tau \end{pmatrix}_{\mathrm{L}}, \tag{15}$$

$$R_{qIu} = (q_{Iu})_{\mathrm{R}} \quad (q_{1u} = u\,,\ q_{2u} = c\,,\ q_{3u} = t)\,, \tag{16}$$

$$R_{qid} = (q_{id})_{\mathrm{R}} \quad (q_{1d} = d\,,\ q_{2d} = s\,,\ q_{3d} = b)\,, \tag{17}$$

$$L_{qI} = \begin{pmatrix} q_{Iu} \\ V^{-1}_{Ii} q_{id} \end{pmatrix}_{\mathrm{L}}, \tag{18}$$

where L and R denote the respective left- and right-handed components of the spinors,

$$\psi_{\mathrm{R,L}} = \frac{1 \pm \gamma_5}{2}\, \psi\,, \tag{19}$$

and V_{iI} is the Kobayashi – Maskawa matrix. The neutrinos in the SM are assumed to be left-handed and massless. The Lagrangian L_{f} is

$$L_{\mathrm{f}} = \sum_{k=1}^{3} \left[\mathrm{i} \bar{L}_k \hat{D}_{\mathrm{L}} L_k + \mathrm{i} \bar{R}_k \hat{D}_{\mathrm{R}} R_k + \mathrm{i} \bar{L}_{qk} \hat{D}^q_{\mathrm{L}} L_{qk} + \mathrm{i} \bar{R}_{qku} \hat{D}^q_{\mathrm{R}} R_{qku} + \mathrm{i} \bar{R}_{qkd} \hat{D}^q_{\mathrm{R}} R_{qkd} \right], \tag{20}$$

where $\hat{D}_{\mathrm{L}} = \gamma^\mu D_{\mathrm{L}\mu}$, $\hat{D}_{\mathrm{R}} = \gamma^\mu D_{\mathrm{R}\mu}$, $\hat{D}^q_{\mathrm{L}} = \gamma^\mu D^q_{\mathrm{L}\mu}$, and $\hat{D}^q_{\mathrm{R}} = \gamma^\mu D^q_{\mathrm{R}\mu}$. The Lagrangian L_{Yuk} is responsible for generation of the fermion mass terms. For massless neutrinos, the Yukawa coupling of the fermions to the Higgs field isodoublet has the form

$$L_{\mathrm{Yuk}} = -\sum_{k=1}^{3} \left[h_{lk} \bar{L}_k H R_k + h_{dk} \bar{L}_{dk} H R_{dk} + h_{uk} \bar{L}_{uk} (\mathrm{i} \sigma^2 H^*) R_{uk} \right] + \mathrm{h.c.} \tag{21}$$

For $M^2 > 0$, the potential

$$V_0(H) = -M^2 H^+ H + \frac{\lambda}{2} (H^+ H)^2$$

leads to spontaneous symmetry breaking. The doublet H acquires the finite vacuum expectation value

$$\langle H \rangle = \begin{pmatrix} 0 \\ \dfrac{v}{\sqrt{2}} \end{pmatrix}, \tag{22}$$

where $v = 246$ GeV. In the unitary gauge, there can be no unphysical Goldstone fields, with the result that the isodoublet of the Higgs fields depends only on a single physical scalar field (the Higgs field)

$$H(x) = \left(\begin{array}{c} 0 \\ \dfrac{v}{\sqrt{2}} + \dfrac{H(x)}{\sqrt{2}} \end{array} \right) . \tag{23}$$

Because of spontaneous gauge symmetry breaking, the gauge electroweak fields, except for the photon, acquire mass. The diagonalization of the mass matrix yields

$$W^{\pm}_{\mu} = \frac{1}{\sqrt{2}} (W^1_{\mu} \mp W^2_{\mu}) , \qquad M_{\mathrm{W}} = \frac{1}{2}\, g_2 v , \tag{24}$$

$$Z_{\mu} = \frac{1}{\sqrt{g_2^2 + g_1^2}} (g_2 W^3_{\mu} - g_1 W^0_{\mu}) , \qquad M_{\mathrm{Z}} = \frac{1}{2} \sqrt{g_2^2 + g_1^2}\, v , \tag{25}$$

$$A_{\mu} = \frac{1}{\sqrt{g_2^2 + g_1^2}} (g_1 W^3_{\mu} + g_2 W^0_{\mu}) , \qquad M_A = 0 , \tag{26}$$

where $W^{\pm}_{\mu}$ and Z_{μ} are the respective fields of charged and neutral electroweak bosons and A_{μ} is the photon field. At this point, it is convenient to introduce the rotation angle θ_{W} between (W^3, W^0) and (Z, A), commonly known as the Weinberg angle, as

$$\sin\theta_{\mathrm{W}} \equiv \frac{g_1}{\sqrt{g_1^2 + g_2^2}} . \tag{27}$$

The experimental value of the Weinberg angle is such that $\sin^2\theta_{\mathrm{W}} \approx 0.23$ [16]. The formula for the electron charge e is

$$e = \frac{g_2 g_1}{\sqrt{g_2^2 + g_1^2}} . \tag{28}$$

At the tree level, the Higgs boson mass is given by

$$m_{\mathrm{H}} = \sqrt{2}\, M = \sqrt{\lambda}\, v . \tag{29}$$

In the unitary gauge, the Lagrangian L_{HYM} is given by

$$L_{\mathrm{HYM}} = \frac{1}{2}\, \partial^{\mu} H \partial_{\mu} H + M_{\mathrm{W}}^2 \left(1 + \frac{H}{v}\right)^2 W^+_{\mu} W^{\mu} + + \frac{1}{2}\, M_Z^2 \left(1 + \frac{H}{v}\right)^2 Z^{\mu} Z_{\mu} , \tag{30}$$

while

$$L_{\mathrm{Yuk}} = - \sum_i m_{\psi_i} \left(1 + \frac{H}{v}\right) \bar{\psi}_i \psi_i . \tag{31}$$

3.2 Limits on the Higgs boson mass

According to the experiments done at the LEP accelerator, the lower limit on the Higgs boson mass in the SM is $m_{\mathrm{H}} \geqslant 114.4$ GeV with a 95% confidence [14]. An analysis of precision measurements of the electroweak observables leads to the upper bound $m_{\mathrm{H}} \leqslant 193$ GeV [17] (with 95% confidence) on the Higgs boson mass, and hence the Higgs boson should be fairly light in the SM.

An upper limit on the Higgs boson mass can be placed by requiring that the effective Higgs self-coupling constant have no Landau poles [18] and that the electroweak vacuum be stable [19]. The idea of deriving the limit from the condition that there should be no Landau pole is as follows (see Ref. [18]). We suppose that the Standard Model is valid up to the scale Λ. The requirement that there be no Landau pole in the effective coupling constant $\bar{\lambda}(E)$ of the self-coupling of the Higgs fields at energies $E \leqslant \Lambda$ can be used to place an upper limit on the Higgs boson mass. For Λ equal to 10^3, 10^4, 10^6, 10^8, 10^{12}, and 10^{14} GeV and $m_{\mathrm{t}}^{\mathrm{pole}} = 175$ GeV, we can find the respective limits on the Higgs boson mass $m_{\mathrm{H}} \leqslant 400$, 300, 240, 200, 180, 170, and 160 GeV (see Ref. [12]). The limit from the vacuum stability requirement (see Ref. [19]) follows from the requirement that the electroweak minimum of the effective potential be the deepest minimum of the effective potential for $|H| \leqslant \Lambda$. For $|H| \gg v$, the mass terms in the effective potential can be ignored compared to the term describing the self-coupling of the scalar fields. The vacuum stability requirement then means that the effective coupling constant of the self-interaction of the Higgs isodoublet $\bar{\lambda}(\mu)$ is nonnegative, $\bar{\lambda}(\mu) \geqslant 0$, for $\mu \leqslant \Lambda$. For Λ equal to 10^3, 10^4, 10^6, 10^8, 10^{12}, and 10^{14} GeV and $m_{\mathrm{t}}^{\mathrm{pole}} = 175$ GeV, the lower limit on the Higgs boson mass is numerically given by $m_{\mathrm{H}} \geqslant 78$, 101, 121, 129, 136, and 137 GeV, respectively (see Ref. [12]). In the minimal supersymmetric model, taking the radiative corrections into account leads to an increase in the mass of the lightest Higgs boson [20] up to 135 GeV [21]. As noted in Ref. [22], by measuring the Higgs boson mass, one can distinguish between the SM and MSSM or at least estimate the scale Λ beginning at which one can expect deviations from the SM to come into play.

3.3 Higgs boson decays

The tree-level Higgs boson coupling to gauge bosons and fermions can be found from Lagrangians (30) and (31). Of these, $\mathrm{HW^+W^-}$, HZZ, and $\mathrm{H}\bar{\psi}\psi$ are phenomenologically the most important. The Higgs boson decay width into a fermion–antifermion pair is [15]

$$\Gamma(\mathrm{H} \to \psi\bar{\psi}) = \frac{G_{\mathrm{F}} m_{\psi}^2 m_{\mathrm{H}} N_{\mathrm{c}}}{4\pi\sqrt{2}} \left(1 - \frac{4 m_{\psi}^2}{m_{\mathrm{H}}^2}\right)^{3/2} , \tag{32}$$

where N_{c} is the number of color fermion states. For $m_{\mathrm{H}} \leqslant 2m_{\mathrm{W}}$, the Higgs boson decays mainly (with approximately 90% probability) into a b-quark–antiquark pair and with approximately 7% probability, into a τ-lepton–antilepton pair. Allowing for QCD corrections amounts to replacing the pole mass of the b-quark by the effective mass $\bar{m}_{\mathrm{b}}(m_{\mathrm{H}})$ in Eqn (32). We note that the relation between the perturbative pole mass m_{Q} of the quark and the $\overline{MS}$ effective quark mass $\bar{m}_{\mathrm{Q}}(m_{\mathrm{Q}})$ is [23]

$$m_{\mathrm{Q}} = \left[1 + \frac{4}{3}\, \frac{\alpha_{\mathrm{s}}(m_{\mathrm{Q}})}{\pi} + K_{\mathrm{Q}} \left(\frac{\alpha_{\mathrm{s}}(m_{\mathrm{Q}})}{\pi}\right)^2\right] \bar{m}_{\mathrm{Q}}(m_{\mathrm{Q}}) , \tag{33}$$

where numerically $K_{\mathrm{t}} \approx 10.9$, $K_{\mathrm{b}} \approx 12.4$, and $K_{\mathrm{c}} \approx 13.4$.

For $m_{\mathrm{H}} \geqslant 2M_{\mathrm{W}}$, the Higgs boson decays into gauge bosons with the decay widths

$$\Gamma(\mathrm{H} \to \mathrm{W^+W^-}) = \frac{G_{\mathrm{F}} m_{\mathrm{H}}^3}{32\pi\sqrt{2}} (4 - 4a_{\mathrm{W}} + 3a_{\mathrm{W}}^2)(1 - a_{\mathrm{W}})^{1/2} , \tag{34}$$

$$\Gamma(\mathrm{H} \to \mathrm{Z^0 Z^0}) = \frac{G_{\mathrm{F}} m_{\mathrm{H}}^3}{64\pi\sqrt{2}} (4 - 4a_{\mathrm{Z}} + 3a_{\mathrm{Z}}^2)(1 - a_{\mathrm{Z}})^{1/2} , \tag{35}$$

where $a_{\mathrm{W}} = 4M_{\mathrm{W}}^2/m_{\mathrm{H}}^2$ and $a_{\mathrm{Z}} = 4M_Z^2/m_{\mathrm{H}}^2$. For the heavy Higgs boson ($2m_{\mathrm{Z}} \leqslant m_{\mathrm{H}} \leqslant 800$ GeV), the decay into gauge bosons is predominant. For instance, for $m_{\rm H} \gg 2m_{\rm Z}$, we have the asymptotic formula

$$\Gamma(\mathrm{H} \to \mathrm{W}^+\mathrm{W}^-) = 2\Gamma(\mathrm{H} \to \mathrm{ZZ}) \simeq \frac{G_{\rm F} m_{\rm H}^3}{8\pi\sqrt{2}} . \quad (36)$$

The dependence of the $m_{\rm H}^3$-type follows from the existence of the W and Z boson states with the transverse polarization. We note that the width of the Higgs boson decay into a fermion–antifermion pair increases only linearly with the Higgs boson mass. Therefore, for Higgs boson masses much larger than $2m_{\rm Z}$, the total width of the Higgs boson decay is mainly determined by the width of the decay into gauge bosons, and the Higgs boson decay into $\mathrm{t\bar{t}}$ can be ignored. We have the heavy Higgs boson decay width

$$\Gamma_{\rm tot}(\mathrm{H}) \simeq 0.48\ \mathrm{TeV}\left(\frac{m_{\rm H}}{1\ \mathrm{TeV}}\right)^3 . \quad (37)$$

Off-shell decays into gauge bosons are important from the phenomenological standpoint. The width of such a decay is given by the formula [24]

$$\Gamma(\mathrm{H} \to \mathrm{VV}^*) = \delta_{\rm V}\, \frac{3G_{\rm F}^2 M_{\rm V}^4 m_{\rm H}}{16\pi^3}\, R\left(\frac{M_{\rm V}^2}{m_{\rm H}^2}\right), \quad (38)$$

where V = W and Z,

$$\delta_{\rm W} = 1\,, \qquad \delta_{\rm Z} = \frac{7}{12} - \frac{10}{9}\sin^2\theta_{\rm W} + \frac{40}{27}\sin^4\theta_{\rm W}\,,$$

$$R(x) = 3\,\frac{1-8x+20x^2}{\sqrt{4x-1}}\arccos\frac{3x-1}{2x^{3/2}} - \frac{1-x}{2x}(2-13x+47x^2) - \frac{3}{2}(1-6x+4x^2)\log x\,, \quad (39)$$

with $x = M_{\rm V}^2/m_{\rm H}^2$. For a Higgs boson that is slightly heavier than two gauge bosons, the width of the decay into two off-shell gauge bosons plays an important role. The corresponding formulas can be found in Ref. [24].

We note that there are a number of important interactions of the Higgs boson that are absent from the tree level but appear at the one-loop level. Among these, the interaction of the Higgs boson with gluons and photons plays a very important role in the search for the Higgs boson in supercolliders. The one-loop interaction of the Higgs boson with two gluons emerges because of a virtual top-quark exchange in a loop [25] and leads to the effective Lagrangian

$$L_{\rm Hgg}^{\rm eff} = \frac{8g_2\alpha_{\rm s}}{24\pi m_{\rm W}}\, HG_{\mu\nu}^a G^{a\mu\nu}\,. \quad (40)$$

In the lowest-order perturbation theory, the corresponding decay width is [24]

$$\Gamma_{\rm LO}(\mathrm{H} \to \mathrm{gg}) = \frac{G_{\rm F}^2\alpha_{\rm s}^2 m_{\rm H}^3}{36\sqrt{2}\,\pi^3}\left|\sum_{\rm Q} A_{\rm Q}^{\rm H}(\tau_{\rm Q})\right|^2 , \quad (41)$$

$$A_{\rm Q}^{\rm H}(\tau) = \frac{3}{2}\,\tau\big[1 + (1-\tau)f(\tau)\big]\,, \quad (42)$$

$$f(\tau) = \arcsin^2\frac{1}{\sqrt{\tau}}\,, \qquad \tau \geqslant 1\,, \quad (43)$$

$$f(\tau) = -\frac{1}{4}\left(\log\frac{1+\sqrt{1-\tau}}{1-\sqrt{1-\tau}} - \mathrm{i}\pi\right)^2 , \qquad \tau < 1\,. \quad (44)$$

The parameter $\tau_{\rm Q} = 4m_{\rm Q}^2/m_{\rm H}^2$ is determined by the pole mass $M_{\rm Q}$ of the heavy quark in the loop. For such a quark, $A_{\rm Q}^{\rm H}(\tau_{\rm Q}) \to 1$. The radiative QCD corrections prove to be very large [26], precisely, the decay width increases by 60–70% in the most interesting mass range 100 GeV $\leqslant m_{\rm H} \leqslant$ 500 GeV. Three-loop QCD corrections have been calculated in the heavy top-quark limit and have been found to increase the decay width by approximately 10% [27].

Also very important is the one-loop induced Higgs boson interaction with two photons. The width of the Higgs boson decay into two photons is given by the formula [24]

$$\Gamma(\mathrm{H} \to \gamma\gamma) = \frac{G_{\rm F}\alpha^2 m_{\rm H}^3}{128\sqrt{2}\,\pi^3}\left|\sum_{\rm f} N_{\rm cf} e_{\rm f}^2 A_{\rm f}^{\rm H}(\tau_{\rm f}) + A_{\rm W}^{\rm H}(\tau_{\rm W})\right|^2 , \quad (45)$$

where

$$A_{\rm f}^{\rm H}(\tau) = 2\tau\big[1 + (1-\tau)f(\tau)\big]\,, \quad (46)$$

$$A_{\rm W}^{\rm H}(\tau) = -\big[2 + 3\tau + 3\tau(2-\tau)f(\tau)\big]\,, \quad (47)$$

and $\tau_i = 4M_i^2/m_{\rm H}^2$, with $i = \mathrm{f, W}$. The function $f(\tau)$ is defined in Eqns (43) and (44). The W-boson loop provides the main contribution in the intermediate mass range. The corresponding diagrams for the Higgs boson decay widths are presented in Fig. 3.

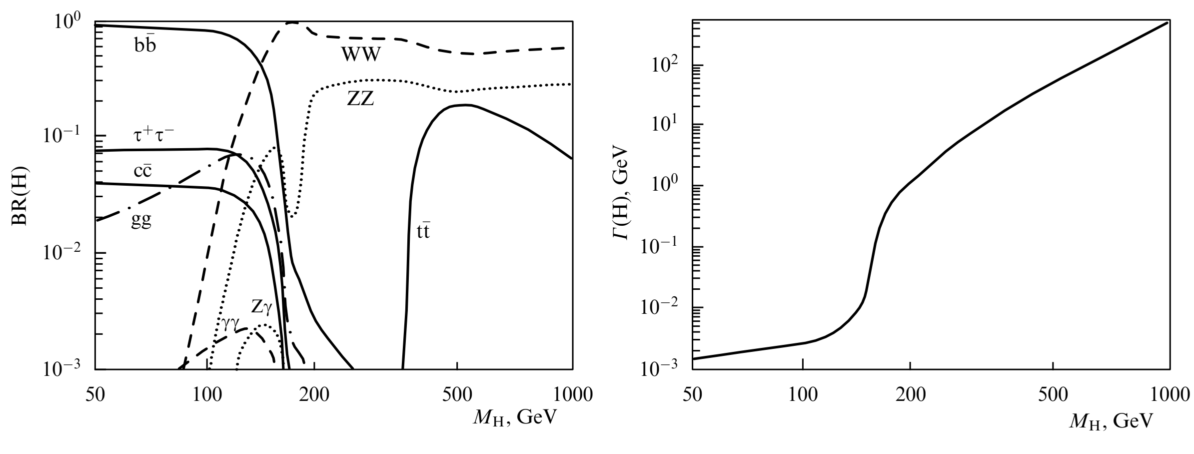

Figure 3. Branching ratios and the decay width for the Higgs boson.

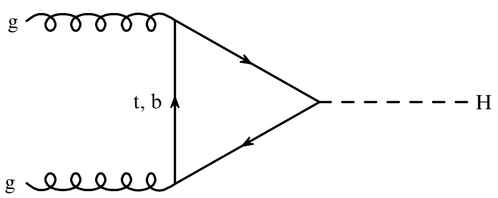

Figure 4. Diagram demonstrating the contribution to Higgs boson production in gluon – gluon collisions.

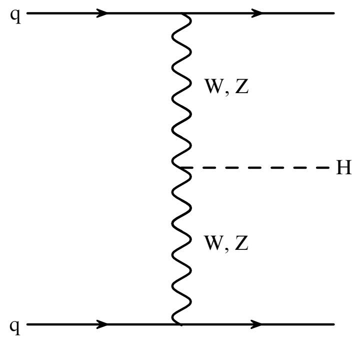

Figure 5. Diagram demonstrating the contribution to $qq \to qqV^*V^* \to qqH$.

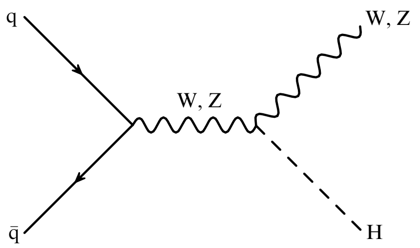

Figure 6. Diagram demonstrating the contribution to $q\bar{q} \to V^* \to VH$.

3.4 Higgs boson production at the LHC

The typical processes in which Higgs bosons are produced and which can be used at the LHC are [28, 24]:

- gluon fusion: $gg \to H$ (Fig. 4);
- WW and ZZ fusion: $W^+W^-, ZZ \to H$ (Fig. 5);
- 'Higgs-strahlung' of W and Z: $q\bar{q}W, Z \to W, Z + H$ (Fig. 6); and
- 'Higgs-strahlung' of the top quark: $q\bar{q}, gg \to t\bar{t} + H$ (Fig. 7).

The mechanism of gluon fusion plays a dominant role in the entire range of allowed masses, while WW/ZZ fusion becomes more and more important as the Higgs boson mass increases. The last two mechanisms are important only for light Higgs bosons.

The gluon-fusion mechanism [25]

$$pp \to gg \to H \tag{48}$$

is the most important mechanism of Higgs boson production up to 1-TeV masses. The interaction of the Higgs boson with gluons emerges at the one-loop level as a result of a top-quark exchange in the loop. In the leading-order perturbation theory, the partonic cross section is proportional to the width of Higgs boson decay into two gluons,

$$\sigma_{\rm LO}(gg \to H) = \sigma_0 m_H^2 \delta(s - m_H^2)\,, \tag{49}$$

$$\sigma_0 = \frac{\pi^2}{8m_H^2}\,\Gamma_{\rm LO}(H \to gg)\,, \tag{50}$$

where $\tau_Q = 4M_Q^2/m_H^2$, s denotes the squared energy of the partonic system, and the form factor $A_Q^H(\tau_Q)$ is defined in Eqns (42) – (44). The hadronic cross section can be written as

$$\sigma_{\rm LO}(pp \to H) = \sigma_0 \tau_H \frac{dL^{gg}}{d\tau_H}\,, \tag{51}$$

where $dL^{gg}/d\tau_H$ denotes the gg luminosity of the pp collider and $\tau_H = m_H^2/s$. The QCD corrections to the one-loop gluon-fusion cross section are positive and highly essential [24, 26, 27] — they stabilize the theoretical predictions concerning the cross section under variations in the renormalization and factorization scales. The theoretically predicted behavior of the Higgs boson production cross section for the LHC is shown in Fig. 8. The cross section decreases with increasing the Higgs boson mass on the whole because of the decrease in the gg partonic luminosity with increasing the invariant mass. The process that is second in importance for Higgs boson production at the LHC is the fusion of vector bosons: $ZZ, W^+W^- \to H$. For large Higgs boson masses, this mechanism competes with the gluon fusion mechanism, while in the intermediate mass region, the cross section is approximately ten times smaller. The respective formulas can be found in Ref. [29]. The mechanism based on the reaction $q\bar{q} \to V^* \to VH$ $(V = W, Z)$ plays an important role in the search for the light Higgs boson at the LHC. Although the cross section of this reaction is approximately a hundred times smaller than the gluon-fusion cross section, leptonic decays of vector bosons are extremely useful in separating signal from background. The corresponding formulas for the cross section can be found in Ref. [30].

The $gg, q\bar{q} \to t\bar{t}H$ process is important for small Higgs boson masses. The analytic expression for the partonic cross section is extremely cumbersome [31]. We also note that the Higgs-strahlung from a top quark makes it possible to experimentally determine the $Ht\bar{t}$ Yukawa coupling con-

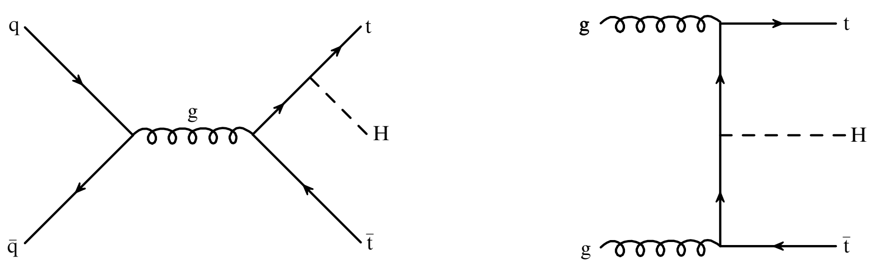

Figure 7. Diagrams demonstrating the contribution to $q\bar{q}/gg \to Ht\bar{t}$.

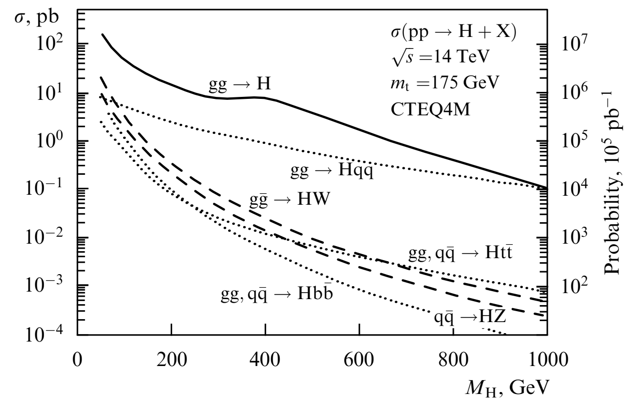

Figure 8. Higgs boson production cross section for different mechanisms as a function of the Higgs boson mass [24].

stant. The cross section $\sigma(\mathrm{pp} \to \mathrm{t\bar{t}H} + \ldots)$ is directly proportional to the square of the Yukawa coupling constant of the top-quark – Higgs boson interaction.

Clearly, three classes of processes can be distinguished here. Gluon fusion is a universal process dominating over the entire range of Higgs boson masses. The Higgs-strahlung from electroweak bosons or top quarks is important for small Higgs boson masses. By contrast, the WW/ZZ fusion mechanism becomes more and more important with increasing the Higgs boson mass.

3.5 $\mathrm{H} \to \gamma\gamma$

One of the main reactions in the search for the Higgs boson at the LHC is

$$\mathrm{pp} \to (\mathrm{H} \to \gamma\gamma) + \ldots, \qquad (52)$$

which is especially promising [32] in the search for the Higgs boson in the most interesting mass range

$$100 \leqslant m_{\mathrm{H}} \leqslant 150 \text{ GeV}.$$

The signal significance $S = N_S/\sqrt{N_B}$ for the CMS detector is estimated to be 6.6 (9) for $m_{\mathrm{H}} = 110\,(130)$ GeV at a low luminosity of 30 fb^{-1} and 10 (13) for $m_{\mathrm{H}} = 110\,(130)$ GeV and a high luminosity of 100 fb^{-1} [8]. The general conclusion was that at the level of 5σ, the CMS detector allows detecting a Higgs boson[2] in the interval $95 \leqslant m_{\mathrm{H}} \leqslant 145$ GeV in the low-luminosity stage, while in the high-luminosity stage, the corresponding interval for Higgs boson masses is $85 \leqslant m_{\mathrm{H}} \leqslant 150$ GeV (Fig. 9). The results of ATLAS simulations coincide with the corresponding results of calculations done for the CMS detector (in terms of signal significance) with an accuracy up to 30% [34].

3.6 $\mathrm{H} \to \gamma\gamma$ plus hadronic jets

The idea of searching for Higgs boson signals associated with hadronic jets was put forward in Ref. [35], where the matrix elements of the signal subprocesses $\mathrm{gg} \to \mathrm{g} + \mathrm{H}$, $\mathrm{gq} \to \mathrm{q} + \mathrm{H}$, and $\mathrm{q\bar{q}} \to \mathrm{g} + \mathrm{H}$ were calculated in the leading perturbation-theory order in the strong coupling constant, α_s^3. For the Higgs boson mass in the $100 \leqslant M_{\mathrm{H}} \leqslant 150$-GeV range and the integrated luminosity 10 fb^{-1}, this channel produces several dozen signal events, with the number of background events being only two or three times larger [35]. The signal significance is $N_S/\sqrt{N_B} \sim 4$, 5, and 4 for $M_{\mathrm{H}} = 100$, 120, and 140 GeV, respectively, which is especially promising for detecting a light Higgs boson in the low-luminosity stage. These results also imply that in the high-luminosity stage with the integrated luminosity 100 fb^{-1}, the signal significance is roughly 12.

3.7 $\mathrm{H} \to \mathrm{WW}^* \to \mathrm{l}^+\nu\mathrm{l}'^-\nu'$

The reaction $\mathrm{pp} \to \mathrm{H} \to \mathrm{WW}^* \to \mathrm{l}^+\nu\mathrm{l}'^-\bar{\nu}'$ [36] ensures the detection of the Higgs boson in the least accessible range of masses from 155 to 180 GeV. It is important that the reaction $\mathrm{H} \to \mathrm{WW}^* \to \mathrm{l}^+\nu\mathrm{l}'^-\nu$ allows detecting a Higgs boson with a mass close to 170 GeV, where the $\mathrm{H} \to 4\mathrm{l}$ branching ratio is especially small and the use of a four-lepton signature does not help, in the low-luminosity stage at least. The use of this reaction does not impose rigorous constraints on the detector operation and requires a relatively low integrated luminosity of approximately 5 fb^{-1} for Higgs boson detection.

The results in Ref. [36] show that this reaction not only ensures the detection of a Higgs boson with a mass in the 155 – 180-GeV range with $S/B \geqslant 0.35$ but also helps in the detection of a Higgs boson with a mass in the 120 – 500-GeV range. The results of the calculations in Ref. [38], which used the total simulation of the detector response, corroborate the results in Ref. [36].

3.8 $\mathrm{pp} \to \mathrm{H} + 2$ forward jets

The mechanism of vector boson fusion $\mathrm{qq} \to \mathrm{qqH}$ leads to energetic jets in forward and backward directions and to the absence of color exchange in the hard process [39 – 41], which makes it possible to strongly suppress the background of $\mathrm{t\bar{t}}$, QCD jets, and W and Z production and to balance the smallness of the Higgs boson production cross section in the mechanism of vector boson fusion compared to the mechanism of gluon fusion $\mathrm{gg} \to \mathrm{H}$. We note that the process of Higgs boson production in the vector boson fusion mechanism with the tagging of jets propagating within the small-azimuthal-angle region was examined earlier in Ref. [42] in the reactions $\mathrm{H} \to \mathrm{ZZ} \to 4\mathrm{l}, 2\mathrm{l}2\nu$. The reaction $\mathrm{pp} \to (\mathrm{H} \to \gamma\gamma) + 2$ forward jets was studied at the lepton level in Ref. [39] and with the rapid simulation of the CMS detector in Ref. [43]. The main conclusion in Ref. [43] is that the signal significance $S = N_S/\sqrt{N_B} = 5$ is attained at the luminosity 25 – 35 fb^{-1} for $m_{\mathrm{H}} = 115$ – 145 GeV. An additional advantage of this signature is that the signal-to-background ratio is $S/B \sim 1$ compared to $S/B \sim 1/15$ for the inclusive reaction $\mathrm{pp} \to (\mathrm{H} \to \gamma\gamma) + \ldots$.

The signature $\mathrm{H} \to \mathrm{W^*W} \to \mathrm{e}^{\pm}\mu^{\mp}p_T^{\mathrm{mis}}$ in the mechanism of vector boson fusion with forward-jet tagging has been studied in Ref. [40]. Spin correlations, which lead to small angles between the charged leptons, were used to suppress background events. This mode ensures the detection of Higgs bosons with masses $m_{\mathrm{H}} \geqslant 120$ GeV.

3.9 $\mathrm{H} \to \mathrm{ZZ}^*(\mathrm{ZZ}) \to 4$ leptons

The decay channel $\mathrm{H} \to \mathrm{ZZ}^* \to 4\mathrm{l}$ is the most promising for detecting a Higgs boson with a mass in the 130 – 180-GeV

[2] It must be noted at this point that a more appropriate characteristic for future experiments [33] is the probability of discovery, i.e., the probability that the number of events N_{ev} measured in the experiment will be such that the probability that the standard physics reproduces N_{ev} events is lower than 5.7×10^{-7} (5σ). For instance, in the search for the standard Higgs boson with $m_{\mathrm{H}} = 110$ GeV and the luminosity $L = 30$ fb^{-1} (20 fb^{-1}), the standard signal significance is 6.6 (5.4). In the language of probabilities, this means that [33] the CMS detector will make it possible to detect a Higgs boson at a level $\geqslant 5\sigma$ with a 96 (73)% probability.

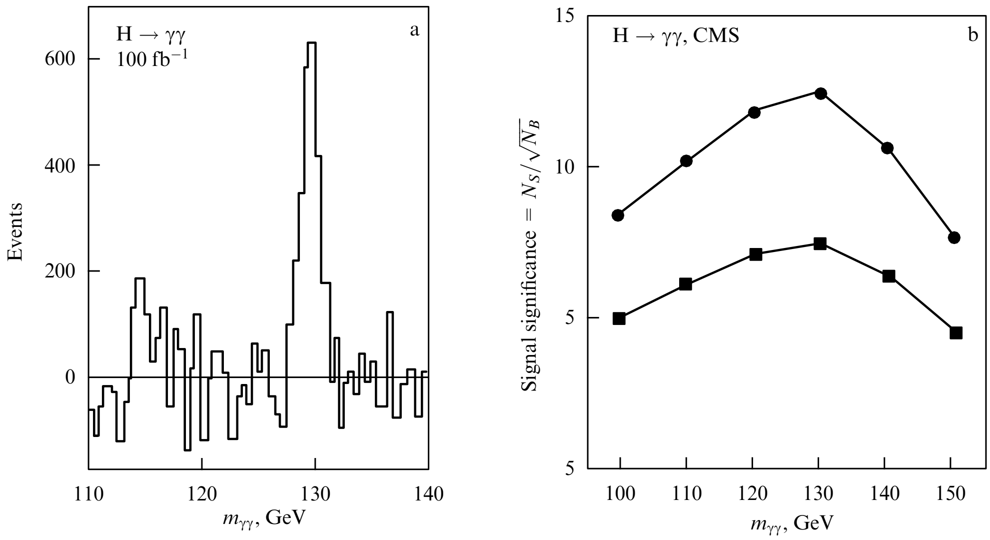

Figure 9. Mass peak (a) and signal significance (b) for $H \to \gamma\gamma$: ■, low luminosity (30 fb^{-1}); and ●, high luminosity (100 fb^{-1}) [8].

range. Below $2M_Z$, the number of events is small, and reducing background events is complicated because one Z is off the mass shell. Within this mass range, the Higgs boson decay width is small, $\Gamma_H < 1$ GeV, and the experimentally observed width is fully determined by the detector resolution. The signal significance is proportional to the square root of the resolution of the four-lepton invariant mass ($S = N_S/\sqrt{N_B}$, $N_{S,B} \sim \sigma_{4l}$), and it is therefore highly important to exactly determine the energy/momentum of the lepton.[3] The discovery potentials of the CMS and ATLAS detectors for the $H \to ZZ^* \to 4l$ reaction were compared by Poggioli [44], whose main conclusion was that in terms of signal significances, the discovery potentials of the CMS and ATLAS detectors are roughly the same (to within 20%). For the mass range $130 \leqslant m_H \leqslant 180$ GeV and for the integrated luminosity 100 fb^{-1}, the CMS detector [32] allows detecting a Higgs boson with a signal significance $\geqslant 5\sigma$ within all mass ranges, except for a narrow region near 170 GeV, where $\sigma \times \mathrm{BR}$ is at its maximum due to the opening of the $H \to WW$ channel and a decrease in the $H \to ZZ^*$ branching ratio.

For the mass range $180 \leqslant m_H \leqslant 600$ GeV, the four-lepton signature is considered the most promising for the discovery of the Higgs boson at the LHC, because the expected number of events is sufficiently large and the background level is low. The main background to the $H \to ZZ \to 4l^{\pm}$ process is the irreducible ZZ production from $q\bar{q} \to ZZ$ and $gg \to ZZ$. The background from $t\bar{t}$ and $Zb\bar{b}$ is fairly small and can be diminished by a cutoff in the Z-boson mass. The use of this signature will make it possible to detect a Higgs boson with a signal significance $\geqslant 5\sigma$ up to $m_H \approx 400$ GeV at the luminosity 10 fb^{-1} and up to $m_H \approx 650$ GeV at the luminosity 100 fb^{-1} [32].

3.10 WH($t\bar{t}$H) → γγ + lepton + ...

The $WH \to l\gamma\gamma + X$ and $t\bar{t}H \to l\gamma\gamma + X$ final states are other promising signatures in the search for the Higgs boson. Here, the production cross section is smaller than that of the inclusive reaction $H \to \gamma\gamma$ by a factor of approximately 30. However, the use of an isolated lepton from the W and t decays makes it possible to achieve strong background reduction. For the integrated luminosity 165 fb^{-1} in both channels, $pp \to WH$ and $pp \to t\bar{t}H$, within the range of diphoton invariant masses $M_H - 1\ \mathrm{GeV} \leqslant M_{\gamma\gamma} \leqslant M_H + 1$ GeV, we have roughly 100 signal events at $M_H = 120$ GeV and about 20 background events [35].

3.11 $t\bar{t}H \to t\bar{t}b\bar{b}$

The large $H \to b\bar{b}$ branching at $m_H \leqslant 150$ GeV can be used in the associated $t\bar{t}H$-production channel. Extracting a Higgs boson signal from the $t\bar{t}H \to l^{\pm}\nu q\bar{q}b\bar{b}b\bar{b}$ channel requires tagging four b-jets, reconstructing the Higgs boson mass from two b-jets, and identifying two top quarks. The use of this channel will make it possible to detect a light Higgs boson with a mass $m_H \leqslant 120$ GeV [32].

3.12 H → WW → llνν, H → WW → lνjj, and H → ZZ → lljj

The decay $H \to ll\nu\nu$ has a branching six times larger than the decay $H \to 4l^{\pm}$. The main background comes from ZZ, ZW, $t\bar{t}$, and Z + jets. By using this channel one can detect the Higgs boson [8, 34] within the mass range $400 \leqslant m_H \leqslant (800-900)$ GeV at the integrated luminosity 100 fb^{-1}.

The channels $H \to WW \to l\nu jj$ and $H \to ZZ \to lljj$ are very important for the region near $m_H \approx 1$ TeV, in which the large branching of $W, Z \to q\bar{q}$ is used. Two hard hadronic jets from the hadron decay W/Z plus one or two high-p_T leptons from the W/Z decays are used to reduce the background.

The main background is from Z + jets, W + jets, ZW, WW, and $t\bar{t}$. At $m_H \approx 1$ TeV, the Higgs boson is extremely wide ($\Gamma_H \approx 0.5$ TeV) and the WW/ZZ-fusion mechanism yields about 50% of the total production cross section, and therefore the use of signatures with two forward jets is essential. The decays $H \to WW \to l\nu jj$ and $H \to ZZ \to lljj$ make it possible to detect a heavy Higgs boson with a mass up to 1 TeV at the integrated luminosity 100 fb^{-1} [8, 34].

3.13 Studies of the properties of the Higgs boson

In the most interesting range of Higgs boson masses, $114.4 \leqslant m_H \leqslant 193$ GeV, the decays $H \to \gamma\gamma$ and $H \to ZZ/ZZ^* \to 4l^{\pm}$ ensure an accuracy of determining the mass

[3] Typical resolutions in this range of Higgs boson masses are $\sigma_{4\mu} \approx 1$ GeV and $\sigma_{4e} \approx 1.5$ GeV (CMS) [8], and $\sigma_{4\mu} \approx 1.6$ GeV and $\sigma_{4e} \approx 1.6$ GeV (ATLAS) [9].

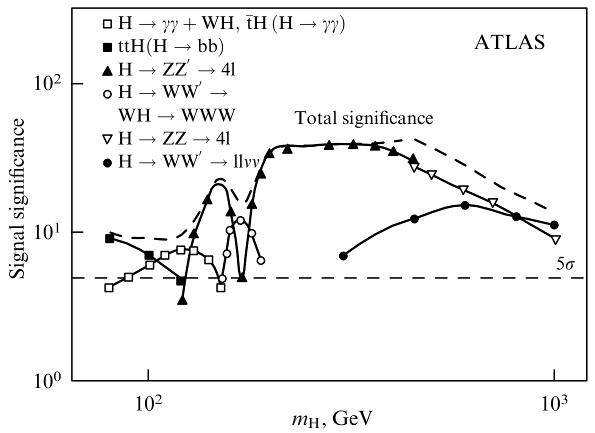

Figure 10. Potential of discovery of the SM Higgs boson for an integrated luminosity of 100 fb^{-1} in the ATLAS detector without the k-factor [34].

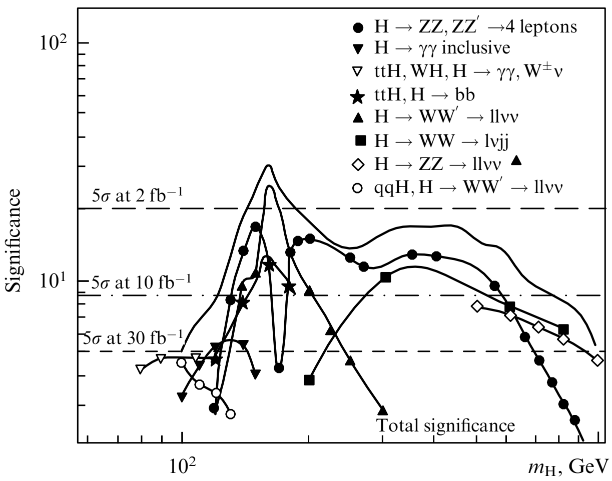

Figure 11. Potential of discovery of the SM Higgs boson for an integrated luminosity of 30 fb^{-1} in the CMS detector without the k-factor [34].

that is better than 10^{-2} [32, 37, 34]. Direct measurement of the decay width is possible only in the mass range $m_H \geqslant 200$ GeV, in which the decay width exceeds the experimental resolution by roughly 1 GeV in mass. An accuracy at the level of $O(10^{-2})$ is expected from the use of the $H \to ZZ^* \to 4l^\pm$ reaction. The mechanism of vector boson fusion and the decays $H \to WW^*$ and $H \to \gamma\gamma$ allow extracting information about the HWW coupling constant. The Higgs boson decay ratio Γ_W/Γ_Z can be measured in the direct production of a Higgs boson via the relation

$$\frac{\sigma_H \times BR(H \to WW^*)}{\sigma_H \times BR(H \to ZZ^*)} = \frac{\Gamma_W}{\Gamma_Z} .$$

Simultaneous use of the $H \to \gamma\gamma$ and $H \to ZZ^*$ channels makes it possible to determine

$$\frac{\sigma_H \times BR(H \to \gamma\gamma)}{\sigma_H \times BR(H \to ZZ^*)} = \frac{\Gamma(H \to \gamma\gamma)}{\Gamma(H \to ZZ^*)} .$$

An accuracy better than 20% is expected for these measurements at the integrated luminosity 300 fb^{-1} [32, 37].

3.14 Main conclusions

The LHC provides the means for discovering the Higgs boson in the mass range from the lower LEP limit $m_H \geqslant 114.4$ GeV to $m_H = 1$ TeV (see Figs 9–11). Within this range, the Higgs boson has a large decay width, $\Gamma_H \approx 0.5$ TeV, and it is therefore meaningless to treat the Higgs boson as an elementary particle. The decay modes most important for the Higgs boson search at the LHC are

$$H \to \gamma\gamma ,$$
$$H \to ZZ^*, ZZ \to 4l^\pm ,$$
$$H \to WW^* \to l^+\nu l'^-\nu ,$$
$$H \to ZZ, WW \to ll\nu\nu, lljj, l\nu jj .$$

The simultaneous use of different channels will allow finding the Higgs boson width ratio.

4. Search for supersymmetry within the MSSM

4.1 The MSSM

Supersymmetry, or SUSY, is a new type of symmetry that links bosons with fermions [4, 5]. Locally supersymmetric theories inevitably involve gravity [45]. SUSY also serves as an essential ingredient of superstring theories [46]. The interest in SUSY is also related to the observation that the results of measurements of gauge constants on the LEP1 accelerator favor the supersymmetric GUT with superparticle masses smaller than $O(1)$ TeV [5]. Moreover, supersymmetric electroweak models produce the simplest solution to the problem of gauge hierarchies [5]. In real life, however, supersymmetry is violated, and for the problem of gauge hierarchies to have a solution, the superparticle masses must be smaller than $O(1)$ TeV. Supergravity provides a natural explanation for supersymmetry breaking [47]; namely, allowing for supersymmetry breaking in the hidden sector leads to a weak supersymmetry breaking in the observable sector.

An elegant formulation of supersymmetry is achieved by introducing the concept of superspace [45]. Two anticommuting coordinates θ_α and $\bar{\theta}_{\dot{\alpha}}$ are introduced. This extends the initial four-dimensional space–time x_μ to the superspace $(x_\mu, \theta_\alpha, \bar{\theta}_{\dot{\alpha}})$. There are two types of fields in this superspace: a chiral field and a vector field [45]. For the chiral superfield, the Taylor expansion has the form

$$\Phi(y, \theta) = A(y) + \sqrt{2}\,\theta\psi(y) + \theta\theta F(y) , \qquad (53)$$

where $y = x + i\theta\sigma\bar{\theta}$. The chiral superfield $\Phi(y, \theta)$ has two bosonic (the complex-valued scalar field A) and two fermionic (the Weyl spinor ψ) degrees of freedom. The component superfields A and ψ are called superpartners. The field F is an auxiliary field and has no physical interpretation. The auxiliary field can be eliminated via the equations of motion. The following expansion holds for an arbitrary function of chiral superfields:

$$W(\Phi_i) = W(A_i + \sqrt{2}\,\theta\psi_i + \theta\theta F_i)$$
$$= W(A_i) + \frac{\partial W}{\partial A_i}\sqrt{2}\,\theta\psi_i + \theta\theta\left(\frac{\partial W}{\partial A_i}F_i - \frac{1}{2}\frac{\partial^2 W}{\partial A_i \partial A_j}\psi_i\psi_j\right) . \qquad (54)$$

Here, W is usually called the superpotential, i.e., a generalization of the ordinary concept of a potential to the case of superfields. To construct gauge-invariant interactions, we must introduce a real-valued complex superfield $V = V^+$. Under an Abelian supergauge transformation, the superfield

V transforms as

$$V \to V + \Phi + \Phi^{+}, \tag{55}$$

where Φ is the gauge superfield. A gauge (known as the Wess–Zumino gauge) can be chosen such that

$$V = -\theta\sigma^{\mu}\bar{\theta}v_{\mu}(x) + \mathrm{i}\theta\theta\bar{\theta}\bar{\lambda}(x) - \mathrm{i}\bar{\theta}\bar{\theta}\theta\lambda(x) + \frac{1}{2}\,\theta\theta\bar{\theta}\bar{\theta}D(x)\,. \tag{56}$$

The physical degrees of freedom corresponding to the real-valued vector superfield V are the gauge vector field $v_{\mu}(x)$ and the Majorana spinor field $\lambda(x)$. Here, $D(x)$ is an auxiliary field and can be eliminated via equations of motion. The chiral superfield of the stress tensor can be defined (by analogy with $F_{\mu\nu}$ in gauge theories) as

$$W_{\alpha} = -\frac{1}{4}\,\bar{D}^{2}e^{gV}D_{\alpha}e^{-gV}\,, \tag{57}$$

$$\bar{W}_{\dot{\alpha}} = -\frac{1}{4}\,D^{2}e^{gV}\bar{D}_{\dot{\alpha}}e^{-gV}\,. \tag{58}$$

The superfield of the stress tensor in the Wess–Zumino gauge has the form

$$W_{\alpha} = T^{a}\left(-\mathrm{i}\lambda_{\alpha}^{a} + \theta^{\alpha}D^{a} - \frac{\mathrm{i}}{2}(\sigma^{\mu}\bar{\sigma}^{\nu}\theta)_{\alpha}F_{\mu\nu}^{a} + \theta^{2}\sigma^{\mu}D_{\mu}\bar{\lambda}^{a}\right), \tag{59}$$

where

$$F_{\mu\nu}^{a} = \partial_{\mu}v_{\nu}^{a} - \partial_{\nu}v_{\mu}^{a} + gf^{abc}v_{\mu}^{b}v_{\nu}^{c}\,, \tag{60}$$

$$D_{\mu}\bar{\lambda}^{a} = \partial_{\mu}\bar{\lambda}^{a} + gf^{abc}v_{\mu}^{b}\bar{\lambda}^{c}\,. \tag{61}$$

Here, the T^{a} and f^{abc} are the generators and structure constants of the group G.

Supersymmetry-invariant Lagrangians can be built in an elegant way by introducing integration over the superspace according to the rules [45]

$$\int \mathrm{d}\theta_{\alpha} = 0\,, \qquad \int \theta_{\alpha}\,\mathrm{d}\theta_{\beta} = \delta_{\alpha\beta}\,. \tag{62}$$

We first consider the case of chiral fields without gauge interactions. The renormalizable Lagrangian can be written as (see Ref. [45])

$$L = \int \mathrm{d}^{2}\theta\,\mathrm{d}^{2}\bar{\theta}\;\Phi_{i}^{+}\Phi_{i} + \int \mathrm{d}^{2}\theta\;W_{3} + \mathrm{h.c.}\,, \tag{63}$$

where

$$W_{3} = \lambda_{i}\Phi_{i} + \frac{1}{2}\,m_{ij}\Phi_{i}\Phi_{j} + \frac{1}{3}\,h_{ijk}\Phi_{i}\Phi_{j}\Phi_{k}\,. \tag{64}$$

Integration over the anticommuting variables yields

$$\begin{aligned} L = {} & \mathrm{i}\partial_{\mu}\bar{\psi}_{i}\bar{\sigma}^{\mu}\psi_{i} + \partial^{\mu}A_{i}^{*}\partial_{\mu}A_{i} + F_{i}^{*}F_{i} \\ & + \left[\lambda_{i}F_{i} + m_{ij}\left(A_{i}F_{j} - \frac{1}{2}\,\psi_{i}\psi_{j}\right)\right. \\ & \left. + h_{ijk}(A_{i}A_{j}F_{k} - \psi_{i}\psi_{j}A_{k}) + \mathrm{h.c.}\right]. \end{aligned} \tag{65}$$

Eliminating the auxiliary fields F_{i} and F_{i}^{*} via the equations of motion, we obtain

$$\begin{aligned} L = {} & \mathrm{i}\partial_{\mu}\bar{\psi}_{i}\bar{\sigma}^{\mu}\psi_{i} + \partial^{\mu}A_{i}^{*}\partial_{\mu}A_{i} \\ & - \left(\frac{1}{2}\,m_{ij}\psi_{i}\psi_{j} + h_{ijk}\psi_{i}\psi_{j}A_{k} + \mathrm{h.c.}\right) \\ & - \left|\lambda_{k} + m_{ik}A_{i} + h_{ijk}A_{i}A_{j}\right|^{2}. \end{aligned} \tag{66}$$

We now examine the case of gauge fields. The supersymmetric generalization of the Yang–Mills Lagrangian is

$$L_{\mathrm{SYM}} = \frac{1}{4}\int \mathrm{d}^{2}\theta\;\mathrm{Tr}\,(W^{\alpha}W_{\alpha}) + \mathrm{h.c.} \tag{67}$$

In terms of the component fields, Lagrangian (67) can be written as

$$L_{\mathrm{SYM}} = -\frac{1}{4}\,F_{\mu\nu}^{a}F^{a\mu\nu} - \mathrm{i}\lambda^{a}\sigma^{\mu}D_{\mu}\bar{\lambda}^{a} + \frac{1}{2}\,D^{a}D^{a}\,. \tag{68}$$

The supersymmetric gauge-invariant renormalizable Lagrangian has the form

$$\begin{aligned} L_{\mathrm{SUSYYM}} = {} & \frac{1}{4}\left(\int \mathrm{d}^{2}\theta\;\mathrm{Tr}\,(W^{\alpha}W_{\alpha}) + \mathrm{h.c.}\right) \\ & + \int \mathrm{d}^{2}\theta\,\mathrm{d}^{2}\bar{\theta}\;\Phi_{ia}^{+}(e^{gV})_{b}^{a}\Phi_{i}^{b} + \left(\int \mathrm{d}^{2}\theta\;W_{3}(\Phi_{i}) + \mathrm{h.c.}\right), \end{aligned} \tag{69}$$

where $W_{3}(\Phi_{i})$ is a gauge-invariant superpotential. In terms of the component fields, Lagrangian (69) can be written as

$$\begin{aligned} L_{\mathrm{SUSYYM}} = {} & -\frac{1}{4}\,F_{\mu\nu}^{a}F^{a\mu\nu} - \mathrm{i}\lambda^{a}\sigma^{\mu}D_{\mu}\bar{\lambda}^{a} + \frac{1}{2}\,D^{a}D^{a} \\ & + (\partial_{\mu}A_{i} - \mathrm{i}gv_{\mu}^{a}T^{a}A_{i})^{+}(\partial^{\mu}A_{i} - \mathrm{i}gv_{\mu}^{a}T^{a}A_{i}) \\ & - \mathrm{i}\bar{\psi}_{i}\bar{\sigma}^{\mu}(\partial_{\mu}\psi_{i} - \mathrm{i}gv_{\mu}^{a}T^{a}\bar{\psi}_{i}) - gD^{a}A_{i}^{+}T^{a}A_{i} \\ & - (\mathrm{i}\sqrt{2}\,gA_{i}^{+}T^{a}\lambda^{a}\psi_{i} + \mathrm{h.c.}) \\ & + F_{i}^{+}F_{i} + \left(\frac{\partial W}{\partial A_{i}}\,F_{i} - \frac{1}{2}\,\frac{\partial^{2}W}{\partial A_{i}\,\partial A_{j}}\,\psi_{i}\psi_{j} + \mathrm{h.c.}\right). \end{aligned} \tag{70}$$

After integration over the auxiliary fields D^{a} and F_{i}, we obtain the ordinary Lagrangian.

The simplest generalization of the SM is the MSSM [5, 48]. The MSSM is based on the use of the standard gauge group $\mathrm{SU_c}(3)\otimes\mathrm{SU_L}(2)\otimes\mathrm{U}(1)$ in which the electroweak symmetry is broken by finite vacuum expectation values of two Higgs isodoublets. The MSSM consists of the SM plus the appropriate interactions involving superparticles. We note that the MSSM contains two isodoublets of Higgs fields with hypercharges $Y = \pm 1$, which follows from the requirement that there be no γ_{5} anomalies. The two isodoublets of Higgs fields are also needed in order that the 'upper' and 'lower' fermions acquire mass.

The SUSY generalization of the SM Lagrangian can be written as

$$L_{\mathrm{SUSY}} = L_{\mathrm{Gauge,\,M}} + L_{\mathrm{Yukawa}}\,, \tag{71}$$

where

$$\begin{aligned} L_{\mathrm{Gauge,\,M}} = {} & \sum_{\mathrm{SU(3),\,SU(2),\,U(1)}} \frac{1}{4}\left(\int \mathrm{d}^{2}\theta\;\mathrm{Tr}\,W^{\alpha}W_{\alpha} + \mathrm{h.c.}\right) \\ & + \sum_{\mathrm{matter}} \int \mathrm{d}^{2}\theta\,\mathrm{d}^{2}\bar{\theta}\,\Phi_{i}^{+}e^{gV}\Phi_{i}\,, \end{aligned} \tag{72}$$

$$L_{\mathrm{Yukawa}} = \int \mathrm{d}^{2}\theta\,(W_{R} + W_{NR}) + \mathrm{h.c.} \tag{73}$$

The renormalizable potential W_R in the MSSM determines the Yukawa coupling of quarks and leptons and preserves the global $B-L$ symmetry. Here, B is the baryonic number and L is the leptonic number. The superpotential W_R that preserves the R-parity has the form

$$W_R = \epsilon_{ij}(h^U_{ab} Q^j_a U^c_b H^i_2 + h^D_{ab} Q^j_a D^c_b H^i_1 + h^L_{ab} L^j_a E^c_b H^i_1 + \mu H^i_1 H^j_2)\,, \tag{74}$$

where $i, j = 1, 2, 3$ are SU(2) indices, $a, b = 1, 2, 3$ are indices of generations, and the color indices are omitted. The last term in the right-hand side of Eqn (74) describes the Higgs boson mixing. The most general expression for the superpotential W_{NR} is of the form

$$W_{NR} = \epsilon_{ij}(\lambda^L_{abd} L^i_a L^j_b E^c_d + \lambda^L_{1abd} L^i_a Q^j_b D^c_d + \mu'_a L^i_a H^j_2) + \lambda^B_{abd} U^c_a D^c_b D^c_d\,. \tag{75}$$

Effective superpotential (75) contains terms breaking the $B-L$ symmetry, which may lead to problems with proton decay. To eliminate such dangerous terms in the superpotential, the conservation of R-parity is postulated [49], with $R = (-1)^{3(B-L)+2S}$ for a particle with spin S. For ordinary particles, $R = 1$ and for the corresponding superparticles, $R = -1$. If we postulate the R-parity conservation, then $W_{NR} = 0$. The experimental limits to the coupling constants that violate the R-parity are as follows [16, 50]:

$$\lambda^L_{abc} < O(10^{-4})\,, \tag{76}$$

$$\lambda^L_{1abc} < O(10^{-4})\,, \tag{77}$$

$$\lambda^B_{abc} < O(10^{-9})\,. \tag{78}$$

The requirement of the R-parity conservation leads to nontrivial consequences for supersymmetry phenomenology. The most important consequence of the R-parity conservation is that the lightest supersymmetric particle (LSP) is stable. Cosmological constraints imply that the LSP must be electrically neutral and colorless. Another important consequence of the R-parity conservation is that superparticles are produced in supercolliders in pairs, and hence at least two LSPs must be present in the decay of heavy unstable superparticles. Because LSPs are weakly interacting particles, they are not recorded by detectors, with the result that the missing transverse energy/momentum is the classical signature for supersymmetry theories with R-parity conservation.

In real life, supersymmetry must be broken. At present, the most popular mechanism of supersymmetry breaking is described by a scenario based on the use of the hidden sector [5, 47, 51]. According to this scenario, there are two sectors: ordinary matter enters the apparent sector, while the hidden sector of the theory contains fields that lead to supersymmetry breaking. These two sectors interact via certain fields that mediate SUSY breaking from the hidden sector to the apparent sector. At present, the two most developed scenarios for SUSY breaking are

(1) mediation via gravity (SUGRA), and

(2) gauge mediation.

In the SUGRA scenario [47, 5], the apparent and hidden sectors interact via gravity. Some scalar fields in the hidden sector acquire finite vacuum expectation values for their F-components, which leads to spontaneous SUSY breaking. Because supersymmetry is local in SUGRA, spontaneous SUSY breaking leads to the existence of a Goldstone particle, which is a fermion. Due to the super-Higgs effect, this fermion is absorbed into the additional component of a spin-3/2 particle, the gravitino, which becomes massive in analogy with the standard Higgs mechanism. SUSY breaking is mediated to the apparent sector via gravitational interactions, and this leads to the SUSY breaking scale $M_{\rm SUSY} \sim m_{3/2}$, where $m_{3/2}$ is the gravitino mass. The effective low-energy Lagrangian contains explicit terms with soft supersymmetry breaking:

$$L_{\rm soft} = -\sum_{i,j} m^2_{ij} A_i A^*_j - \sum_i M_i(\lambda_i\lambda_i + \bar\lambda_i\bar\lambda_i) - \left[BW^{(2)}(A) + BW^{(3)}(A) + \text{h.c.}\right]. \tag{79}$$

Here, $W^{(2)}$ and $W^{(3)}$ are, respectively, the quadratic and cubic terms of the apparent superpotential. The mass parameters in Lagrangian (79) are proportional to the gravitino mass $m_{3/2}$.

In the gauge mechanism [51] of supersymmetry breaking mediation, SUSY breaking is conveyed to the apparent sector by gauge interactions. The transmitting agents are gauge bosons or matter fields of the SM. In this scenario, it is possible to construct a renormalizable model with dynamic SUSY breaking in which all the parameters can be calculated (at least theoretically). In the scenario with gauge SUSY breaking mediation, all soft SUSY-violating terms correlate with the gauge constants. Furthermore, this scenario encounters no problems with terms that violate flavor. The lightest superparticle in this scenario is the gravitino. The soft terms that violate SUSY have the dimension not greater than three.

In the MSSM, supersymmetry is softly broken at a certain scale M by the soft terms

$$\begin{aligned} -L_{\rm soft} &= m_0(A^u_{ij} U^c_i Q_j H_2 + A^d_{ij} D^c_i G_j H_1 \\ &\quad + A^l_{ij} E^c_i L_j H_1 + \text{h.c.}) + (m^2_{\rm q})_{ij} Q^+_i Q_j + (m^2_{\rm u})_{ij} (U^c_i)^+ U^c_j \\ &\quad + (m^2_{\rm d})_{ij} (D^c_i)^+ D^c_j + (m^2_{\rm l})_{ij} (L^c_i)^+ L^c_j + (m^2_{\rm e})_{ij} (E^c_i)^+ E^c_j \\ &\quad + m^2_1 H_1 H^+_1 + m^2_2 H_2 H^+_2 + (Bm^2_0 H_1 H_2 + \text{h.c.}) \\ &\quad + \left[\frac{1}{2}\, m_a(\lambda_a\lambda_a) + \text{h.c.}\right]. \end{aligned} \tag{80}$$

In the general case, all soft SUSY-breaking terms are arbitrary, which makes phenomenological analysis more difficult and reduces the predictive power of the theory. The mSUGRA model [5, 48] postulates the universality of the parameters of soft SUSY breaking at the GUT scale. Precisely, all spin-0 particles (squarks, sleptons, and Higgs bosons) have the same mass m_0. All gauginos in this model have the same mass $m_{1/2}$ at the GUT scale and, in addition, the universality of the quadratic and cubic terms B and A is postulated at the same scale. We note that the mSUGRA model is a very special one and can be considered only as a 'toy model' for specific applications.

Thus, in the mSUGRA model, the soft SUSY-breaking masses and coupling constants are postulated equal at the GUT scale, i.e.,

$$\begin{aligned} &A^u_{ij}(M_{\rm GUT}) = Ah^u_{ij}(M_{\rm GUT})\,, \quad A^d_{ij}(M_{\rm GUT}) = Ah^d_{ij}(M_{\rm GUT})\,, \\ &A^l_{ij}(M_{\rm GUT}) = Ah^l_{ij}(M_{\rm GUT})\,, \end{aligned} \tag{81}$$

$$\begin{aligned} (m^2_{\rm q})_{ij}(M_{\rm GUT}) &= (m^2_{\rm u})_{ij}(M_{\rm GUT}) = (m^2_{\rm d})_{ij}(M_{\rm GUT}) \\ &= (m^2_{\rm l})_{ij}(M_{\rm GUT}) = (m^2_{\rm e})_{ij}(M_{\rm GUT}) \\ &= \delta_{ij} m^2_1(M_{\rm GUT}) = \delta_{ij} m^2_2(M_{\rm GUT}) = \delta_{ij} m^2_0\,, \end{aligned} \tag{82}$$

$$m_1(M_{\rm GUT}) = m_2(M_{\rm GUT}) = m_3(M_{\rm GUT}) = m_{1/2}\,. \tag{83}$$

We note that it is more proper to impose boundary conditions not at the GUT scale but at the Planck scale $M_{\rm Pl} = 2.4 \times 10^{18}$ GeV. Allowing for the effects of renormalization between the scales $M_{\rm Pl}$ and $M_{\rm GUT}$ may substantially change the features of the superparticle spectrum. For instance, if we assume that the physics between $M_{\rm Pl}$ and $M_{\rm GUT}$ is described by the SU(5) supersymmetric model, then allowing for the evolution between $M_{\rm Pl}$ and $M_{\rm GUT}$ [52, 53] may dramatically change the slepton spectrum at $m_0 \ll m_{1/2}$ [53]. The renormalization-group equations for SUSY-breaking effective parameters, in which all Yukawa coupling constants are ignored with the exception of the one-loop Yukawa constant for the top quark, have the form [54, 48]

$$\frac{d\tilde{m}_{\rm L}^2}{dt} = \left(3\tilde{\alpha}_2 M_2^2 + \frac{3}{5}\,\tilde{\alpha}_1 M_1^2\right), \tag{84}$$

$$\frac{d\tilde{m}_{\rm E}^2}{dt} = \left(\frac{12}{5}\,\tilde{\alpha}_1 M_1^2\right), \tag{85}$$

$$\frac{d\tilde{m}_{\rm Q}^2}{dt} = \left(\frac{16}{3}\,\tilde{\alpha}_3 M_3^2 + 3\tilde{\alpha}_2 M_2^2 + \frac{1}{15}\,\tilde{\alpha}_1 M_1^2\right) - \delta_{i3} Y_{\rm t}(\tilde{m}_{\rm Q}^2 + \tilde{m}_{\rm U}^2 + m_2^2 + A_{\rm t}^2 m_0^2 - \mu^2), \tag{86}$$

$$\frac{d\tilde{m}_{\rm U}^2}{dt} = \left(\frac{16}{3}\,\tilde{\alpha}_3 M_3^2 + \frac{16}{15}\,\tilde{\alpha}_1 M_1^2\right) - \delta_{i3} 2 Y_{\rm t}(\tilde{m}_{\rm Q}^2 + \tilde{m}_{\rm U}^2 + m_2^2 + A_{\rm t}^2 m_0^2 - \mu^2), \tag{87}$$

$$\frac{d\tilde{m}_{\rm D}^2}{dt} = \left(\frac{16}{3}\,\tilde{\alpha}_3 M_3^2 + \frac{4}{15}\,\tilde{\alpha}_1 M_1^2\right), \tag{88}$$

$$\frac{d\mu^2}{dt} = 3\left(\tilde{\alpha}_2 + \frac{1}{5}\,\tilde{\alpha}_1 - Y_{\rm t}\right)\mu^2, \tag{89}$$

$$\frac{dm_1^2}{dt} = 3\left(\tilde{\alpha}_2 M_2^2 + \frac{1}{5}\,\tilde{\alpha}_1 M_1^2\right) + 3\left(\tilde{\alpha}_2 + \frac{1}{5}\,\tilde{\alpha}_1 - Y_{\rm t}\right)\mu^2, \tag{90}$$

$$\frac{dm_2^2}{dt} = 3\left(\tilde{\alpha}_2 M_2^2 + \frac{1}{5}\,\tilde{\alpha}_1 M_1^2\right) + 3\left(\tilde{\alpha}_2 + \frac{1}{5}\,\tilde{\alpha}_1\right)\mu^2 - 3 Y_{\rm t}(\tilde{m}_{\rm Q}^2 + \tilde{m}_{\rm U}^2 + m_2^2 + A_{\rm t}^2 m_0^2), \tag{91}$$

$$\frac{dA_{\rm t}}{dt} = -\left(\frac{16}{3}\,\tilde{\alpha}_3\,\frac{M_3}{m_0} + 3\tilde{\alpha}_2\,\frac{M_2}{m_0} + \frac{13}{15}\,\tilde{\alpha}_1\,\frac{M_1}{m_0}\right) - 6 Y_{\rm t} A_{\rm t}, \tag{92}$$

$$\frac{dB}{dt} = -3\left(\tilde{\alpha}_2\,\frac{M_2}{m_0} + \frac{1}{5}\,\tilde{\alpha}_1\,\frac{M_1}{m_0}\right) - 3 Y_{\rm t} A_{\rm t}, \tag{93}$$

$$\frac{dM_i}{dt} = -b_i \tilde{\alpha}_i M_i, \tag{94}$$

$$b_1 = \frac{33}{5}, \qquad b_2 = 1, \qquad b_3 = -3. \tag{95}$$

Here, $\tilde{m}_{\rm U}$, $\tilde{m}_{\rm D}$, and $\tilde{m}_{\rm E}$ are the masses of the superpartners of the quark and lepton singlets, while $\tilde{m}_{\rm Q}$ and $\tilde{m}_{\rm L}$ are the masses of the isodoublet superpartners; m_1, m_2, m_3, and μ are the mass parameters for the potential of the Higgs fields; A and B are the coupling constants in the Lagrangian $L_{\rm soft}$, as defined above; and the M_i are the gaugino masses before mixing. The renormalization-group equation for the Yukawa coupling constant for the top quark is

$$\frac{dY_{\rm t}}{dt} = Y_{\rm t}\left(\frac{16}{3}\,\tilde{\alpha}_3 + 3\tilde{\alpha}_2 + \frac{13}{15}\,\tilde{\alpha}_1\right) - 6 Y_{\rm t}^2, \tag{96}$$

and the renormalization-group equations for the gauge coupling constants are

$$\frac{d\tilde{\alpha}_i}{dt} = -b_i \tilde{\alpha}_i^2. \tag{97}$$

Here,

$$\tilde{\alpha}_i = \frac{\alpha_i}{4\pi}, \qquad Y_{\rm t} = \frac{h_{\rm t}^2}{16\pi^2}, \qquad t = \ln\frac{M_{\rm GUT}^2}{Q^2}, \tag{98}$$

and the Yukawa coupling constant $h_{\rm t}$ is related to the running top quark mass as

$$m_{\rm t} = h_{\rm t}(m_{\rm t})\,\frac{v}{\sqrt{2}}\sin\beta. \tag{99}$$

The boundary conditions at $Q^2 = M_{\rm GUT}^2$ are given by

$$\tilde{m}_{\rm Q}^2 = \tilde{m}_{\rm U}^2 = \tilde{m}_{\rm D}^2 = \tilde{m}_{\rm E}^2 = \tilde{m}_{\rm L}^2 = m_0^2, \tag{100}$$

$$\mu = \mu_0; \quad m_1^2 = m_2^2 = \mu_0^2 + m_0^2; \quad m_3^2 = B\mu_0 m_0, \tag{101}$$

$$M_i = m_{1/2}, \quad \tilde{\alpha}_i(0) = \tilde{\alpha}_{\rm GUT}; \quad i = 1, 2, 3. \tag{102}$$

For gauginos, which correspond to the gauge group $\mathrm{SU_L}(2) \otimes \mathrm{U}(1)$, we must take the mixing with higgsinos (the superpartners of Higgs bosons) into account. The mass terms can be written as

$$L_{\text{gaugino-higgsino}} = -\frac{1}{2}\,M_3 \bar{\lambda}_3^a \lambda_3^a - \frac{1}{2}\,\bar{\chi} M^{(0)} \chi - (\bar{\psi} M^{(c)} \psi + \text{h.c.}), \tag{103}$$

where the λ_3^a denote the eight Majorana gluino fields and

$$\chi = \begin{pmatrix} \tilde{B}^0 \\ \tilde{W}^3 \\ \tilde{H}_1^0 \\ \tilde{H}_2^0 \end{pmatrix}, \tag{104}$$

$$\psi = \begin{pmatrix} \tilde{W}^+ \\ \tilde{H}^+ \end{pmatrix} \tag{105}$$

are the Majorana neutralino and Dirac chargino fields. The mass matrices are given by

$$M^{(0)} = \begin{pmatrix} M_1 & 0 & -A & B \\ 0 & M_2 & C & -D \\ -A & C & 0 & -\mu \\ B & -D & -\mu & 0 \end{pmatrix}, \tag{106}$$

$$M^{(c)} = \begin{pmatrix} M_2 & \sqrt{2} M_{\rm W} \sin\beta \\ \sqrt{2} M_{\rm W} \cos\beta & \mu \end{pmatrix}, \tag{107}$$

where

$$A = M_{\rm Z} \cos\beta \sin\theta_{\rm W}, \qquad B = M_{\rm Z} \sin\beta \sin\theta_{\rm W}, \tag{108}$$

$$C = M_{\rm Z} \cos\beta \cos\theta_{\rm W}, \qquad D = M_{\rm Z} \sin\beta \cos\theta_{\rm W}. \tag{109}$$

Solving the appropriate renormalization-group equations with $\alpha_{\rm GUT} = 1/24.3$, $M_{\rm GUT} = 2.0 \times 10^{16}$ GeV, $\sin^2\theta_{\rm W} = 0.2324$, $\tan\beta = 1.65$, and $A_{\rm t}(0) = 0$, we obtain the numerical values of the effective squares of the squark and slepton masses on the electroweak scale [48]:

$$\tilde{m}^2_{\mathrm{E_L}}(M_\mathrm{Z}) = m_0^2 + 0.52m_{1/2}^2 - 0.27\cos 2\beta M_\mathrm{Z}^2\,, \qquad (110)$$

$$\tilde{m}^2_{\nu_\mathrm{L}}(M_\mathrm{Z}) = m_0^2 + 0.52m_{1/2}^2 + 0.5\cos 2\beta M_\mathrm{Z}^2\,, \qquad (111)$$

$$\tilde{m}^2_{\mathrm{E_R}}(M_\mathrm{Z}) = m_0^2 + 0.15m_{1/2}^2 - 0.23\cos 2\beta M_\mathrm{Z}^2\,, \qquad (112)$$

$$\tilde{m}^2_{\mathrm{U_L}}(M_\mathrm{Z}) = m_0^2 + 6.5m_{1/2}^2 + 0.35\cos 2\beta M_\mathrm{Z}^2\,, \qquad (113)$$

$$\tilde{m}^2_{\mathrm{D_L}}(M_\mathrm{Z}) = m_0^2 + 6.5m_{1/2}^2 - 0.42\cos 2\beta M_\mathrm{Z}^2\,, \qquad (114)$$

$$\tilde{m}^2_{\mathrm{U_R}}(M_\mathrm{Z}) = m_0^2 + 6.1m_{1/2}^2 + 0.15\cos 2\beta M_\mathrm{Z}^2\,, \qquad (115)$$

$$\tilde{m}^2_{\mathrm{D_R}}(M_\mathrm{Z}) = m_0^2 + 6.0m_{1/2}^2 - 0.07\cos 2\beta M_\mathrm{Z}^2\,, \qquad (116)$$

$$\tilde{m}^2_{\mathrm{b_R}}(M_\mathrm{Z}) = \tilde{m}^2_{\mathrm{D_R}}\,, \qquad (117)$$

$$\tilde{m}^2_{\mathrm{b_L}}(M_\mathrm{Z}) = \tilde{m}^2_{\mathrm{D_L}} - 0.49m_0^2 - 1.21m_{1/2}^2\,, \qquad (118)$$

$$\tilde{m}^2_{\mathrm{t_R}}(M_\mathrm{Z}) = \tilde{m}^2_{\mathrm{U_R}}(M_\mathrm{Z}) + m_\mathrm{t}^2 - 0.99m_0^2 - 2.42m_{1/2}^2\,, \qquad (119)$$

$$\tilde{m}^2_{\mathrm{t_L}}(M_\mathrm{Z}) = \tilde{m}^2_{\mathrm{U_L}}(M_\mathrm{Z}) + m_\mathrm{t}^2 - 0.49m_0^2 - 1.21m_{1/2}^2\,. \qquad (120)$$

After mixing, the values of the stop quark masses are

$$\begin{aligned}\tilde{m}^2_{\mathrm{t}_{1,2}}(M_\mathrm{Z}) &\approx \frac{1}{2}\left[0.5m_0^2 + 9.1m_{1/2}^2 + 2m_\mathrm{t}^2 + 0.5\cos 2\beta M_\mathrm{Z}^2\right] \\ &\mp \frac{1}{2}\left[(1.5m_{1/2}^2 + 0.5m_0^2 + 0.2\cos 2\beta\, M_\mathrm{Z}^2)^2 \right. \\ &\left. + 4m_\mathrm{t}^2\left(A_\mathrm{t}m_0 - \frac{\mu}{\tan\beta}\right)^2\right]^{1/2}. \qquad (121)\end{aligned}$$

Gauginos and higgsinos have the same quantum numbers, which leads to mixing. The two eigenstates of the chargino $\tilde{\chi}^\pm_{1,2}$ are given by

$$\begin{aligned}M_{1,2}^2 &= \frac{1}{2}\left[M_2^2 + \mu^2 + 2M_\mathrm{W}^2\right] \\ &\mp \frac{1}{2}\left[(M_2^2 - \mu^2)^2 + 4M_\mathrm{W}^4\cos^2 2\beta \right. \\ &\left. + 4M_\mathrm{W}^2(M_2^2 + \mu^2 + 2M_2\mu\sin 2\beta)\right]^{1/2}, \qquad (122)\end{aligned}$$

and at the GUT scale, the masses of the gauginos corresponding to the gauge groups SU(3), $\mathrm{SU_L}(2)$, and U(1) are $m_{1/2}$. The characteristic values of the 4×4 neutralino mass matrix can be found numerically. For the frequently encountered case where the parameter μ is much larger than M_1 and M_2, the mass states are

$$\tilde{\chi}_i^0 = \left[\tilde{B}, \tilde{W}_3, \frac{1}{\sqrt{2}}(\tilde{H}_1 - \tilde{H}_2), \frac{1}{\sqrt{2}}(\tilde{H}_1 + \tilde{H}_2)\right] \qquad (123)$$

with the moduli of the eigenstates being $|M_1|$, $|M_2|$, $|\mu|$, and $|\mu|$.

At the tree level, the potential of Higgs fields in the MSSM is

$$\begin{aligned}V_0(H_1, H_2) &= m_1^2|H_1|^2 + m_2^2|H_2|^2 - m_3^2(H_1H_2 + \mathrm{h.c}) \\ &+ \frac{g_2^2 + g_1^2}{8}\left(|H_1|^2 - |H_2|^2\right)^2 + \frac{g_2^2}{2}|H_1^+H_2|^2\,. \qquad (124)\end{aligned}$$

Minimization of the effective potential $V_0(H_1, H_2)$ leads to the equations

$$v^2 = \frac{8(m_1^2 - m_2^2\tan^2\beta)}{(g_2^2 + g_1^2)(\tan^2\beta - 1)}\,, \qquad (125)$$

$$\sin 2\beta = \frac{2m_3^2}{m_1^2 + m_2^2}\,. \qquad (126)$$

After diagonalization of the appropriate mass matrix, the CP-odd neutral Higgs boson $\mathrm{A}(x)$ acquires the mass $m_\mathrm{A}^2 = m_1^2 + m_2^2$, the charged Higgs boson $\mathrm{H}^+(x)$ acquires the mass $m_{\mathrm{H}^+}^2 = m_\mathrm{A}^2 + M_\mathrm{W}^2$, and the CP-even Higgs bosons $\mathrm{H}(x)$ and $\mathrm{h}(x)$ have the masses

$$m_{\mathrm{H,h}}^2 = \frac{1}{2}\left[m_\mathrm{A}^2 + M_\mathrm{Z}^2 \pm \sqrt{(m_\mathrm{A}^2 + M_\mathrm{Z}^2)^2 - 4m_\mathrm{A}^2M_\mathrm{Z}^2\cos^2 2\beta}\right], \qquad (127)$$

where

$$\langle H_1\rangle = v_1 = \frac{v\cos\beta}{\sqrt{2}}\,, \quad \langle H_2\rangle = v_2 = \frac{v\sin\beta}{\sqrt{2}}\,, \quad \tan\beta = \frac{v_2}{v_1}\,.$$

At the tree level, the following relations hold:

$$m_\mathrm{h}^2 + m_\mathrm{H}^2 = m_\mathrm{A}^2 + M_\mathrm{Z}^2\,, \qquad (128)$$

$$m_\mathrm{h} \leqslant m_\mathrm{A} \leqslant m_\mathrm{H}\,, \qquad (129)$$

$$m_\mathrm{h} \leqslant M_\mathrm{Z}|\cos 2\beta| \leqslant M_\mathrm{Z}\,. \qquad (130)$$

Hence, the lightest Higgs boson is lighter than the Z boson at the tree level. However, radiative corrections increase the mass of the lightest Higgs boson in the MSSM [20]. The upper limit for the Higgs boson mass depends on the top-quark and stop-quark masses. At $m_{\mathrm{t,\,pole}} = 175$ GeV and a stop-quark mass smaller than 1 TeV, the mass of the lightest Higgs boson is smaller than 135 GeV [21].

After the appropriate equations for determining the nontrivial electroweak minimum have been solved, the number of unknown parameters decreases by two. At present, a more or less standard set of parameters in the mSUGRA model includes m_0, $m_{1/2}$, $\tan\beta$, A, and sign μ.

4.2 Superparticle production cross sections

Superparticles can be produced at the LHC in the reactions [55] (Fig. 12)

(a) $\mathrm{gg, qq, qg} \to \tilde{\mathrm{g}}\tilde{\mathrm{g}}, \tilde{\mathrm{g}}\tilde{\mathrm{q}}, \tilde{\mathrm{q}}\tilde{\mathrm{q}}\,,$

(b) $\mathrm{qq, gq} \to \tilde{\mathrm{g}}\tilde{\chi}_i^0, \tilde{\mathrm{g}}\tilde{\chi}_i^\pm, \tilde{\mathrm{q}}\tilde{\chi}_i^0, \tilde{\mathrm{q}}\tilde{\chi}_i^\pm\,,$

(c) $\mathrm{qq} \to \tilde{\chi}_i^\pm\tilde{\chi}_j^\mp, \tilde{\chi}_i^\pm\tilde{\chi}_j^0, \tilde{\chi}_i^0\tilde{\chi}_j^0\,,$

(d) $\mathrm{qq} \to \tilde{\mathrm{l}}\tilde{\nu}, \tilde{\mathrm{l}}\tilde{\mathrm{l}}, \tilde{\nu}\tilde{\nu}\,.$

In this section, following Ref. [55], we list the main formulas for the cross sections at the quark – gluon level. The differential production cross section for two gauge fermions to be produced in quark – antiquark collisions has the form

$$\begin{aligned}&\frac{\mathrm{d}\sigma}{\mathrm{d}t}(\mathrm{q\bar{q}'} \to \text{gaugino 1} + \text{gaugino 2}) \\ &= \frac{\pi}{s^2}\left[A_\mathrm{s}\frac{(t - m_2^2)(t - m_1^2) + (u - m_1^2)(u - m_2^2) + 2sm_1m_2}{(s - M_\mathrm{s}^2)^2}\right. \\ &+ A_\mathrm{t}\frac{(t - m_1^2)(t - m_2^2)}{(t - M_\mathrm{t}^2)^2} + A_\mathrm{u}\frac{(u - m_1^2)(u - m_2^2)}{(u - M_\mathrm{u}^2)^2} \\ &+ A_\mathrm{st}\frac{(t - m_1^2)(t - m_2^2) + m_1m_2s}{(s - M_\mathrm{s}^2)(t - M_\mathrm{t}^2)} + A_\mathrm{tu}\frac{m_1m_2s}{(t - M_\mathrm{t}^2)(u - M_\mathrm{u}^2)} \\ &\left. + A_\mathrm{su}\frac{(u - m_1^2)(u - m_2^2) + m_1m_2s}{(s - M_\mathrm{s}^2)(u - M_\mathrm{u}^2)}\right], \qquad (131)\end{aligned}$$

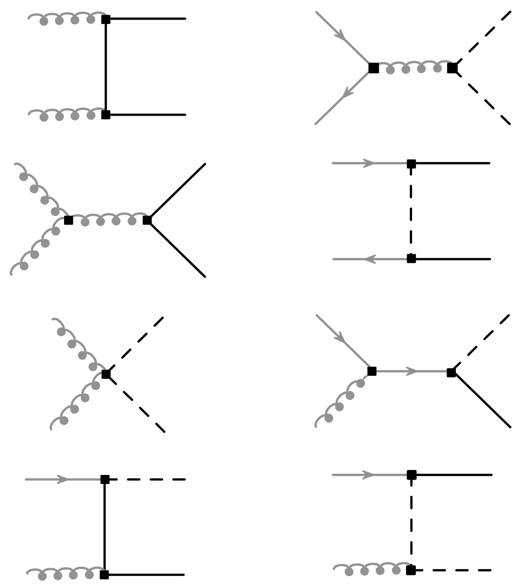

Figure 12. Diagrams describing squark and gluino production.

where m_1 and m_2 are the masses of the produced gauginos and M_s, M_t, and M_u are the masses of the particles that exchange in the s, t, and u channels, respectively. The coefficients A_x are given in Ref. [55]. For instance, when two gluinos are produced in quark–antiquark collisions, the coefficients A_x are [55]

$$A_t = \frac{4}{9} A_s , \quad A_u = A_t , \quad A_{st} = A_s , \quad A_{su} = A_{st} ,$$

$$A_{tu} = \frac{1}{9} A_s , \quad A_s = \frac{8\alpha_s^2}{3} \delta_{qq'} .$$

The differential cross section of the production of gluino pairs in gluon–gluon collisions is

$$\frac{d\sigma}{dt}(gg \to \tilde{g}\tilde{g}) = \frac{9\pi\alpha_s^2}{4s^2} \left\{ \frac{2(t - m_{\tilde{g}}^2)(u - m_{\tilde{g}}^2)}{s^2} + \left[\left(\frac{(t - m_{\tilde{g}}^2)(u - m_{\tilde{g}}^2) - 2m_{\tilde{g}}^2(t + m_{\tilde{g}}^2)}{(t - m_{\tilde{g}}^2)^2} + \frac{(t - m_{\tilde{g}}^2)(u - m_{\tilde{g}}^2) + m_{\tilde{g}}^2(u - t)}{s(t - m_{\tilde{g}}^2)} \right) + (t \leftrightarrow u) \right] + \frac{m_{\tilde{g}}^2(s - 4m_{\tilde{g}}^2)}{(t - m_{\tilde{g}}^2)(u - m_{\tilde{g}}^2)} \right\} , \tag{132}$$

and the total production cross section is

$$\sigma(gg \to \tilde{g}\tilde{g}) = \frac{3\pi\alpha_s^2}{4s} \left[3\left(1 + \frac{4m_{\tilde{g}}^2}{s} - \frac{4m_{\tilde{g}}^4}{s^2}\right) \ln \frac{s + L}{s - L} - \left(4 + \frac{17m_{\tilde{g}}^2}{s}\right) \frac{L}{s} \right] , \tag{133}$$

where $L = [s^2 - 4m_{\tilde{g}}^2 s]^{1/2}$.

The differential cross section for the reaction $q_i q_j \to \tilde{q}_i \tilde{q}_j$ in the case of equal masses of left- and right-handed quarks can be written as

$$\frac{d\sigma}{dt}(q_i q_j \to \tilde{q}_i \tilde{q}_j) = \frac{4\pi\alpha_s^2}{9s^2} \left[-\frac{(t - m_i^2)(t - m_j^2) + st}{(t - m_{\tilde{g}}^2)^2} - \delta_{ij} \frac{(u - m_i^2)(u - m_j^2) + su}{(u - m_{\tilde{g}}^2)^2} + \frac{sm_{\tilde{g}}^2}{(t - m_{\tilde{g}}^2)^2} + \frac{sm_{\tilde{g}}^2}{(u - m_{\tilde{g}}^2)^2} \delta_{ij} - \frac{2sm_{\tilde{g}}^2}{3(t - m_{\tilde{g}}^2)(u - m_{\tilde{g}}^2)} \delta_{ij} \right] , \tag{134}$$

where m_i and m_j are the masses of the produced squarks and $m_{\tilde{g}}$ is the gluino mass.

The differential cross section for the reaction $q_i \bar{q}_j \to \tilde{q}_i \tilde{q}_j^*$ is

$$\frac{d\sigma}{dt}(q_i \bar{q}_j \to \tilde{q}_i \tilde{q}_j^*) = \frac{4\pi\alpha_s^2}{9s^2} \left\{ \frac{ut - m_i^2 m_j^2}{s^2} \times \left[\delta_{ij} \left(2 - \frac{2}{3} \frac{s}{(t - m_{\tilde{g}}^2)} \right) + \frac{s^2}{(t - m_{\tilde{g}}^2)^2} \right] + \frac{sm_{\tilde{g}}^2}{(t - m_{\tilde{g}}^2)^2} \right\} , \tag{135}$$

and for the reaction $gg \to \tilde{q}_i \tilde{q}_i^*$ is

$$\frac{d\sigma}{dt}(gg \to \tilde{q}_i \tilde{q}_i^*) = \frac{\pi\alpha_s^2}{s^2} \left[\frac{7}{48} + \frac{3(u - t)^2}{16s^2} \right] \times \left[1 + \frac{2m^2 t}{(t - m^2)^2} + \frac{2m^2 u}{(u - m^2)^2} + \frac{4m^4}{(t - m^2)(u - m^2)} \right] . \tag{136}$$

Here, m is the mass of the respective squark (the left- and right-handed squarks are assumed to have equal masses).

The differential cross section for the reaction $gq_i \to$ gaugino $+ \tilde{q}_i$ is

$$\frac{d\sigma}{dt}(gq_i \to \text{gaugino} + \tilde{q}_i) = \frac{\pi}{s^2} \left\{ B_s \frac{(\mu^2 - t)}{s} + B_t \frac{[(\mu^2 - t)s + 2\mu^2(m_i^2 - t)]}{(t - \mu^2)^2} + B_u \frac{(u - \mu^2)(u + m_i^2)}{(u - m_i^2)^2} + B_{st} \frac{[(s - m_i^2 + \mu^2)(t - m_i^2) - \mu^2 s]}{s(t - \mu^2)} + B_{su} \frac{[s(u + \mu^2) + 2(m_i^2 - \mu^2)(\mu^2 - u)]}{s(u - m_i^2)} + B_{tu} \frac{1}{2(t - \mu^2)(u - m_i^2)} \left[(m_i^2 - t)(t + 2u + \mu^2) + (t - \mu^2)(s + 2t - 2m_i^2) + (u - \mu^2)(t + \mu^2 + 2m_i^2) \right] \right\} , \tag{137}$$

where μ is the mass of the gauge fermion and m_i is the mass of the scalar quark. The values of the coefficients B_x can be found in Ref. [55]. For instance, when gaugino $\equiv$ gluino,

$$B_s = \frac{4\alpha_s^2}{9} \delta_{ij} , \quad B_t = \frac{9}{4} B_s , \quad B_u = B_s ,$$

$$B_{st} = -B_t , \quad B_{su} = \frac{1}{8} B_s , \quad B_{tu} = \frac{9}{8} B_s .$$

We now examine slepton production. The differential cross section for the production of charged slepton–antislepton pairs is

$$\frac{d\sigma}{dt}(d\bar{u} \to W^* \to \tilde{l}_L \bar{\tilde{\nu}}_L) = \frac{g_2^4 |D_W(s)|^2}{192\pi s^2} (tu - m_{\tilde{l}_L}^2 m_{\tilde{\nu}_L}^2) . \quad (138)$$

For the $\tilde{l}_L$ pair production, the differential cross section is

$$\frac{d\sigma}{dt}(q\bar{q} \to \gamma^*, Z^* \to \tilde{l}_L \bar{\tilde{l}}_L) = \frac{2\pi\alpha^2}{3s^2}(tu - m_{\tilde{l}_L}^4) \left[\frac{q_l^2 q_q^2}{s^2} + (\alpha_l - \beta_l)^2 (\alpha_q^2 + \beta_q^2) |D_Z(s)|^2 + \frac{2 q_l q_q \alpha_q (\alpha_l - \beta_l)(s - M_Z^2)}{s} |D_Z(s)|^2 \right] , \quad (139)$$

where

$$D_V(s) = \frac{1}{s - M_V^2 + i M_V \Gamma_V} ,$$

$$q_l = -1 , \quad q_\nu = 0 , \quad q_u = \frac{2}{3} , \quad q_d = -\frac{1}{3} ,$$

$$\alpha_l = \frac{1}{4}(3t - c) , \quad \alpha_\nu = \frac{1}{4}(c + t) ,$$

$$\alpha_u = -\frac{5}{12} t + \frac{1}{4} c , \quad \alpha_d = -\frac{1}{4} c + \frac{1}{12} t ,$$

$$\beta_l = \frac{1}{4}(c + t) , \quad \beta_\nu = -\frac{1}{4}(c + t) ,$$

$$\beta_u = -\frac{1}{4}(c + t) , \quad \beta_d = \frac{1}{4}(c + t) ,$$

$$c = \cot\theta_W , \quad t = \tan\theta_W .$$

The differential cross section for the production of a pair of sneutrinos can be obtained by replacing α_l, β_l, q_l, and $m_{\tilde{l}}$ with α_ν, β_ν, 0, and $m_{\tilde{\nu}}$, respectively, while for the $\tilde{l}_R$ pair production, the replacements $\alpha_l - \beta_l \to \alpha_l + \beta_l$ and $m_{\tilde{l}_L} \to m_{\tilde{l}_R}$ must be made. We note that the QCD corrections to the tree-level equations for the squark and gluino production cross sections play a very important role [56].

4.3 Superparticle decays

Superparticle decay widths strongly depend on the mass ratios. Here, we only give the main decay modes for superparticles. The formulas for the superparticle decay widths can be found in Ref. [57]. We begin with gluino and squark decays. When $m_{\tilde{g}} > m_{\tilde{q}}$, the main decay modes are

$$\tilde{g} \to \tilde{q}_i \bar{q}_i, \bar{\tilde{q}}_k q_k , \quad (140)$$

$$\tilde{q}_k \to \tilde{\chi}_i^0 q_k , \quad (141)$$

$$\tilde{q}_k \to \tilde{\chi}_j^+ q_m, \tilde{\chi}_j^- q_l . \quad (142)$$

For $m_{\tilde{g}} < m_{\tilde{q}}$, the main decay modes are

$$\tilde{q}_i \to \tilde{g} q_i , \quad (143)$$

$$\tilde{g} \to q\bar{q}' \tilde{\chi}_k^+ , \quad (144)$$

$$\tilde{g} \to q' \bar{q} \tilde{\chi}_k^- , \quad (145)$$

$$\tilde{g} \to q\bar{q}\tilde{\chi}_k^0 . \quad (146)$$

Charginos and neutralinos have many decay modes. Especially interesting from the standpoint of detecting SUSY at the LHC are the leptonic modes, e.g.,

$$\tilde{\chi}_1^\pm \to \tilde{\chi}_1^0 l^\pm \nu , \quad (147)$$

$$\tilde{\chi}_1^\pm \to (\tilde{l}_L^\pm \to \tilde{\chi}_1^0 l^\pm)\nu , \quad (148)$$

$$\tilde{\chi}_1^\pm \to (\tilde{\nu} \to \tilde{\chi}_1^0 \nu) l^\pm , \quad (149)$$

$$\tilde{\chi}_1^\pm \to \tilde{\chi}_1^0 (W^\pm \to l^\pm \nu) , \quad (150)$$

$$\tilde{\chi}_2^0 \to \tilde{\chi}_1^0 l^+ l^- , \quad (151)$$

$$\tilde{\chi}_2^0 \to (\tilde{\chi}_1^\pm \to \tilde{\chi}_1^0 l^\pm \nu) l^\mp \nu , \quad (152)$$

$$\tilde{\chi}_2^0 \to (\tilde{l}_{L,R}^\pm \to \tilde{\chi}_1^0 l^\pm) l^\mp . \quad (153)$$

The two-particle modes of the decay of neutralinos and charginos into Higgs bosons are

$$\tilde{\chi}_i^0 \to \tilde{\chi}_j^0 + h(H) , \quad (154)$$

$$\tilde{\chi}_i^0 \to \tilde{\chi}_k^\pm + H^\mp , \quad (155)$$

$$\tilde{\chi}_i^\pm \to \tilde{\chi}_k^0 + H^\pm , \quad (156)$$

$$\tilde{\chi}_i^\pm \to \tilde{\chi}_j^\pm + h(H) . \quad (157)$$

Left-handed sleptons decay mainly into a chargino and a neutralino via two-particle modes:

$$\tilde{l}_L \to l + \tilde{\chi}_i^0 , \quad (158)$$

$$\tilde{l}_L \to \nu_L + \tilde{\chi}_j^- , \quad (159)$$

$$\tilde{\nu}_L \to \nu_L + \tilde{\chi}_i^0 , \quad (160)$$

$$\tilde{\nu}_L \to l + \tilde{\chi}_j^+ . \quad (161)$$

For relatively light sleptons, only the decays into LSPs and appropriate leptons are possible, and hence decays of light sneutrinos are invisible. Heavier sleptons can decay into charginos and other (not LSPs) particles. These decays are very important because they occur due to the large SU(2) coupling constant and can dominate over the direct decay into LSPs. The SU(2) singlet charged sleptons $\tilde{l}_R$ decay only via the U(1) gauge interaction, and in the limit of vanishing Yukawa coupling constants, their decays into charginos are forbidden. Hence, the main mode of left-handed-slepton decays is

$$\tilde{l}_R \to l + \tilde{\chi}_i^0 . \quad (162)$$

In many cases, the decay into LSPs is the predominant decay mode.

4.4 The search for superparticles at the LHC

Squarks and gluinos. The gluino and squark production cross sections at the LHC are the largest, compared to slepton and gaugino production cross sections. Hence, squark and gluino production at the LHC is most interesting from the standpoint of SUSY detection, with the squark and gluino production cross sections being of the order of 1 pb for squark and gluino masses equal to 1 TeV. The decays of squarks and gluinos lead to events with missing transverse energy plus hadronic jets and leptons from decays of charginos and neutralinos [58].

It is natural to break down the signatures used in the search for squarks and gluinos into the following categories [58]:

(1) jets plus E_T^{miss}-events,
(2) 1l plus jets plus E_T^{miss}-events,
(3) 2l plus jets plus E_T^{miss}-events,

(4) 3l plus jets plus E_T^{miss}-events,
(5) 4l plus jets plus E_T^{miss}-events, and
(6) $\geqslant$ 5l plus jets plus E_T^{miss}-events.

Multileptons appear as a result of cascade decays of neutralinos and charginos into W and Z bosons followed by the decays of W and Z bosons into leptons. For instance, dileptonic events with the same or opposite charges of the leptons occur as a result of the cascade events

$$\tilde{g} \to q'\bar{q}\tilde{\chi}_i^{\pm}, \qquad \tilde{\chi}_i^{\pm} \to W^{\pm}\tilde{\chi}_1^0 \to l^{\pm}\nu\tilde{\chi}_1^0, \tag{163}$$

where l stands for both e and μ. Dileptonic events with opposite charges of the leptons occur as a result of the cascade decay

$$\tilde{g} \to q\bar{q}\tilde{\chi}_i^0, \qquad \tilde{\chi}_i^0 \to Z\tilde{\chi}_1^0 \to l^+l^-\tilde{\chi}_1^0. \tag{164}$$

The main conclusion drawn in Refs [59, 34] is that with the mSUGRA model, the LHC will make it possible to detect supersymmetry with squark and gluino masses up to 2–2.5 TeV at the integrated luminosity 100 fb^{-1} (Fig. 13).

The most important signature for detecting squarks and gluinos in the mSUGRA model is that with multijets and E_T^{miss} [signature (1)]. We note that in the case of the MSSM with arbitrary squark and gluino masses, the SUSY discovery potential depends very strongly on the ratios of the LSP, squark, and gluino masses, and this potential diminishes as the LSP mass grows [60]. With the LSP mass close to the squark or gluino mass, it is possible to detect SUSY with squark and gluino masses up to 1.2–1.5 TeV [60] (Fig. 14). We also note that the multileptonic signatures (2)–(6) emerge because of decays of squarks and gluinos into charginos and neutralinos, which differ from LSPs, followed by decays of

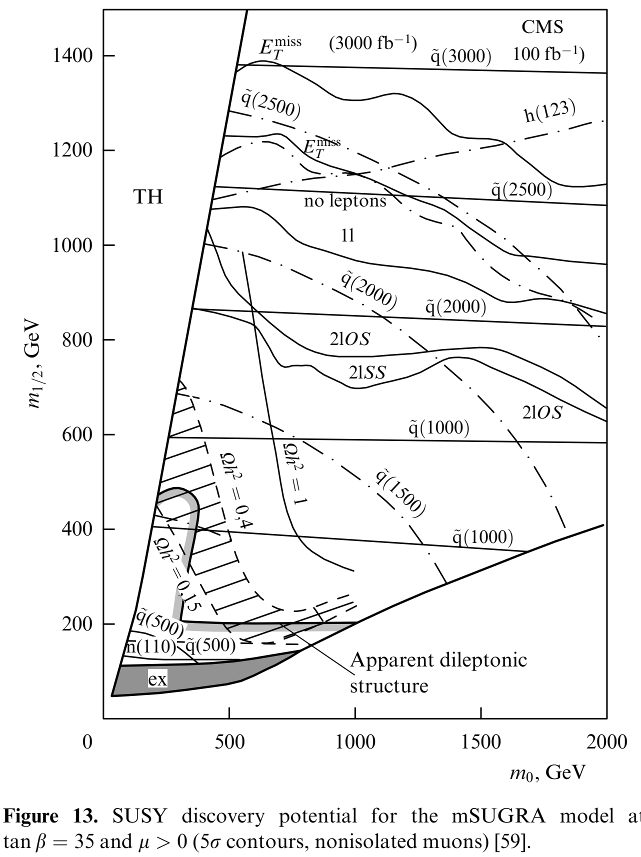

Figure 13. SUSY discovery potential for the mSUGRA model at $\tan\beta = 35$ and $\mu > 0$ (5σ contours, nonisolated muons) [59].

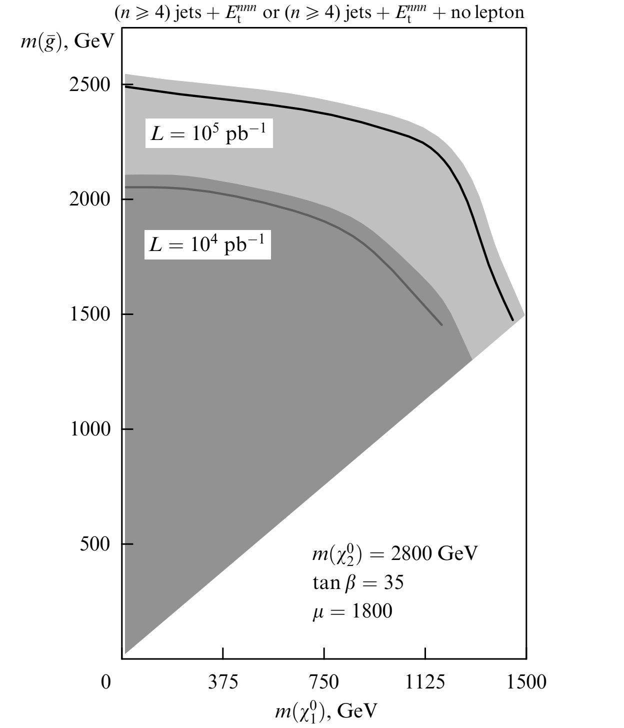

Figure 14. SUSY discovery potential at CMS for different values of $m_{\tilde{\chi}_1^0}$ and $m_{\tilde{g}}$ at $m_{\tilde{q}} = m_{\tilde{g}} + 100$ GeV (the curves correspond to the background level boosted by a factor of 1.5) [60].

charginos and neutralinos into W and Z bosons plus LSPs. However, in the case of nonuniversal chargino masses, a situation may occur where all charginos and neutralinos, with the exception of LSPs, are heavier than gluinos and squarks. Hence, gluinos and squarks would then decay mainly into quarks or gluons plus LSPs, and therefore cascade decays and, as a consequence, multileptons must be negligible.

The search for neutralinos and charginos. Chargino and neutralino pairs produced in the Drell–Yan process $pp \to \tilde{\chi}_1^{\pm}\tilde{\chi}_2^0$ can be detected by leptonic decays $\tilde{\chi}_1^{\mp}\tilde{\chi}_2^0 \to lll + E_T^{\text{miss}}$. Thus, the signature for detecting direct production of charginos and neutralinos is three isolated leptons plus E_T^{miss}. A three-lepton signal is generated by decays (148)–(153), while the undetected neutrino and $\tilde{\chi}_1^0$ in these decays lead to a finite E_T^{miss}. The main background to the three-lepton signature appears because of WZ/ZZ, $t\bar{t}$, $Zb\bar{b}$, and $b\bar{b}$ production followed by the decay into leptonic modes. There may also be a SUSY background, which appears as a result of cascade decays of squarks and gluinos into multileptonic modes.

The typical cutoffs are [59]

(1) three isolated leptons with $p_t^l > 15$ GeV,

(2) veto of hadronic jets with $E_t > 25$ GeV in the region $|\eta| < 3.5$, and

(3) $m_{l\bar{l}} < 81$ GeV or $m_{l\bar{l}} \neq M_Z \pm \delta M_Z$.

The main conclusion is that neutralinos and charginos with masses up to 350 GeV may be detected at the LHC [59]. In addition, the mass difference $M(\tilde{\chi}_2^0) - M(\tilde{\chi}_1^0)$ can be determined by measuring the distribution in the l^+l^- invariant mass, which emerges as a result of the decay $\tilde{\chi}_2^0 \to \tilde{\chi}_1^0 + l^+l^-$ [59].

The search for sleptons. Slepton pairs produced via the Drell–Yan process $pp \to \gamma^*/Z^* \to \tilde{l}^+\tilde{l}^-$ can be detected in their leptonic decays $\tilde{l} \to l + \chi_1^0$. Hence, the typical signature in the search for sleptons at the LHC are events with a dileptonic pair with missing transverse energy and without hadronic jets [59]. With the integrated luminosity 100 fb^{-1}, it will be possible to detect sleptons with masses up to 400 GeV at the LHC [59, 61].

The search for flavor leptonic number violation in sleptonic decays. In the supersymmetric model with the explicit flavor leptonic number violation via SUSY-violating soft massive terms, it is possible to detect flavor leptonic number violation in sleptonic decays [62]. For example, in the case of a finite mixing, $\sin\phi \neq 0$, between a right-handed selectron and a right-handed smuon, the flavor leptonic number is violated in sleptonic decays, i.e., [62]

$$\Gamma(\tilde{\mu}_R \to \mu + \text{LSP}) = \Gamma\cos^2\phi\,, \tag{165}$$

$$\Gamma(\tilde{\mu}_R \to \text{e} + \text{LSP}) = \Gamma\sin^2\phi\,, \tag{166}$$

$$\Gamma(\tilde{\text{e}}_R \to \text{e} + \text{LSP}) = \Gamma\cos^2\phi\,, \tag{167}$$

$$\Gamma(\tilde{\text{e}}_R \to \mu + \text{LSP}) = \Gamma\sin^2\phi\,, \tag{168}$$

$$\Gamma = \frac{g_1^2}{8\pi}\left(1 - \frac{M_{\text{LSP}}^2}{M_{\text{SL}}^2}\right)^2. \tag{169}$$

A typical consequence of finite smuon–selectron mixing is the existence of signal events $\text{e}^{\pm}\mu^{\mp}$ with missing transverse energy, events that emerge as a result of production of slepton pairs followed by decays with flavor leptonic number violation. The possibility of detecting flavor leptonic number violation in sleptonic decays at the LHC has been discussed in Ref. [61]. The main conclusion was that in the most optimistic case of maximum mixing between right-handed sleptons $\tilde{\text{e}}_R$ and $\tilde{\mu}_R$, $\sin\phi = 1/\sqrt{2}$, the detection of flavor leptonic number violation is possible at the LHC for slepton masses up to 275 GeV [61]. Other possibilities of detecting flavor leptonic number violation in sleptonic decays at the LHC have been discussed in Ref. [63].

Measuring superparticle masses. After the discovery of SUSY at the LHC, the main problem will be to separate the different channels that emerge because of cascade decays of SUSY particles and to determine the SUSY parameters (squark, gluino, neutralino, chargino, and slepton masses). In the MSSM, the products of SUSY-particle decays always contain a phantom particle $\tilde{\chi}_1^0$, and hence SUSY particles cannot be reconstructed directly. The most promising approach to measuring the masses of superparticles is to use the kinematical distribution of jets or leptons [64]. For instance, the l^+l^- distribution from the decay $\tilde{\chi}_2^0 \to \tilde{\chi}_1^0\text{l}^+\text{l}^-$ has a kinematical cutoff, which determines the difference $M_{\tilde{\chi}_2^0} - M_{\tilde{\chi}_1^0}$. The distribution from the two-particle decay

$$\tilde{\chi}_2^0 \to \tilde{\text{l}}^{\pm}\text{l}^{\mp} \to \tilde{\chi}_1^0\text{l}^+\text{l}^-$$

has a sharp peak near

$$\sqrt{\frac{(M_{\tilde{\chi}_2^0}^2 - M_{\tilde{\text{l}}}^2)(M_{\tilde{\text{l}}}^2 - M_{\tilde{\chi}_1^0}^2)}{M_{\tilde{\text{l}}}^2}}\,.$$

A larger number of various mass combinations can be determined using longer chains of decays [34, 65]. We also note that as proposed in Ref. [67], the 'hardness' of an event can be characterized by the sum of transverse energies of the four most energetic hadronic jets and the missing transverse energy:

$$E_T^{\text{sum}} = E_T^1 + E_T^2 + E_T^3 + E_T^4 + E_T^{\text{miss}}\,. \tag{170}$$

The value of a local maximum in the E_T^{sum} spectrum for an inclusive SUSY signal ensures good identification of that signal, while the value at a local maximum is related to squark and gluino masses by the formula $M_{\text{peak}} \equiv M_{\text{SUSY}} \approx \min(M_{\tilde{\text{g}}}, M_{\tilde{\text{q}}})$ [64, 66], valid to within 10% in the mSUGRA model. Here, $M_{\tilde{\text{q}}}$ is the average mass of squarks of the first and second generations. By measuring the E_T^{sum} distributions, we can estimate the scale M_{SUSY} with 10 – 20% accuracy.

Supersymmetry breaking via gauge interaction mediation. In models based on supersymmetry violation via gauge interaction mediation [67], the gravitino $\tilde{\text{G}}$ is very light and the phenomenology depends on the type of the next-to-lightest supersymmetric particle (NLSP), which may be either $\tilde{\chi}_1^0$ or a slepton, and the time it takes for them to decay into the gravitino $\tilde{\text{G}}$. In the case where the NLSP is $\tilde{\chi}_1^0$, the main decay follows the scheme $\tilde{\chi}_1^0 \to \tilde{\text{G}}\gamma$, with the result that the SUSY signature contains two energetic isolated photons. If the NLSP is a charged long-lived slepton, it behaves as a nonrelativistic muon with $\beta < 1$. The mass of the long-lived slepton can be determined through the use of muon chambers by measuring the time of flight [34, 68].

4.5 The search for SUSY Higgs bosons

The MSSM has three neutral and one charged Higgs bosons in the spectrum:[4] h, H, A, and $\text{H}^{\pm}$. We note that at the tree level, the MSSM predicts [20] the lightest Higgs boson with a mass smaller than m_Z. But taking the radiative corrections into account [20] may drive the Higgs boson mass up to 135 GeV for stop-quark masses not greater than 1 TeV [21].

In the mSUGRA model, the Higgs sector is mainly described by two parameters, the A-boson mass and $\tan\beta$, the latter being the ratio of the vacuum expectation values of two Higgs bosons. In the limit of a large A-boson mass, the coupling constants for the h boson coincide with those for the SM Higgs boson.

At large values of $\tan\beta$, the H and A bosons decay mainly into $\text{b}\bar{\text{b}}$. However, this mode is not very promising because of the huge $\text{b}\bar{\text{b}}$ background. The decays of H and A into $\tau^+\tau^-$ and $\mu^+\mu^-$ are the most promising modes for detecting A and H bosons [34, 69]. In the MSSM, the decays $\text{H} \to \tau^+\tau^-$ and $\text{A} \to \tau^+\tau^-$ are enhanced at large $\tan\beta$. The production of heavy MSSM Higgs bosons occurs primarily in the reactions $\text{gg} \to H_{\text{SUSY}}$ and $\text{gg} \to \text{b}\bar{\text{b}}\text{H}_{\text{SUSY}}$. The coupling constants for the interaction of the Higgs boson and b-quarks is enhanced at large values of $\tan\beta$, and associative production $\text{gg} \to \text{b}\bar{\text{b}}\text{H}_{\text{SUSY}}$ is predominant (roughly 90% of the total cross section) for $\tan\beta \geqslant 10$ and $M_{\text{H}} \geqslant 300$ GeV. The gluon fusion cross section is determined by quark loops and can be substantially suppressed in the case of strong mixing of stop quarks and small top-quark masses [70]. Because the production mechanism $\text{gg} \to \text{b}\bar{\text{b}}\text{H}_{\text{SUSY}}$ is predominant at large $\tan\beta$, the yield cross sections for the heavy Higgs bosons H and A are insensitive to loop effects.

The light Higgs boson. For SUSY particles heavier than $O(300)$ GeV, the decay widths and the production cross section for the light Higgs boson h are approximately equal to those for the SM Higgs boson, and the most important signature is $\text{h} \to \gamma\gamma$. In addition, the signatures

[4] The lower limits on the masses of the light h and pseudoscalar A bosons produced by LEP 2 experiments are 91.0 and 91.9 GeV, respectively. Moreover, the excluded regions in $\tan\beta$ are $0.5 \leqslant \tan\beta \leqslant 2.4$ for the scenario with maximum mixing and $0.7 \leqslant \tan\beta \leqslant 10.5$ in the absence of mixing [14].

$pp \to t\bar{t}(h \to b\bar{b})$ and $pp \to qq(h \to WW^* \to l^+l'^-\nu\bar{\nu})$ are also important. We note that in the case of light stop quarks with $m_{\tilde{t}_1} \leqslant 200$ GeV and strong mixing of stop quarks, the cross section of the reaction $gg \to h \to \gamma\gamma$ may be heavily suppressed due to destructive interference of top and stop quarks, which may result in the Higgs boson not being detected in this mode. For the most difficult region $m_h \sim m_A \sim m_H \sim 100$ GeV and large values of $\tan\beta$, the use of the reaction $gg \to b\bar{b}h \to b\bar{b}\mu^+\mu^-$ helps to detect the Higgs boson [32, 69, 71].

The heavy neutral A and H bosons. The states $\tau\bar{\tau}$ can be sought in 2-lepton, lepton + τ-jet, and 2 τ-jet final states [32, 34]. For states with one lepton and one τ-jet, a background appears because of the reactions $Z, \gamma^* \to \tau\bar{\tau}$; $t\bar{t} \to \tau\bar{\tau} + X, \tau + X$; and $b\bar{b} \to \tau\bar{\tau} + X, \tau X$. Effective τ-jet identification based on the low multiplicity, narrowness, and insularity of τ-jets in the reaction $H, A \to \tau\tau$ makes it possible to obtain a suppression factor $\geqslant 1000$ for QCD jets. The Higgs boson can be reconstructed from the channel $H \to \tau\tau$ by using the apparent momentum of the τ-lepton (leptons or τ-jets) and the collinear approximation for the neutrinos from τ-decays. The accuracy in determining the Higgs boson mass is estimated at $\leqslant 10\%$ for the $A, H \to \tau\tau$ channel at large values of $\tan\beta$. The A and H bosons may be detected via the $\tau\tau$ decay modes with masses up to 600 – 800 GeV [32, 69, 34] (Fig. 15).

In the MSSM, the branching ratio of $A, H \to \mu\mu$ is very small ($\sim 3 \times 10^{-4}$), but dissociative production in $gg \to b\bar{b}H(A)$ is predominant at large values of $\tan\beta$. The Drell – Yan process $\gamma^*, Z^* \to \mu^+\mu^-$ is the main background and can be suppressed by b-tagging [32]. The accuracy of measuring the Higgs boson mass is expected to be 0.1 – 1.5% for this mode.

Thus, the heavy H and A bosons can be detected at large values of $\tan\beta$ by using the $\tau\tau$ and $\mu\mu$ decay modes. At the LHC, the discovery potential begins at $\tan\beta \geqslant 10$ for $m_A \leqslant 200$ GeV [32]. For $\tan\beta \leqslant 10$, the decays of H and A bosons into superparticles can be used. The channel $A, H \to \tilde{\chi}_2^0\tilde{\chi}_2^0 \to 4l^{\pm} + X$ is the most promising one [72] for detecting heavy neutral bosons if neutralinos and sleptons are sufficiently light, and hence the branching of $\tilde{\chi}_2^0 \to \tilde{l}l \to \tilde{\chi}_1^0 l^+l^-$ is substantial. With this channel, H and A bosons with masses of 200 – 400 GeV could be detected [69, 34].

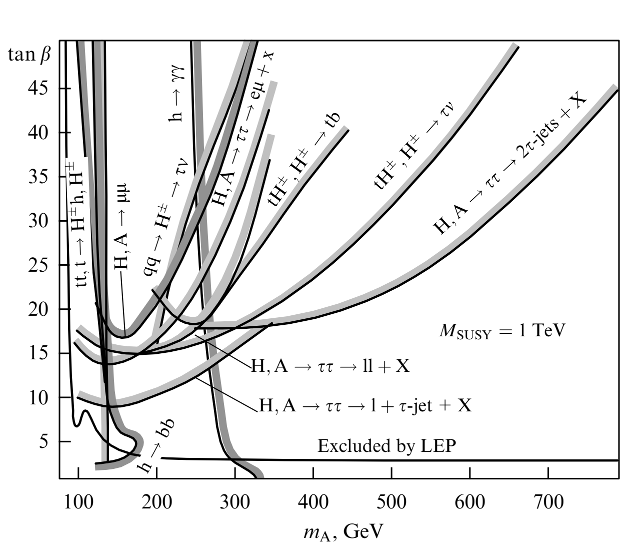

Figure 15. The expected 5σ discovery potential for the MSSM Higgs bosons in the case of maximum mixing in the CMS detector at the total luminosity 30 fb^{-1} [32].

The charged Higgs boson. The search for the charged Higgs boson at the LHC is important for understanding the nature of the Higgs sector. Indeed, the discovery of the charged Higgs boson will be a clear indication that there is physics beyond the SM. For $m_{H^{\pm}} < m_{top}$, the charged Higgs boson $H^{\pm}$ decays primarily into $\tau\nu$. At $m_{H^{\pm}} > 200$ GeV, the decay $H^{\pm} \to tb$ is predominant, but $BR(H^{\pm} \to \nu\tau)$ approaches 0.1 at $m_{H^{\pm}} \geqslant 400$ GeV. For the light charged Higgs boson ($m_{H^{\pm}} < m_{top}$), the main $H^{\pm}$ production mechanism is the production of $t\bar{t}$ followed by the decay $t \to H^{\pm}b$. The use of the decay mode $H^{\pm} \to \tau\nu$ makes it possible to detect $H^{\pm}$ almost irrespective of the value of $\tan\beta$ for the light charged Higgs boson [69, 34]. The heavy charged Higgs boson ($m_{H^{\pm}} > m_{top}$) is produced mainly together with a top quark in the $gb \to tH^{\pm}$ and $gg \to tbH^{\pm}$ processes. In this case, the decay mode $H^{\pm} \to \nu\tau$ is also promising for the detection of $H^{\pm}$. The use of τ-polarization in the decay $H^{\pm} \to \nu\tau$ [73] allows suppressing the background from $t\bar{t}$, Wtb, $W \to \tau\nu$.

For purely hadronic final states in the reaction $gb \to t(H^{\pm} \to \nu\tau)$ with hadronic decays of the top quark, the transverse mass reconstructed from the τ-jet and the E_T^{miss} vector makes it possible to estimate the value of the mass of $H^{\pm}$ with an accuracy better than 10%. The discovery range for this signature is shown in Fig. 15.

The decay $H^{\pm} \to tb$ following the reaction $gb \to tH^{\pm}$ was studied for the signature with one isolated lepton, which is produced in the decay of one of the top quarks, in Refs [69, 34]. Extraction of the signal in these multijet events requires tagging three b-jets, reconstructing leptonic and hadronic decays of top quarks, and reconstructing the Higgs boson mass. The discovery potential for this signature is shown in Fig. 15. We also note that the s-channel production of $H^{\pm}$ in the reaction $q\bar{q}' \to H^{\pm} \to \tau\nu$ can be used to detect $H^{\pm}$ [74], but diminishing the huge background from $q\bar{q}' \to W \to \tau\nu$ is extremely difficult. In determining the mass of the charged Higgs boson, an accuracy of roughly 1 – 2% is expected [32]. Moreover, because $\sigma \sim \tan^2\beta$, $\tan\beta$ can be found with an accuracy better than 7% for $\tan\beta > 20$ and $m_{H^{\pm}} = 250$ GeV [32].

The main conclusion drawn in Refs [32, 69, 34] that concern the search for the MSSM Higgs bosons at the LHC at different values of m_A and $\tan\beta$ is that almost the entire range of m_A and $\tan\beta$ can be studied by the decay modes $h \to \gamma\gamma$ and $h \to b\bar{b}$ at the integrated luminosity 30 fb^{-1}. The heavy H and A bosons will be detected at $\tan\beta \geqslant 10$ via the decay modes $H, A \to \tau\tau, \mu\mu$ for A and H boson masses up to 800 GeV. The reaction $gb \to tH^{\pm}, H^{\pm} \to \tau\nu$ is the most important one in the search for the charged Higgs boson $H^{\pm}$, with the discovery region at $\tan\beta \geqslant 20$ extending to $m_{H^{\pm}} \approx 400$ GeV. The most difficult region $110 \leqslant m_A \leqslant 200$ GeV, $3 \leqslant \tan\beta \leqslant 10$ can be studied by using the decays of superparticles if the neutralinos and sleptons are sufficiently light.

5. The search for new physics beyond the SM and MSSM

There are many models that differ from the SM and MSSM. Some of these are briefly discussed below.

5.1 Extra dimensions

Recently, there has been an upsurge of interest in models that involve extra dimensions [75–81]. The main hope is here that the models with a large compactification radius $R_c \geqslant O(1)$ TeV^{-1} of extra dimensions will help to explain the hierarchy between the electroweak and Planck scales. In such models, the new physics may manifest itself on a scale of 1 TeV and can therefore be discovered at the LHC.

In the Arkani-Hamed – Dimopoulos – Dvali (ADD) model [75], the metric has the form

$$ds^2 = g_{\mu\nu}(x)\,dx^\mu\,dx^\nu + \eta_{ab}(x,y)\,dy^a\,dy^b\,, \qquad (171)$$

where $\mu,\nu = 0,1,2,3$ and $a,b = 1,\ldots,d$. All the d extra dimensions are compactified with a characteristic compactification size R_c. The relation between the fundamental mass scale (M_D) in dimension $D = 4 + d$ and the four-dimensional Planck scale $M_{\rm Pl}$ can be written as

$$M_{\rm Pl}^2 = V_d\,M_D^{2+d}\,, \qquad (172)$$

where V_d is the volume of the compactified dimensions [$V_d = (2\pi R_c)^d$ for the toroidal shape of the extra dimensions]. The ADD model involves two free parameters, the number d of extra dimensions and the fundamental scale M_D. The condition $M_D \sim 1$ TeV implies that the compactification radius R_c^{-1} varies from 10^{-3} eV to 10 MeV as d varies from 2 to 6. In the ADD model, all SM gauge fields and matter fields are placed on a three-dimensional brane embedded in the $(3+d)$-dimensional space, and only gravity 'propagates' in the bulk $(3+d)$-volume. This means that the matter energy – momentum tensor can be written as

$$T_{AB}(x,y) = \eta_A^\mu \eta_B^\nu T_{\mu\nu}(x)\delta(y)\,, \qquad (173)$$

where $A,B = 0,1,\ldots,3+d$. The Lagrangian describing the coupling of gravitons to matter is given by

$$L_g = -\frac{1}{\bar{M}_{\rm Pl}}\,G_{\mu\nu}^{(n)}T_{\mu\nu}\,, \qquad (174)$$

where n denotes the Kaluza – Klein (KK) excitation level and $\bar{M}_{\rm Pl} = M_{\rm Pl}/\sqrt{8\pi} = 2.4\times10^{18}$ GeV. The explicit form of Lagrangian (174) suggests that the coupling constants determining the interaction between graviton excitations and matter are universal and very small. The masses of the graviton KK excitations are

$$m_n = \frac{\sqrt{(n_a n^a)}}{R_c}\,, \qquad (175)$$

where $n_a = (n_1, n_2, \ldots, n_d)$. The mass splitting $\Delta m \sim R_c^{-1}$ is very small, and we therefore have an almost continuous spectrum of gravitons. The production cross section for a KK graviton with a mass $m_n \leqslant E$ is given by

$$\sigma_{\rm KK} \sim \frac{E^d}{M_D^{d+2}}\,. \qquad (176)$$

The lifetime of a massive graviton is [75]

$$\tau_n \sim \frac{1}{M_{\rm Pl}}\left(\frac{M_{\rm Pl}}{m_n}\right)^3. \qquad (177)$$

Hence, KK gravitons behave as massive, almost stable, noninteracting particles with spin equal to 2. The typical signature in the search for KK gravitons is the imbalance in the transverse energy of the final states with a continuous distribution in $E_T^{\rm miss}$. The signature that is most promising in the search for graviton KK excitations at the LHC is related to the reaction pp $\to$ jet $+ E_T^{\rm miss}$. We note that at the quark – gluon level, the subprocess gq $\to$ q$G^{(n)}$ provides the main contribution. The main background is from the reactions Z + jet and Z $\to \nu\bar{\nu}$. The use of this signature will make it possible to discover the extra dimensions at the LHC (ATLAS) for the inverse radius smaller than 9 TeV [34]. A very interesting signature for direct production of massive gravitons is provided by the process pp $\to \gamma + E_T^{\rm miss}$, which can be used as an independent check, although with a much smaller cross section. The SM background is mainly from the reaction pp $\to \gamma$(Z $\to \nu\bar{\nu}$).

Another prediction of the ADD model states that taking the graviton resonances into account modifies the SM cross sections at large momentum transfers (e.g., the cross section of lepton pair production). At the tree level, the contribution of massive gravitons to the matrix element is proportional to

$$M \propto \frac{1}{\bar{M}_{\rm Pl}^2}\sum_n \frac{1}{s - m_n^2}\,. \qquad (178)$$

The sum in the right-hand side of (178) diverges for $d \geqslant 2$, and the cutoff M_c should be calculable in the complete theory (at least theoretically). The crude estimate $M \propto 1/M_c^4$ is commonly used in estimating the lower limit on M_c, which can be extracted from the LHC data. Diphoton and Drell – Yan production schemes lead to a sensitivity for M_c up to 7.4 TeV at the LHC.

In the Randall – Sundrum (SR) model [76], gravity exists in the five-dimensional anti-de Sitter space with a single extra dimension compactified on the orbifold S^1/Z_2. The metric has the form

$$ds^2 = \exp\left(-2k|y|\right)\eta_{\mu\nu}\,dx^\mu\,dx^\nu + dy^2\,, \qquad (179)$$

where $y = r_c\theta$ $(0 \leqslant \theta \leqslant \pi)$, r_c is the 'radius' of the extra dimension, and the parameter k determines the scalar curvature of the space. The five-dimensional action integral yields the relation

$$\bar{M}_{\rm Pl}^2 = \frac{M_5^3}{k}\left[1 - \exp\left(-2kr_c\pi\right)\right], \qquad (180)$$

which implies that $k \sim \bar{M}_5 \sim \bar{M}_{\rm Pl}$. In the ADD model, there are two three-dimensional branes with equal but opposite tensions; one is located at the point $y = \pi r_c$ (and is known as the TeV brane) and the other at the point $y = 0$ (and is known as the Planck brane). All SM fields are on the TeV brane, while gravity propagates along the extra dimension. Using the linear expansion of the metric

$$g_{\mu\nu} = \exp\left(-2ky\right)\left(\eta_{\mu\nu} + \frac{2}{M_5^{3/2}}\,h_{\mu\nu}\right), \qquad (181)$$

we obtain the coupling of gravitons to the SM fields,

$$L = -\frac{1}{\bar{M}_{\rm Pl}}\,T^{\mu\nu}h_{\mu\nu}^{(0)}(x) - \frac{1}{\Lambda_\pi}\sum_n T^{\mu\nu}h_{\mu\nu}^{(n)}(x)\,, \qquad (182)$$

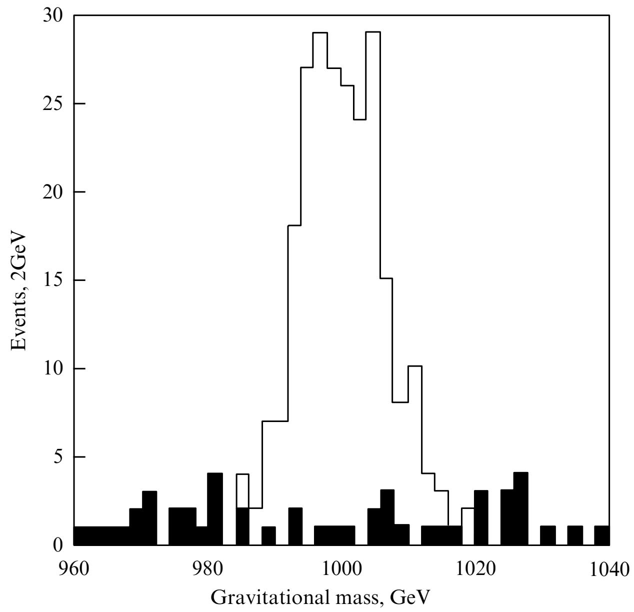

Figure 16. Distribution in the e^+e^- invariant mass for the signal (□) and background (■) from a graviton resonance with a mass of 1 TeV and integrated luminosity of 100 fb^{-1} at the ATLAS detector [34].

where $\Lambda_\pi \sim \bar{M}_{\rm Pl} \exp(-kr_{\rm c}\pi)$. The coupling constants of the massive states are suppressed by Λ_π^{-1}, while the zero mode has the ordinary coupling constant $\bar{M}_{\rm Pl}^{-1}$. The physical scale on the TeV brane is of the order of 1 TeV for $kr_{\rm c} \sim 12$. The KK-resonance graviton masses are given by the formula

$$m_n = kx_n \exp(-kr_{\rm c}\pi)\,, \tag{183}$$

where x_n are the zeros of the Bessel function $J_1(x)$. In the RS model [76], the first graviton excitation has a mass $O(1)$ TeV and decays into jets, leptons, or photons. The most promising mode for detecting a graviton resonance at the LHC is the leptonic mode. The reaction $q\bar{q}, gg \to G_{\rm res1} \to l^+l^-$ has been studied in Ref. [82] (Fig. 16). The signal is detected at $M_{\rm G,\,res1} \leqslant 2$ TeV. Measuring the angular distribution of the leptons at $M_{\rm G,\,res1} \leqslant 1.5$ TeV allows confirming that the resonance has spin 2.

Another nontrivial prediction of the RS model is that there exists a relatively light scalar particle known as the radion, usually denoted by Φ. The radion has a mass m_Φ, a scale Λ_Φ, and a parameter ζ characterizing the mixing with the Higgs boson. The coupling of the radion to the SM fields is given by

$$L_{\rm int} = \frac{\Phi}{\Lambda_\Phi}\, T_\mu^\mu({\rm SM})\,, \tag{184}$$

where $\Lambda_\Phi = \langle \Phi \rangle \sim O(1)$ TeV and

$$T_\mu^\mu({\rm SM}) = \sum_f m_{\rm f} \bar{f} f - 2m_{\rm W}^2 W_\mu^+ W^\mu - m_{\rm Z}^2 Z_\mu Z^\mu + m_{\rm H}^2 H^2 + \ldots \tag{185}$$

Radion couplings are very similar to the couplings of the SM Higgs bosons. We note that the radion has anomalous coupling with a pair of gluons (photons), which follows from the trace anomaly of the energy-momentum tensor, in addition to the interaction related to loop diagrams with a top quark,

$$T_\mu^\mu({\rm SM})^{\rm anom} = \sum_a \frac{\beta_a(g_a)}{2g_a}\, F_{\mu\nu}^a F^{a\mu\nu}\,, \tag{186}$$

where

$$\frac{\beta_{\rm QCD}}{2g_{\rm s}} = -\frac{\alpha_{\rm s}}{8\pi}\left(11 - \frac{2n_{\rm f}}{3}\right) \quad \text{and} \quad \frac{\beta_{\rm QED}}{2e} = -\frac{11}{3}\,\frac{\alpha}{8\pi}\,.$$

Because of the anomalous gluon–radion coupling, gluon fusion is the most promising mechanism for radion production in hadronic collisions. In the general case, a Higgs boson can mix with a radion because of a nonvanishing coupling

$$S_\xi = \xi \int {\rm d}^4x\, \sqrt{g_{\rm vis}}\, R(g_{\rm vis}) H^+ H\,, \tag{187}$$

where $R(g_{\rm vis})$ is the Ricci tensor for the induced metric on the apparent brane.

Radion production subprocesses at the LHC are $gg \to \Phi$ (the main channel), $qq' \to W\Phi$, $q\bar{q} \to Z\Phi$, $qq' \to qq'\Phi$, and $q\bar{q} \to t\bar{t}\Phi$. The most interesting radion decay processes that can be used for detecting Φ are $\Phi \to \gamma\gamma, ZZ, hh$. For the heavy radion ($m_\Phi \geqslant 2M_{\rm Z}$), the purest signature is

$$gg \to \Phi \to ZZ \to 4l\,. \tag{188}$$

At the LHC, the discovery potential for the radion depends on the radion mass and is between $\Lambda_\Phi = 1$ TeV and $\Lambda_\Phi = 10$ TeV [34].

In the ADD and RS models, all SM particles are on a brane, while gravitons can propagate in the extra dimensions. But there are no fundamental reasons for the SM particles to reside on a brane. In the scenario studied in Ref. [83], all particles can propagate in the extra dimensions.[5] In the simplest case of a single extra dimension, momentum conservation in the fifth dimension leads to the KK-number conservation after compactification. In view of this, KK states are produced in pairs at the LHC, similarly to the production of supersymmetric particles in models with R-parity conservation. Hence, the LHC phenomenology is determined by pair production of KK quarks and KK gluons:

$$qq' \to q^{(1)}q'^{(1)}\,, \tag{189}$$

$$q\bar{q} \to q^{(1)}\bar{q}^{(1)}\,, \tag{190}$$

$$gg \to g^{(1)}g^{(1)}\,, \tag{191}$$

$$gg, q\bar{q} \to q^{(1)}\bar{q}^{(1)}\,. \tag{192}$$

Each KK quark $q^{(1)}$ decays into a quark and a KK photon $\gamma^{(1)}$, which leads to events with hadronic jets and missing transverse energy, as in the case of the search for supersymmetric particles. Also very interesting is the chain of decays of $q^{(1)}$ into $W^{(1)}$ and $Z^{(1)}$ followed by the decays of $W^{(1)}$ and $Z^{(1)}$ into leptons, which leads to events involving isolated leptonic, hadronic jets, and missing transverse energy, in analogy with the supersymmetric case. At the LHC, it will be possible to detect KK quarks and gluons with masses up to 1.5 TeV [83].

We note that there is also a mixed scenario in which some of the SM particles reside on a brane while other SM particles can propagate in the extra dimensions. For instance, in the

[5] A similar model was proposed in Refs [77, 84].

5DSM model [85], the fifth dimension y is compactified on the orbifold S^1/Z_2, which has two fixed points, at $y = 0$ and $y = \pi R_c$. The SM gauge fields propagate in the extra dimension, and the SM chiral fields are localized at the fixed points [85]. In this model, the first excitation of the gauge bosons may initiate a process of the Drell – Yan type followed by a decay into leptons, $pp \to Z^{(1)} \to l^+l^-$. At the LHC, it will be possible to produce gauge KK bosons with masses up to 6 TeV [86].

In the ADD model, the scale M_D at which gravity becomes strongly coupled is of the order of 1 TeV for $d = 10$. According to this model, the black hole production is possible at $\sqrt{s} \gg 1$ TeV. Intermediate states with black holes are expected to dominate in the scattering s-channel, because in string theory, the number of such states increases with the black hole mass faster than the number of states in perturbation theory [87]. The Schwarzschild radius of a $(4+d)$-dimensional black hole with mass M_{BH} and spin $J = 0$ is given by [88]

$$R_S(M_{BH}) = \frac{1}{M_D}\left(\frac{M_{BH}}{M_D}\right)^{1/(1+d)} . \tag{193}$$

The cross section of the black hole production by partons a and b is usually assumed to have the simplest geometric form [87]

$$\sigma_{ab \to BH}(s) \approx \pi R_S^2(s) . \tag{194}$$

This cross section rapidly grows with the energy. For gravity, which becomes strongly coupled at the TeV scale, black hole production will be the main process at the LHC. The experimental signature produced by the decay of black holes is very special in the ADD model [81]:

- favor-blind (thermal) processes;
- hard, direct charged leptons and photons (with the energy not lower than 100 GeV);
- hadron-to-lepton activity ratio close to 5 : 1;
- complete cutoff of hadronic jets with $p_T > R_S^{-1}$; and
- low missing transverse energy.

This signature has an almost vanishing background. The LHC discovery potential for black holes is at its maximum for the $e/\mu + X$ channel, and scales up to $M_D \leqslant 9$ TeV can be attained [89]. We note that the above scenario may be considered too optimistic and crude (see Ref. [90]). We believe that the possibility of detecting black holes at the LHC is still unclear and further research in this area is needed.

5.2 Additional gauge bosons

Many supersymmetric electroweak models and Grand Unification models, inspired by superstring models and based on extended gauge groups $(SO(10), E_6, \ldots)$, predict the existence of new relatively light neutron vector Z' bosons and charged W' bosons [91]. The LHC discovery potential for a Z' boson depends on the coupling constant for the interaction of a Z' boson and quarks and leptons and on the Z'-boson mass. The Lagrangian describing the Z' boson and its coupling with the SM fields is [91]

$$L_{Z'} = -\frac{1}{4} F'_{\mu\nu}F'^{\mu\nu} - \frac{\sin\chi}{2} F'_{\mu\nu}F^{\mu\nu} + \frac{1}{2} M_{Z'}^2 Z'_\mu Z'^\mu + \delta M^2 Z'_\mu Z^\mu - \frac{e}{2c_W s_W}\sum_i \bar{\psi}_i\gamma^\mu(f_V^i - g_A^i\gamma_5)\psi_i Z'_\mu , \tag{195}$$

where $c_W = \cos\theta_W$ and $s_W = \sin\theta_W$; $F_{\mu\nu}$ and $F'_{\mu\nu}$ are the respective stress tensor fields for the hypercharge and the Z' boson; and the ψ_i are matter fields carrying the Z'-vector and axial charges f_V^i and g_A^i. The mixing angle between the Z and Z' bosons is given by

$$\xi \approx \frac{\delta M^2}{M_Z^2 - M_{Z'}^2} . \tag{196}$$

If the Z' charges depend on the fermion generation, then flavor-changing neutral currents occur at the tree level in the general case. There are severe constraints imposed on the neutral flavor-changing currents by precise measurements, such as the mass difference $K_L - K_S$ and $BR(\mu \to 3e)$. If the Z' coupling commutes with the standard SM gauge group, there are five independent $Z'\bar{\psi}\psi$ coupling constants per generation, and f_V^u, g_A^u, f_V^d, f_V^e, and g_A^e can be chosen as these constants.

Usually, two Z' models are considered. In the first, the effective $SU_L(2) \otimes U_Y(1) \otimes U_{Y'}(1)$ gauge group follows from breaking of the exceptional gauge group E_6:

$$E_6 \to SO(10) \otimes U(1)_\psi \to SU(5) \otimes U_\chi(1) \otimes U_\psi(1) \to SU_c(3) \otimes SU_L(2) \otimes U_Y(1) \otimes U_{Y'}(1) .$$

The new lightest Z' boson is defined as

$$Z' = Z'_\chi \cos\beta + Z'_\psi \sin\beta , \tag{197}$$

where β is the mixing parameter. In the second model, the new Z' boson appears in $SU_L(2) \otimes SU_R(2) \otimes U_{B-L}(1)$ left – right symmetric models. The Z' boson in such models is coupled to a linear combination of the right-chiral and B – L currents. Sometimes, the unrealistic case of a Z' boson with the same coupling constants as those of the SM Z boson is considered as an example.

The width of the decay of a Z' boson into a massless fermion – antifermion pair is given by

$$\Gamma_{Z'}^f = N_c \frac{\alpha M_{Z'}}{12 c_W^2}\left[(f_V^i)^2 + (g_A^i)^2\right] , \tag{198}$$

where N_c is the color factor and α is the effective electromagnetic coupling constant calculated at the $M_{Z'}$ scale ($\alpha \sim 1/128$). In the models under discussion, the Z' boson is usually narrow [91], with the total decay width $\Gamma_t(Z') \sim O(10^{-2})M_{Z'}$ and with $BR(Z' \to e^+e^-) \sim 0.05$.

Quark – antiquark fusion is the main mechanism of Z'-boson production. The production cross section is of the standard form

$$\sigma(pp \to Z' + \ldots) = \sum_i \frac{12\pi^2\Gamma(Z' \to \bar{q}_i q_i)}{9sM_{Z'}}\int_{M_{Z'}^2/s}^1 \frac{dx}{x} \times \left[\bar{q}_{pi}(x,\mu)q_{pi}(x^{-1}M_{Z'}^2 s^{-1},\mu) + q_{pi}(x,\mu)\bar{q}_{pi}(x^{-1}M_{Z'}^2 s^{-1},\mu)\right], \tag{199}$$

where $\bar{q}_{pi}(x,\mu)$ and $q_{pi}(x,\mu)$ are the parton distributions of the antiquark $\bar{q}_i$ and quark q_i in the proton at the normalization point $\mu \sim M_{Z'}$, and $\Gamma(Z' \to \bar{q}_i q_i)$ is the hadronic width of the Z'-boson decay into a quark – antiquark pair with flavor i. The best way to detect the Z' boson is to use the decay modes $Z' \to e^+e^-, \mu^+\mu^-$, jet jet. Studying the angular distribution of lepton pairs makes it possible to gather nontrivial informa-

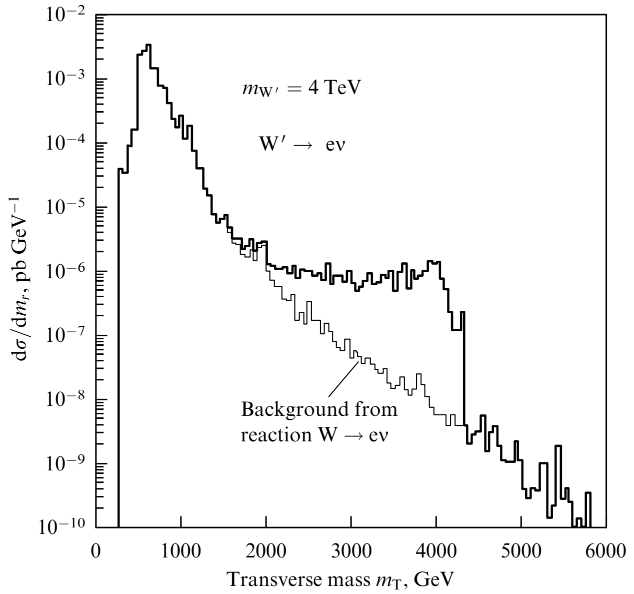

Figure 17. Expected transverse distribution of mass in ATLAS for the decay $W' \to e\nu$ [34].

tion about the coupling constants characterizing the interaction between the Z' boson and quarks and leptons and to confirm that the Z' boson is a spin-1 particle. In the Z'-boson models considered here, a new Z' boson with a mass up to 5 TeV can be detected in the reaction $pp \to Z' \to l^+l^-$ at the integrated luminosity 100 fb^{-1} [8, 34, 92]. Measurements of the lepton forward – backward asymmetry at the Z' peak and in the interference region plus measurements of the Z'-boson rapidity distribution make it possible to distinguish between the different Z'-boson models for Z'-boson masses up to 2 – 2.5 TeV at the integrated luminosity 100 fb^{-1}.

The most promising candidate for W' is the W_R gauge boson in left – right symmetric models [93], which lead to spontaneous violation of parity in electroweak interactions. The gauge group of the left – right symmetric models is

$$SU_c(3) \otimes SU_L(2) \otimes SU_R(2) \otimes U(1)_{B-L}$$

with the SM hypercharge identified as $Y = T_{3R} + \frac{1}{2}(B - L)$, where T_{3R} is the third component of $SU_R(2)$. The fermions are transformed under the gauge group as $q_L(3, 2, 1, 1/3) + q_R(3, 1, 2, 1/3)$ for quarks and $l_L(1, 2, 1, -1) + l_R(1, 1, 2, -1)$ for leptons. The model requires the introduction of a right-handed neutrino ν_R, whose presence plays an important role in explaining the smallness of the neutrino masses on the basis of the 'seesaw' mechanism. The Higgs bidoublet $\Phi(1, 2, 2, 0)$ is usually introduced to generate fermion masses. As in the case of Z'-boson production, the main mechanism of W'-boson production is the quark – antiquark fusion. If the right-handed neutrino ν_R is heavier than W_R, the decay mode $W_R \to \nu_R + l$ is forbidden kinematically, and the decay into two jets is the dominant decay of the W_R boson. If ν_R is lighter than W_R, the decay $W_R \to l_R\nu_R$ is allowed. The decay $\nu_R \to e_R q\bar{q}'$ leads to its jet jet signature. The use of the $pp \to W_R \to e\nu_R \to eeq\bar{q}$ signature allows detecting a W_R boson with masses up to 4.6 TeV at the total luminosity 30 fb^{-1} and $m_{\nu_R} \leqslant 2.8$ TeV [34].

The best way to search for a W' boson with coupling constants to the SM fermions equal to those of the ordinary W boson is to use the leptonic decay mode $W' \to l\nu$. Within this model, a W' boson with a mass up to 6 TeV can be discovered by using leptonic decay modes [34, 8]. By measuring the transverse mass of the W' boson, we can determine its mass to within 50 – 100 GeV [34] (Fig. 17).

5.3 Heavy neutrinos

Left – right symmetric models based on the $SU_c(3) \otimes SU_L(2) \otimes SU_R(2) \otimes U(1)$ gauge group [93] predict the existence of heavy Majorana neutrinos $\nu_{R,e,\mu,\tau}$. For $m_{\nu_R} < M_{W_R}$, such a neutrino can be detected in the decay of the heavy W_R boson via the signature

$$pp \to W_R + ... \to l(\nu_{R,l} \to ljj) + \ldots$$

In view of the Majorana nature of such neutrinos, half of the events involve leptons of the same sign plus two or more hadronic jets from the decay $\nu_{R,l} \to ljj$, which makes the signature with leptons of the same sign most promising both for the ATLAS detector [34] and for the CMS detector [94]. At the integrated luminosity 30 fb^{-1}, it is possible to detect heavy neutrinos with masses up to 2.8 TeV.

5.4 Sgoldstinos

It is well-known that there are models of supergravity symmetry breaking that involve relatively light sgoldstinos (scalar S and pseudoscalar P particles, the superparticles of the goldstino ψ). Such a situation occurs in a number of nonminimal supergravity models [95] and in models of gauge mediation of supersymmetry breaking (see Ref. [96]). In the leading order in $1/F$, where F is the supersymmetry breaking parameter, and in the zeroth order in the MSSM gauge and Yukawa coupling constants, the couplings between the component fields of the goldstino supermultiplet and the MSSM fields were derived in Ref. [97]. They correspond to a process that is most attractive for accelerator applications, a process in which only one of these new particles is in the final state. All the relevant sgoldstino couplings given in Ref. [97] are entirely determined by the MSSM soft supersymmetry breaking terms and the supersymmetry breaking parameter F, while the sgoldstino masses (m_S and m_P) remain free. If the sgoldstino masses are of the order of the electroweak scale and $\sqrt{F} \sim 1$ TeV, the sgoldstino can be detected in the collisions of high-energy particles in supercolliders [98, 99]. Flavor-conserving and flavor-violating couplings of the sgoldstino fields exist. As regards the couplings with flavor conservation, the strongest constraints emerge in astrophysics and cosmology: $\sqrt{F} \geqslant 10^6$ GeV [100, 101], or $m_{3/2} > 600$ eV, for models with $m_{S(P)} < 10$ keV and MSSM soft flavor-conserving terms of the order of the electroweak scale. For intermediate sgoldstino masses (up to several megaelectronvolts), astrophysical constraints and constraints from reactor experiments lead to $\sqrt{F} \geqslant 300$ TeV [101]. For heavier sgoldstinos, low-energy processes (such as rare meson decays) lead to constraints at the level of $\sqrt{F} \geqslant 500$ GeV [101].

Collider experiments have the same sensitivity level for light sgoldstinos as rare meson decays [102 – 105]. The search for heavier sgoldstinos at accelerators leads to similar constraints on the supersymmetry breaking scale. The most powerful existing accelerators (LEP and TEVATRON) yield the constraint of the order of 1 TeV on the supersymmetry breaking scale in models with light sgoldstinos. For instance, an analysis carried out by the DELPHI collaboration [106] yields the constraint $\sqrt{F} > 500 – 200$ GeV for sgoldstino masses $m_{S,P} = 10-150$ GeV and $M_{soft} \sim 100$ GeV. This constraint depends on the parameters of soft supersymmetry breaking in the MSSM, In particular, it is stronger by several hundred gigaelectronvolts in models with degenerate gauginos. At TEVATRON, several events in the $p\bar{p} \to S\gamma(Z)$ channel and approximately 10^4 events in the $p\bar{p} \to S$ channel would be produced at $\sqrt{F} = 1$ TeV and $M_{soft} \sim 100$ GeV at the integrated luminosity 100 pb^{-1} and the sgoldstino mass of the order of 100 GeV [99]. This makes it possible to detect sgoldstinos provided that they decay into photons inside the detector and that $\sqrt{F}$ is not greater than 1.5 – 2 TeV.

In terms of the scalar $SU(3)_c \times SU(2)_L \times U(1)_Y$-fields, the effective Lagrangian is given by [97]

$$\begin{aligned} L_S = &- \sum_{\substack{\text{all gauge}\\ \text{fields}}} \frac{M_\alpha}{2\sqrt{2}F} S F^\alpha_{a\,\mu\nu} F^{\alpha\,\mu\nu}_a \\ &- \frac{\mathcal{A}^L_{ab}}{\sqrt{2}F} y^L_{ab} S(\epsilon_{ij} l^j_a e^c_b h^i_D + \text{h.c.}) \\ &- \frac{\mathcal{A}^D_{ab}}{\sqrt{2}F} y^D_{ab} S(\epsilon_{ij} q^j_a d^c_b h^i_D + \text{h.c.}) \\ &- \frac{\mathcal{A}^U_{ab}}{\sqrt{2}F} y^U_{ab} S(\epsilon_{ij} q^i_a u^c_b h^j_U + \text{h.c.}) \,, \end{aligned} \qquad (200)$$

$$\begin{aligned} L_P = &\sum_{\substack{\text{all gauge}\\ \text{fields}}} \frac{M_\alpha}{4\sqrt{2}F} P F^\alpha_{a\,\mu\nu} \epsilon^{\mu\nu\lambda\rho} F^\alpha_{a\,\lambda\rho} \\ &- \mathrm{i}\, \frac{\mathcal{A}^L_{ab}}{\sqrt{2}F} y^L_{ab} P(\epsilon_{ij} l^j_a e^c_b h^i_D - \text{h.c.}) \\ &- \mathrm{i}\, \frac{\mathcal{A}^D_{ab}}{\sqrt{2}F} y^D_{ab} P(\epsilon_{ij} q^j_a d^c_b h^i_D - \text{h.c.}) \\ &- \mathrm{i}\, \frac{\mathcal{A}^U_{ab}}{\sqrt{2}F} y^U_{ab} P(\epsilon_{ij} q^i_a u^c_b h^j_U - \text{h.c.}) \,, \end{aligned} \qquad (201)$$

$$\begin{aligned} L_{\psi,S,P} = &\, \mathrm{i}\partial_\mu \bar{\psi} \bar{\sigma}^\mu \psi + \partial_\mu S \partial^\mu S \\ &- \frac{1}{2} m_S^2 S^2 + \partial_\mu P \partial^\mu P - \frac{1}{2} m_P^2 P^2 \\ &+ \frac{m_S^2}{2\sqrt{2}F} S(\psi\psi + \bar{\psi}\bar{\psi}) - \mathrm{i}\, \frac{m_S^2}{2\sqrt{2}F} P(\psi\psi - \bar{\psi}\bar{\psi}) \,, \end{aligned} \qquad (202)$$

where M_α are the gaugino masses and $\mathcal{A}_{\alpha\beta}$ and $y_{\alpha\beta}$ are the soft trilinear coupling constants. The values $\mathcal{A}_{ab} = A$ and $y_{ab} \propto \delta_{ab}$ are usually taken for numerical estimates.

At hadronic colliders, sgoldstinos will be mainly produced in the gluon fusion reaction $gg \to S(P)$ [99]. For the relevant parameter ranges, sgoldstinos are expected to decay inside the detector not very far from the collision point. Under the assumption that the supersymmetric partners (excluding the gravitino $\tilde{G}$) are too heavy to be essential in sgoldstinos decays, the following main decay channels are possible:

$$S(P) \to gg, \gamma\gamma, \tilde{G}\tilde{G}, f\bar{f}, \gamma Z, WW, ZZ\,.$$

The respective decay widths have been calculated in Refs [98, 99].

For sgoldstinos that decay into pairs of massless gauge bosons, we have

$$\Gamma(S(P) \to \gamma\gamma) = \frac{M^2_{\gamma\gamma} m^3_{S(P)}}{32\pi F^2}\,, \qquad \Gamma(S(P) \to gg) = \frac{M^2_3 m^3_{S(P)}}{4\pi F^2}\,,$$

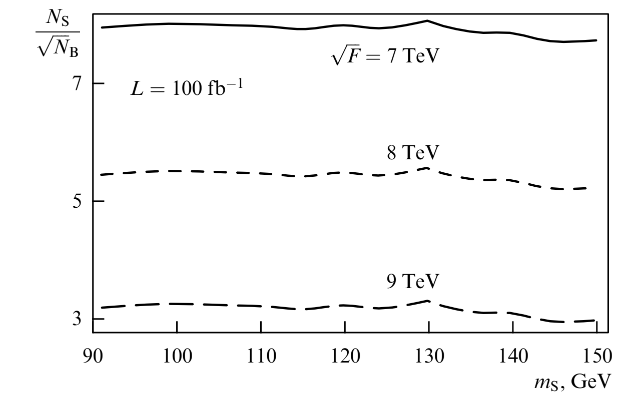

Figure 18. Signal significance for the $\gamma\gamma$ channel as a function of the sgoldstino mass m_S for model II [107].

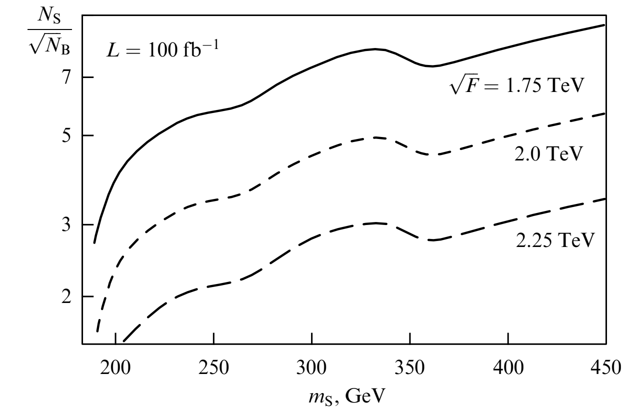

Figure 19. Signal significance for the ZZ channel as a function of the sgoldstino mass m_S for model I [107].

where $M_{\gamma\gamma} = M_1 \cos^2\theta_W + M_2 \sin^2\theta_W$, with θ_W the Weinberg angle. We note that for $M_{\gamma\gamma} \sim M_3$, the gluon mode dominates over the photon mode because of the presence of the color factor $N_c^2 - 1$.

For values of the parameter $\sqrt{F}$ that are interesting from the phenomenological standpoint, the gravitino with its mass in the range $m_{\tilde{G}} = \sqrt{8\pi/3}\, F/M_{Pl} \simeq 10^{-3} - 10^{-1}$ eV is extremely light. The width of the sgoldstino decay into two gravitinos is given by

$$\Gamma(S(P) \to \tilde{G}\tilde{G}) = \frac{m^5_{S(P)}}{32\pi F^2}$$

and becomes comparable to the width of sgoldstino decay into two photons for heavy sgoldstinos, i.e., such that $m_{S(P)} \sim M_{\gamma\gamma}$.

The discovery potential for sgoldstinos at the LHC has been discussed in Ref. [107]. There, two sets of soft supersymmetry breaking parameters were examined (see Table 1). The most reliable signatures with $\gamma\gamma$ and ZZ in the final state have been studied. The main conclusion is that the LHC allows detecting sgoldstinos with $\sqrt{F} \leqslant 2-8$ TeV (Figs 18 and 19).

Table 1. Sets of parameters (in GeV) and the corresponding LHC sensitivity toward the detection of sgoldstinos.

Model	M_1	M_2	M_3	A
I	100	300	500	300
II	300	300	300	300

5.5 Scalar leptoquarks

Scalar leptoquarks (LQ) are particles that have nonzero leptonic and baryonic numbers. Their existence is predicted in many models [108] with the gauge symmetry larger than $SU_c(3) \otimes SU_L(2) \otimes U(1)$. Leptoquarks decay mainly into a quark and a lepton. At the LHC, there can be both pair and single leptoquark production:

$$q + g \to LQ + l \to 2l + j\,, \qquad (203)$$

$$g + g \to LQ + LQ \to 2l + 2j\,. \qquad (204)$$

The single leptoquark production cross section depends on the unknown Yukawa coupling constant that characterizes the interaction of a leptoquark with a lepton and a quark. The pair leptoquark production cross section depends mainly on the leptoquark mass. Pair production of leptoquarks at the LHC was studied in Refs [109, 34]. The main signature is here represented by events with two hadronic jets and two isolated leptons produced as a result of decays of leptoquarks, with the invariant jet-leptonic mass equal to the leptoquark mass. For the first and second generations of leptoquarks, the LHC allows detecting them for masses up to 1.6 TeV at the integrated luminosity 100 fb^{-1} [109, 34].

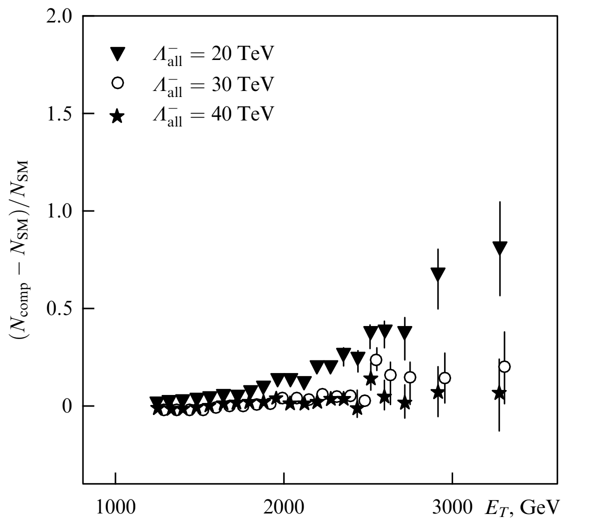

Figure 20. The difference between the SM prediction and the effect of compositeness for the E_T distribution of hadronic jets normalized to the SM prediction. The error corresponds to the integrated luminosity 300 fb^{-1} for different values of scale Λ [34].

5.6 Compositeness

In the SM, quarks and leptons are fundamental point particles. But the growing number of quarks and leptons has led to speculations that these particles have a complex structure and are bound states of components (which became knows preons) that are more fundamental. If quarks have an inner structure, this may manifest itself in a deviation of the cross sections of hadronic jets from those predicted by QCD. This deviation can be parameterized by the coupling

$$\delta L = \frac{4\pi}{\Lambda^2}\, \bar{q}\gamma^{\mu} q \bar{q}\gamma_{\mu} q\,, \qquad (205)$$

which becomes strong at the Λ scale. Comparing the QCD predictions for hadronic jet production cross sections for large values of p_T with the data places a constraint on Λ (Fig. 20). At the LHC (ATLAS) with the integrated luminosity 300 fb^{-1}, a constraint on Λ can be obtained at the level of $\Lambda \geqslant 20$ TeV, provided that the systematic uncertainties are smaller than the statistical ones [34].

The possibility of searching for the quark–lepton coupling

$$\delta L = \frac{4\pi}{\Lambda^2_{\rm ql}}\, \bar{l}\gamma^{\mu} l \bar{q}\gamma_{\mu} q \qquad (206)$$

at the LHC was studied in Ref. [110]. The Drell–Yan process $pp \to q\bar{q} \to \gamma^*/Z^* \to l^+l^-$ was investigated. The coupling in (206) modifies the SM prediction for the Drell–Yan cross sections when the dielectron has a large invariant mass. At the integrated luminosity 100 fb^{-1}, the lower limit $\Lambda_{\rm ql} \geqslant 35$ TeV can be obtained at the LHC (CMS).

5.7 *R*-parity violation

In most works on supersymmetric phenomenology, it is assumed that the MSSM preserves *R*-parity. But at present, there is no profound theoretical justification for the *R*-parity conservation. The phenomenology of supersymmetric models with explicit *R*-parity violation was studied in Ref. [111]. The terms in superpotential (75) violate the baryonic and leptonic numbers and generate an unacceptably large proton decay amplitude, suppressed only by the inverse square of the squark mass. The *R*-parity prohibits the appearance of dangerous terms in superpotential (75). But the *R*-parity conservation is not the only way to build a minimal extension of the SM. The symmetries that are alternatives to the *R*-parity and allow nonvanishing couplings in (75) can easily be found. For instance, under the transformation

$$(Q, U, D) \to -(Q, U, D)\,, \quad (L, E, H_{1,2}) \to +(L, E, H_{1,2})\,, \qquad (207)$$

only the quark superfields change sign. For the superpotential (75) invariant under transformation (207), only the last term *UDD*, which violates the baryonic number, is forbidden. There are similar symmetries that forbid the appearance of terms violating leptonic numbers.

Thus, in the direct search for supersymmetric particles, the phenomenology changes dramatically when *R*-parity violating terms are included in the superpotential. Generally, the mechanisms of production and decay of SUSY particles may then change. In addition to pair production of supersymmetric particles, *R*-odd states may also be produced. If all the supersymmetric particles decay inside the detector, we may no longer have the standard signature with the missing transverse energy $E_T^{\rm miss}$. The LSPs will mainly decay into three-particle final states [111]. But except for the LSPs, all other particles will basically decay, as in the MSSM case, with *R*-parity conservation. We examine the case where an LSP decays inside the detector. If the leptonic number is violated, the SUSY signal contains leptons from LSP decays $\tilde{\chi}^0_1 \to l^+l^-\nu, lq\bar{q}$ [111]. If the baryonic number is violated, the LSP decays into hadronic jets $\tilde{\chi}^0_1 \to qqq$, which results in a large number of jets without missing transverse energy. Extracting such a signal from the huge QCD background would constitute a formidable problem. The SUSY signal could be detected by using cascade decays containing leptons, e.g., $\tilde{\chi}^0_2 \to \tilde{l}^{\pm}l^{\mp} \to qqql^+l^-$.

We also note that a model with superweak R-parity violation and with a relatively long-lived ($t \sim 10^{-1} - 10^{-9}$ s) charged slepton $\tilde{\tau}_R$ (which acts as an LSP) can be built [112]. The phenomenology of such a model is similar to that of the GMSB (gauge mediation of supersymmetry breaking) model [67], with $\tilde{\tau}_R$ acting as a superparticle following the LSP in the mass scale. [6]

5.8 Additional Higgs bosons with large Yukawa coupling constants

A model with many Higgs doublets in which each Higgs isodoublet is related to its own quark via a relatively large Yukawa coupling constant was examined in Ref. [113]. For a large Yukawa coupling constant, the main reaction of the Higgs isodoublet production corresponding to the first or second generation is the quark – antiquark fusion. The phenomenology of Higgs isodoublets corresponding to the third generation is very similar to the phenomenology of the model with two Higgs isodoublets. The Higgs boson production cross section for the quark – antiquark fusion in the approximation of an infinitely narrow resonance is given by the standard formula

$$\sigma(\mathrm{AB} \to \mathrm{H}_{\mathrm{q}_i\mathrm{q}_j} + \mathrm{X}) = \frac{4\pi^2 \Gamma(\mathrm{H}_{\mathrm{q}_i\mathrm{q}_j} \to \bar{\mathrm{q}}_i \mathrm{q}_j)}{9sM_\mathrm{H}} \int_{M_\mathrm{H}^2/s}^{1} \frac{\mathrm{d}x}{x}$$

$$\times \left[\bar{q}_{\mathrm{A}i}(x,\mu) q_{\mathrm{B}j}(x^{-1}M_\mathrm{H}^2 s^{-1},\mu) + q_{\mathrm{A}j}(x,\mu)\bar{q}_{\mathrm{B}i}(x^{-1}M_\mathrm{H}^2 s^{-1},\mu)\right] . \quad (208)$$

Here, $\bar{q}_{\mathrm{A}i}(x,\mu)$ and $q_{\mathrm{A}j}(x,\mu)$ are the parton distributions of the antiquark $\bar{\mathrm{q}}_i$ and the quark q_i in the hadron A at the normalization point $\mu \sim M_\mathrm{H}$, and $\Gamma(\mathrm{H}_{\mathrm{q}_i\mathrm{q}_j} \to \bar{\mathrm{q}}_i\mathrm{q}_j)$ is the width of the hadronic decay of the Higgs boson into a quark – antiquark pair. For the Lagrangian

$$L_\mathrm{Y} = h_{\mathrm{q}_i\mathrm{q}_j} \bar{q}_{\mathrm{L}i} q_{\mathrm{R}j} H_{\mathrm{q}_i\mathrm{q}_j} + \mathrm{h.c.} \quad (209)$$

the width of the hadronic decay of the Higgs boson into massless quarks is

$$\Gamma(\mathrm{H}_{\mathrm{q}_i\mathrm{q}_j} \to \bar{\mathrm{q}}_i\mathrm{q}_j) = \frac{3M_\mathrm{H} h^2_{\mathrm{q}_i\mathrm{q}_j}}{16\pi} . \quad (210)$$

The model being discussed involves Higgs bosons related to both quarks and leptons, and hence the best signature is the search for an electrically neutral Higgs boson decaying into $\mathrm{e}^+\mathrm{e}^-$ or $\mu^+\mu^-$ pairs. For charged Higgs bosons, the best search method is to use the decays of such bosons into charged leptons and neutrinos. The Higgs doublets related to top quarks in the model with a massless neutrino are not related to leptons, and therefore the only way to detect them is to search for a resonance structure in the distribution in the invariant mass of two-jet events. But the accuracy of determining the invariant mass of two jets is approximately 10%, with the result that it is very difficult to detect the Higgs boson at the LHC by measuring the two-jet differential cross section. In the model under discussion, in view of the smallness of the vacuum expectation values for the Higgs isodoublets corresponding to the quarks u, d, s, and c, after the electroweak symmetry breaking, the mass splitting within the Higgs isodoublets is small. Hence, in such a model, the search for a neutral Higgs boson that decays into a leptonic pair is actually the search for the entire Higgs isodoublet. The Drell – Yan process provides the main background in the search for neutral Higgs bosons decaying into leptonic pairs. The main conclusion here is that [113] at the LHC with the integrated luminosity 100 fb^{-1} and the Yukawa coupling constant $h_\mathrm{Y} = 1$, it will be possible to detect such bosons with masses up to 4.5 – 5 TeV.

5.9 Astrophysical applications

We now briefly discuss an interesting suggestion for using the CMS detector in astrophysical applications. [7] One of the basic features of a CMS detector is the presence of a strong magnetic field inside a large volume. This provides a unique possibility of searching for cosmic scalar or pseudoscalar particles, such as the axion, that interact with two photons. The new particles (if they exist, of course) will pass through the hadron calorimeter, which will be used as a veto system that excludes the interaction with cosmic rays, and will then be observed in the electromagnetic calorimeter due to their conversion into photons in the external magnetic fields of the CMS superconducting solenoid. At high energies, the axion – photon conversion is a coherent process inside the CMS detector, which makes it possible to substantially increase the sensitivity to the axion mass up to $0 \leqslant m_\mathrm{a} \leqslant 32\sqrt{E_\mathrm{a}[\mathrm{GeV}]}$, where m_a is the axion mass in electronvolts. The CMS detector will allow limiting the product of the coupling constant of the new particle with two photons and the integrated flux of particles passing through the CMS detector.

6. Conclusion

There is no doubt that the key problem in contemporary experimental high-energy physics is the search for the Higgs boson, the last undiscovered particle of the Standard Model. The LHC will make it possible to detect this boson and to verify its properties. The experimental discovery of the Higgs boson will be a triumph for the idea of renormalizability in local quantum field theory (in a certain sense, this will be the 'experimental proof' of the renormalizability of electroweak interactions). The LHC will allow detecting supersymmetry with squark and gluino masses as large as 2.5 TeV. There is also a small probability of detecting something new in addition to the SM and MSSM (extra dimensions, Z′ bosons, W′ bosons, compositeness, etc.). In any case, after research at the LHC, we will know the mechanism of electroweak gauge symmetry breaking (the Higgs boson or even something more exotic, perhaps) and the main elements of the structure of matter at the TeV scale.

The authors are grateful to their colleagues from the Department of Theoretical Physics of the Institute of Nuclear Research, Russian Academy of Sciences, for fruitful discussions. The work done by N V Krasnikov was supported financially by the Russian Foundation for Basic Research (Grant No. 0.3-02-16933).

[6] We recall that in the GMSB model, the gravitino $\tilde{\mathrm{G}}$ becomes the LSP. The neutralino $\tilde{\chi}_1^0$ or the slepton $\tilde{\tau}_R$ may follow the LSP in mass and be long-lived particles. The $\tilde{\tau}_R$ appears as a 'heavy muon' that passes through the detector with a speed much less than that of light. Its time of flight can be measured and hence its mass $m_{\tilde{\tau}_R}$ can be calculated [68, 34].

[7] S N Gninenko, private communication, to be published.

References

1. Glashow S L *Nucl. Phys.* **22** 579 (1961); Weinberg S *Phys. Rev. Lett.* **19** 1264 (1967); Salam A, in *Elementary Particle Theory* (Ed. N Svartholm) (Stockholm: Almquist & Wiksell, 1964); Politzer H D *Phys. Rev. Lett.* **30** 1346 (1973); Gross D J, Wilczek F *Phys. Rev. Lett.* **30** 1343 (1973)
2. Bogolyubov N N, Shirkov D V *Vvedenie v Teoriyu Kvantovannykh Poleĭ* (Introduction to the Theory of Quantized Fields) (Moscow: Nauka, 1976) [Translated into English (New York: John Wiley, 1979)]
3. Fukuda Y et al. (Super-Kamiokande Collab.) *Phys. Rev. Lett.* **81** 1562 (1998); Eguchi K et al. (KamLAND Collab.) *Phys. Rev. Lett.* **90** 021802 (2003); Ahn M H et al. *Phys. Rev. Lett.* **90** 041801 (2003)
4. Gol'dfand Yu A, Likhtman E P *Pis'ma Zh. Eksp. Teor. Fiz.* **13** 452 (1971) [*JETP Lett.* **13** 323 (1971)]; Volkov D V, Akulov V P *Pis'ma Zh. Eksp. Teor. Fiz.* **16** 621 (1972) [*JETP Lett.* **16** 438 (1972)]; Wess J, Zumino B *Phys. Lett. B* **49** 52 (1974)
5. Barbieri R *Riv. Nuovo Cimento* **11** 1 (1988); Lahanas A B, Nanopoulos D V *Phys. Rep.* **145** 1 (1987); Haber H E, Lane G L *Phys. Rep.* **117** 75 (1985); Nilles H P *Phys. Rep.* **110** 1 (1984)
6. Weinberg S *Phys. Rev. D* **19** 1277 (1979); Susskind L *Phys. Rev. D* **20** 2619 (1979); Dimopoulos S, Susskind L *Nucl. Phys. B* **155** 237 (1979); Eichten E, Lane K *Phys. Lett. B* **90** 125 (1980)
7. The Large Hadron Collider, CERN/AC/95-05
8. CMS, Technical Proposal, CERN/LHCC/94-38
9. ATLAS, Technical Proposal, CERN/LHCC/94-43
10. ALICE, Technical Proposal, CERN/LHCC/95-71
11. LHC-B, Technical Proposal, CERN/LHCC/95-XX
12. Krasnikov N V, Matveev V A *Fiz. Elem. Chastits At. Yadra* **28** 1125 (1997) [*Phys. Part. Nucl.* **28** 441 (1997)]; *Teor. Mat. Fiz.* **132** 349 (2002) [*Theor. Math. Phys.* **132** 1189 (2002)]
13. Higgs P W *Phys. Lett.* **12** 132 (1964); Englert F, Brout R *Phys. Rev. Lett.* **13** 321 (1964)
14. The LEP working group for Higgs boson searches, CERN-EP/2001-055
15. Okun' L B *Leptony i Kvarki* (Leptons and Quarks) (Moscow: Nauka, 1981) [Traslated into English (Amsterdam: North-Holland, 1984)]; Cheng T-P, Li L-F *Gauge Theory of Elementary Particle Physics* (Oxford: Clarendon Press, 1984); Pokorski S *Gauge Field Theories* (Cambridge: Cambridge Univ. Press, 1987); Bailin D, Love A *Introduction to Gauge Field Theory* (Bristol: A. Hilger, 1986); Borodulin V I, Rogalyov R N, Slabospitsky S R, Preprint 95-50 (Protvino: IHEP, 1995); Gunion J F et al. *The Higgs Hunter's Guide* (Redwood City, CA: Addison-Wesley, 1990)
16. Hagiwara K et al. (Particle Data Group) "Review of particle physics" *Phys. Rev. D* **66** 010001 (2002)
17. Grunewald M W *Nucl. Phys. B Proc. Suppl.* **117** 280 (2003); hep-ex/0210003
18. Cabibbo N et al. *Nucl. Phys. B* **158** 295 (1979); Lindner M *Z. Phys. C* **31** 295 (1986)
19. Krasnikov N V *Yad. Fiz.* **28** 549 (1978) [*Sov. J. Nucl. Phys.* **28** 279 (1978)]; Hung P Q *Phys. Rev. Lett.* **42** 873 (1979); Politzer H D, Wolfram S *Phys. Lett. B* **82** 242 (1979); Ansel'm A A *Pis'ma Zh. Eksp. Teor. Fiz.* **29** 590 (1979) [*JETP Lett.* **29** 590 (1979)]; Lindner M, Sher M, Zaglauer H W *Phys. Lett. B* **228** 139 (1989)
20. Ellis J, Ridolfi G, Zwirner F *Phys. Lett. B* **257** 83 (1991); Haber H E, Hempfling R *Phys. Rev. Lett.* **66** 1815 (1991); Yamada A *Phys. Lett. B* **263** 233 (1991); Barbieri R, Frigeni M, Caravaglios F *Phys. Lett. B* **258** 167 (1991); Chankowski P H, Pokorski S, Rosiek J *Phys. Lett. B* **274** 191 (1992)
21. Degrassi G et al. *Eur. Phys. J. C* **28** 133 (2003)
22. Krasnikov N V, Pokorski S *Phys. Lett. B* **288** 184 (1992); Díaz M A, ter Veldhuis T A, Weiler T J *Phys. Rev. Lett.* **74** 2876 (1995)
23. Cray N et al. *Z. Phys. C* **48** 673 (1990)
24. Spira M *Fortschr. Phys.* **43** 203 (1998)
25. Ellis J, Gaillard M K, Nanopoulos D V *Nucl. Phys. B* **106** 292 (1976)
26. Spira M et al. *Nucl. Phys. B* **453** 17 (1995); Inami T, Kubota T, Okada Y *Z. Phys. C* **18** 69 (1983)
27. Chetyrkin K G, Kniehl B A, Steinhauser M *Phys. Rev. Lett.* **79** 353 (1997)
28. Krasnikov N V, Matveev V A *Fiz. Elem. Chastits At. Yadra* **31** 525 (2000) [*Phys. Part. Nucl.* **31** 255 (2000)]; hep-ph/9909490
29. Cahn R N, Dawson S *Phys. Lett. B* **136** 196 (1984); Hikasa K-I *Phys. Lett. B* **164** 385 (1985); Altarelli G, Mele B, Pitolli F *Nucl. Phys. B* **287** 205 (1987); Han T, Valencia G, Willenbrock S *Phys. Rev. Lett.* **69** 3274 (1992)
30. Glashow S L, Nanopoulos D V, Yildiz A *Phys. Rev. D* **18** 1724 (1978)
31. Kunszt Z *Nucl. Phys. B* **247** 339 (1984); Gunion J F *Phys. Lett. B* **261** 510 (1991); Marciano W J, Paige F E *Phys. Rev. Lett.* **66** 2433 (1991)
32. Kinnunen R, CMS CR 2002/020; Lassila-Perini, CMS CR 2001/018
33. Bityukov S I, Krasnikov N V *Mod. Phys. Lett. A* **13** 3235 (1998)
34. ATLAS Collaboration, ATLAS Detector and Physics Performance, Technical Design Report, CERN/LHCC/99-14
35. Dubinin M N, Ilyin V A, Savrin V I, CMS Note 1997/101
36. Dittmar M, Dreiner H *Phys. Rev. D* **55** 167 (1997)
37. Branson J G et al. (ATLAS Collab., CMS Collab.), hep-ph/0110021
38. Green D et al., CMS Note 1998/089
39. Rainwater D, Zeppenfeld D *JHEP* **9712** 005 (1997)
40. Rainwater D, Zeppenfeld D, Hagiwara K *Phys. Rev. D* **59** 014037 (1999)
41. Rainwater D, Zeppenfeld D, Hagiwara K, hep-ph/9808468
42. Cahn R N et al. *Phys. Rev. D* **35** 1626 (1987); Kleiss R, Stirling W J *Phys. Lett. B* **200** 193 (1988)
43. Dubinin M N, CMS Note 2001/022
44. Poggioli L, ATLAS Internal Note, PHYS-No-066 (1995)
45. Wess J, Bagger J *Supersymmetry and Supergravity* (Princeton, NJ: Princeton Univ. Press, 1983); West P *Introduction to Supersymmetry and Supergravity* (Singapore: World Scientific, 1986)
46. Green M B, Schwarz J H, Witten E *Superstring Theory* (Cambridge: Cambridge Univ. Press, 1987)
47. Nilles H P *Phys. Lett. B* **115** 193 (1982); Barbieri R, Ferrara S, Savoy C A *Phys. Lett. B* **119** 343 (1982); Cremmer E, Fayet P, Girardello L *Phys. Lett. B* **122** 41 (1983); Ibáñez L *Phys. Lett. B* **118** 73 (1982); Chamseddine A H, Arnowitt R, Nath P *Phys. Rev. Lett.* **49** 970 (1982)
48. Kazakov D I, hep-ph/0012288
49. Fayet P *Phys. Lett. B* **69** 489 (1977); Salam A, Strathdee J *Nucl. Phys. B* **87** 85 (1975)
50. Dreiner H, Ross G G *Nucl. Phys. B* **365** 597 (1991); Enqvist K, Masiero A, Riotto A *Nucl. Phys. B* **373** 95 (1992); Barger V et al. *Phys. Rev. D* **53** 6407 (1996)
51. Dine M, Nelson A E *Phys. Rev. D* **48** 1277 (1993); Dine M, Nelson A E, Shirman Y *Phys. Rev. D* **51** 1362 (1995); Dine M et al. *Phys. Rev. D* **53** 2658 (1996)
52. Polonsky N, Pomarol A *Phys. Rev. Lett.* **73** 2292 (1994)
53. Krasnikov N V, Popov V V, hep-ph/9611298
54. Ibáñez L E, López C, Muñoz C *Nucl. Phys. B* **256** 218 (1985)
55. Eichten E et al. *Rev. Mod. Phys.* **56** 579 (1984)
56. Beenakker W et al. *Phys. Rev. Lett.* **74** 2905 (1995); *Z. Phys. C* **69** 163 (1995); *Nucl. Phys. B* **492** 51 (1997)
57. Baer H et al. *Phys. Lett. B* **161** 175 (1985); Gamberini G *Z. Phys. C* **30** 605 (1986); Baer H et al. *Phys. Rev. D* **36** 96 (1987); Gamberini G et al. *Phys. Lett. B* **203** 453 (1988); Barnett R M, Gunion J F, Haber H E *Phys. Rev. D* **37** 1892 (1988); Bartl A et al. *Z. Phys. C* **52** 477 (1991)
58. Baer H et al. *Mod. Phys. A* **4** 4111 (1989)
59. Abdullin S et al., CMS Note 1998/006
60. Bityukov S I, Krasnikov N V *Phys. Lett. B* **469** 149 (1999); *Yad. Fiz.* **65** 1374 (2002) [*Phys. At. Nucl.* **65** 1341 (2002)]; hep-ph/0210269
61. Krasnikov N V *Pis'ma Zh. Eksp. Teor. Fiz.* **65** 139 (1997) [*JETP Lett.* **65** 148 (1997)]; hep-ph/9611282; Bityukov S I, Krasnikov N V *Yad. Fiz.* **62** 1288 (1999) [*Phys. At. Nucl.* **62** 1213 (1999)]; hep-ph/9806504
62. Krasnikov N V *Mod. Phys. Lett. A* **9** 791 (1994); *Phys. Lett. B* **388** 783 (1996); Arkani-Hamed N et al. *Phys. Rev. Lett.* **77** 1937 (1996)
63. Agashe K, Graesser M *Phys. Rev. D* **61** 075008 (2000); Hinchliffe I, Paige F E *Phys. Rev. D* **63** 115006 (2001); Hisano J, Kitano R, Nojiri M M, hep-ph/0202129; Porod W, Majerotto W, hep-ph/0210326; Kalinowski J *Acta Phys. Pol. B* **33** 2613 (2002); hep-ph/0207051
64. Hinchliffe I et al. *Phys. Rev. D* **55** 5520 (1997)
65. Alessia A, CMS CR 2002/022
66. Tovey D R *Phys. Lett. B* **498** 1 (2001)

67. Giudice G F, Rattazzi R *Phys. Rep.* **322** 419 (1999); Gorbunov D S, Dubovskiĭ S L, Troitskiĭ S V *Usp. Fiz. Nauk* **169** 705 (1999) [*Phys. Usp.* **42** 623 (1999)]
68. Wrochna G, CMS CR 2002/015
69. Denegri D et al., CMS Note 2001/032
70. Djouadi A *Phys. Lett. B* **435** 101 (1998)
71. Boos E, Djouadi A, Nikitenko A *Phys. Lett. B* **578** 384 (2004); hep-ph/0307079
72. Abdullin S, Denegri D, Moortgat F, CMS Note 2001/042
73. Roy D P *Phys. Lett. B* **459** 607 (1999)
74. Slabospitsky S, hep-ph/0203094
75. Arkani-Hamed N, Dimopoulos S, Dvali G *Phys. Lett. B* **429** 263 (1998); *Phys. Rev. D* **59** 086004 (1999)
76. Randall L, Sundrum R *Phys. Rev. Lett.* **83** 3370, 4690 (1999)
77. Antoniadis I et al. *Phys. Lett. B* **436** 257 (1998); Antoniadis I, Benakli K *Phys. Lett. B* **326** 69 (1994); Antoniadis I, Benakli K, Quirós M *Phys. Lett. B* **331** 313 (1994); Antoniadis I *Phys. Lett. B* **246** 377 (1990)
78. Krasnikov N V *Phys. Lett. B* **273** 246 (1991)
79. Giudice G F, Rattazzi R, Wells J D *Nucl. Phys. B* **544** 3 (1999)
80. Rubakov V A *Usp. Fiz. Nauk* **171** 913 (2001) [*Phys. Usp.* **44** 871 (2001)]
81. Hewett J, Spiropulu M *Annu. Rev. Nucl. Part. Sci.* **52** 397 (2002); hep-ph/0205106; Kisselev A V, hep-ph/0303090; Cheung K, hep-ph/0305003
82. Traczyk P, Wrochna G, CMS IN 2002/061; Lemaire M-C, Pansart J-P, CMS IN 2002/63
83. Cheng H-C, Matchev K T, Schmaltz M *Phys. Rev. D* **66** 036005, 056006 (2002)
84. Appelquist T, Cheng H-C, Dobrescu B A *Phys. Rev. D* **64** 035002 (2001)
85. Pomarol A, Quirós M *Phys. Lett. B* **438** 255 (1998); Masip M, Pomarol A *Phys. Rev. D* **60** 096005 (1999)
86. Rizzo T G *Phys. Rev. D* **61** 055005 (2000); Antoniadis I, Benakli K, Quirós M *Phys. Lett. B* **460** 176 (1999)
87. Giddings S B, Thomas S *Phys. Rev. D* **65** 056010 (2002)
88. Myers R C, Perry M J *Ann. Phys.* (New York) **172** 304 (1986)
89. Dimopoulos S, Landsberg G *Phys. Rev. Lett.* **87** 161602 (2001)
90. Han T, Kribs G D, McElrath B *Phys. Rev. Lett.* **90** 031601 (2003); Kotwal A V, Hays C *Phys. Rev. D* **66** 116005 (2002); Argyres P C, Dimopoulos S, March-Russell J *Phys. Lett. B* **441** 96 (1998); Casadio R, Harms B *Int. J. Mod. Phys. A* **17** 4635 (2002); Cavaglià M, Das S, Maartens R *Class. Quantum Grav.* **20** L205 (2003); hep-ph/0305223
91. Hewett J L, Rizzo T G *Phys. Rep.* **183** 193 (1989); Leike A *Phys. Rep.* **317** 143 (1999)
92. Dittmar M, Nicollerat A-S, Djouadi A *Phys. Lett. B* **583** 111 (2004); Dittmar M, Djouadi A, Nicollerat A-S, hep-ph/0307020
93. Pati J C, Salam A *Phys. Rev. D* **10** 275 (1974); Mohapatra R N, Pati J C *Phys. Rev. D* **11** 566 (1975); Senjanovic G, Mohapatra R N *Phys. Rev. D* **12** 1502 (1975)
94. Gninenko S N et al., hep-ph/0301140
95. Ellis J, Enqvist K, Nanopoulos D V *Phys. Lett. B* **147** 99 (1984); **151** 357 (1985)
96. Giudice G F, Rattazzi R *Phys. Rep.* **322** 419 (1999); Gorbunov D S, Dubovskiĭ S L, Troitskiĭ S V *Usp. Fiz. Nauk* **169** 705 (1999) [*Phys. Usp.* **42** 623 (1999)]
97. Gorbunov D S, Semenov A V, LAPTH-884/01
98. Perazzi E, Ridolfi G, Zwirner F *Nucl. Phys. B* **574** 3 (2000)
99. Perazzi E, Ridolfi G, Zwirner F *Nucl. Phys. B* **590** 287 (2000)
100. Nowakowski M, Rindani S D *Phys. Lett. B* **348** 115 (1995)
101. Gorbunov D S *Nucl. Phys. B* **602** 213 (2001)
102. Dicus D A, Nandi S, Woodside J *Phys. Rev. D* **41** 2347 (1990)
103. Dicus D A, Roy P *Phys. Rev. D* **42** 938 (1990)
104. Dicus D A, Nandi S, Woodside J *Phys. Rev. D* **43** 2951 (1991)
105. Dicus D A, Nandi S *Phys. Rev. D* **56** 4166 (1997)
106. Abreu P et al. *Phys. Lett. B* **494** 20 (2000)
107. Gorbunov D S, Krasnikov N V *JHEP* **0207** 043 (2002); hep-ph/0203078
108. Pati J C, Salam A *Phys. Rev. D* **10** 275 (1974); Buchmüller W, Rückl R, Wyler D *Phys. Lett. B* **191** 442 (1987); Abbott L F, Farhi E *Phys. Lett. B* **101** 69 (1981)
109. Wrochna G, CMS CR-1996/003; Abdullin S, Charles F, Luckel F, CMS Note 1999/027
110. Gupta A K, Jain S, Mondal N K, CMS Note 1999/075
111. Dimopoulos S et al. *Phys. Rev. D* **41** 2099 (1990); Dawson S *Nucl. Phys. B* **261** 297 (1985); Ross G G, Dreiner H *Nucl. Phys. B* **365** 397 (1988); Barbieri R et al., hep-ph/9810232
112. Krasnikov N V *Phys. Lett. B* **386** 161 (1996)
113. Krasnikov N V *Mod. Phys. Lett. A* **10** 2675 (1995)